Addis Ababa University
አዲስ፡አበባ፡ዩኒቨርሲቲ
SEEK WISDOM, ELEVATE YOUR INTELLECT AND SERVE HUMANITY !

**ADDIS ABABA INSTITUTE OF TECHNOLOGY**

**SCHOOL OF CIVIL AND ENVIRONMENTAL ENGINEERING**

**THESIS PAPER ON**

# COMPARATIVE ASSESSMENT OF LOW IMPACT DEVELOPMENT CONTROLS ON FLOOD MITIGATION

# (THE CASE OF WOLLO SEFER TO GOTERA ROUTE, ADDIS ABABA)

**By**

**Biniam Berhe**

**A thesis submitted and presented to the school of graduate studies of Addis Ababa University in partial fulfillment of the degree of Masters of Science in Civil and Environmental Engineering**

**(Major: Water Supply and Environmental Engineering)**

**Advisor**
**Dr.-Ing. Geremew Sahilu**

**Addis Ababa, Ethiopia**
**November, 2021**

# Addis Ababa University
# Addis Ababa Institute of Technology
# School of Graduate Studies

This is to certify that the thesis prepared by Biniam Berhe, entitled: Comparative Assessment of Low Impact Development Controls on Flood Mitigation (The case of Wollo Sefer to Gotera route: Addis Ababa) and submitted in partial fulfillment of the requirements for the degree of Masters of Science in Civil Engineering (Major in Water Supply and Environmental Engineering) complies with the regulations of the university and meets the accepted standards with respect to originality and quality.

## Approval by Board of Examiners

| | | |
|---|---|---|
| Advisor | Signature | Date |
| (Dr. Ing. Geremew Sahilu) | ...................... | ............... |
| Internal Examiner | Signature | Date |
| (Dr. Ing. Dereje Hailu) | ...................... | ............... |
| External Examiner | Signature | Date |
| (Professor Yilma Seleshi) | ...................... | ............... |

# Certification

The undersigned certify that he has read the Thesis titled "Comparative Assessment of Low Impact Development Controls on Flood Mitigation (The case of Wollo Sefer to Gotera Route, Addis Ababa)" and hereby recommend for acceptance by the Addis Ababa University in partial fulfillment of the requirements for the degree of Masters of Science.

……………………………………………

Dr.-Ing. Geremew Sahilu
(Advisor)

………………………………………………………………
Date

# Declaration and Copy Right

I declare that this thesis has been composed only by me and that it has not been submitted, in whole or in part, in any previous application for a degree. Except where stated otherwise by reference or acknowledgment, the work presented is entirely my own.

Signature___________________________

Date____________________________



Biniam Berhe

Email: Bbiniambirhane213@gmail.com

Phone No. 0901118188

November, 2021

# Acknowledgement

First and foremost, thanks to the Gracious GOD for giving me the chance to know him. Knowing him helped me a lot in focusing on my work and finishes it successfully.

Second, I would like to thank my Advisor Dr.-Ing. Geremew Sahilu for his sufficient guidance throughout the preparation of this paper.

Last but not least, I would like to thank my family and friends who supported me a lot in finalizing this work.

# Dedication

I dedicate this work to my mother whose support and affection has been a source of confidence to me while preparing it.

# ABSTRACT

Urbanization alters hydrological cycle and increases runoff by changing permeable surfaces into impermeable ones. In Addis Ababa, which is found in Awash catchment; rapid urbanization and development is altering permeable surfaces into impermeable ones; including impermeable roof surfaces. This phenomenon lowers the capacity of the land to infiltrate and store stormwater, and contributes in increased runoff volume and rate; causing flood damage as a result; which is not adequately managed by the current conventional drainage systems of the city. The study area which is the route from Wollo sefer to Gotera is one of the areas found in the city affected by flood due to immense urbanization. By decreasing runoff volume and increasing storage and infiltration, Low Impact Development (LID) practices are capable of minimizing and even avoiding flood risk if integrated with the existing drainage system. The objectives of the study are, evaluating the performance of the existing drainage system of the study area, apply four hypothetical LID controls (bio-retention cells, rain barrels, green roofs, and permeable pavements) to see the difference, comparing the LID controls on the basis of avoiding flood with a minimum area of application, and selecting the feasible one using storm water management modeling (SWMM) tool. The study revealed that the area has eleven subcatchments and flooding problem exists in it; because the drainage system is not found to adequately prevent this issue solely. Calibration of the model resulted in $R^2 = 0.9714$, and RMSE = 4.867; which proved a good agreement between the model and the actual values. Trials and errors testified that the minimum area on which LID controls can be applied to avoid flood risk was 58320m² (36%) of the area of the third subcatchment. If the aforementioned LID controls except green roofs were applied on such an area, flood problems would be avoided. Since, building areas were found to cover 60% of the third subcatchment, rain barrels were chosen as the feasible LID controls that can be installed on the least area possible to avoid flooding problems.

**Key Words**: Urbanization, Flood risk, Low Impact Development Controls, SWMM, Feasibility

# Table of Contents

# List of Abbreviations and Acronyms

A: Drainage area

AACRA: Addis Ababa City Road Authority

AMSL: Above mean sea level

A2: Rainfall Region Classification of Ethiopian Road Authority

C: Conduit

c: factor

cm: centimeter

CMS: Cubic meter per second

D/M/Y: Day, Month, Year

Daily Max: Maximum daily rainfall

DEM: Digital Elevation Model

Dmod: Simulated/modeled Depth

Dobs: Actual/ observed/ measured depth

ERA: Ethiopian Road Authority

f: factor

g: Gravitational acceleration

G.C: Gregorian calendar

GIS: Geographic Information System

Ha/ha: hectare

hr: hours

IDF: Intensity duration frequency

in: inches

J: Junction/node

Kn: Critical Deviate

KT: Frequency factor

LID: Low Impact Development

Ltr: Liters

m: meter

mm: millimeters

$m^2$: square meter

m/s: meter per second

$m^3/s$: cubic meter per second

Min: minutes

n: manning's roughness coefficient

O: Outfall

OBS: Observatory Station

Q: flow rate

R: Hydraulic Radius

RF: Rainfall

S: Subcatchment

SWMM: Storm Water Management Model

T: Return Periods

US EPA: United States Environmental Protection Agency

V: Velocity

z: Critical Deviate

# List of Figures

# List of Tables

# List of Pictures



# List of Tables and Figures in Appendix

# CHAPTER ONE

# 1. INTRODUCTION

## 1.1 Background

Urbanization and the need for development alters hydrologic cycle by introducing impermeable surfaces; which reduces stormwater losses and increases runoff; enhancing flood risk as a result. Sediment erosion, non-point source pollution of water bodies, flooding of flood plain areas, property losses, traffic disruption, and public health issues are some of the repercussions result because of the increased amount of runoff [1,2].

A good indicator of the effect of urbanization on flood management is the five-fold increment in the quantity of runoff from impervious surfaces in a typical city block compared with that from a natural woodland area of the same size [3]. Conventional stormwater management systems that collect, transport, and dispose of stormwater are not adequate to meet the requirements of the rapid land development and continuously increasing degree of imperviousness due to installation of streets, parking lots, and rooftops. Integrating structural management technique with non-structural is vital to increase stormwater losses and avoid flood risk. To achieve this, conventional stormwater management systems should be integrated with best management practices (BMPs) or low impact development (LID) controls [2].

LID controls are green infrastructures (GIs) designed to capture surface runoff and provide some combination of detention, infiltration, and evapotranspiration to it, capable of integrating the developmental activities with the environmental preservations. They are designed to retrofit the effect of urbanization on flood issues and decrease the load on artificial drainage systems. Green roofs, porous pavement, vegetative swales, rain barrels, rooftop disconnection, infiltration trench, rain garden, and bioretention cell can be mentioned as LID controls [4].

In urbanized and developed countries, these practices are gaining an increasing acceptance. This is primarily driven by the increasing urbanization, climate change, and sustainability issues [3]. In developing cities like Addis

Ababa; which has increasingly been growing economically in the last couple of decades, urbanization is one of the major issues with regard to urban flood management. The city keeps on developing, altering the permeability nature of the land by building infrastructures using impermeable materials [5].

The impermeable nature of these infrastructures plays a vital role in the overall runoff generated in the area. The stormwater that is transported from the roof to the downstream areas uses gutters and downspouts; which decreases the time for the flow to reach its peak and may cause sudden flooding damage. Infiltration and storage decreases when the stormwater runs off on impermeable roads, pedestrian walk ways, and impermeable building roofs [1,2].

Adopting LID controls such as rain barrels, green roofs, bioretention cells, and permeable pavements ensure the minimization of flood risks if applied and integrated with the existing drainage systems [6]. These approaches are best management practices which can balance development with environmental concerns, and address social, environmental, economic, and scientific aspects [7]. These four LID controls were analyzed and compared in this research, on the basis feasible flood mitigation.

In certain highly urbanized areas, green roofs constitute of between 30 and 50% of the roof surfaces [5,6]. Experiments on vegetated roofs reveal that they are capable of decreasing overall runoff peaks and volumes by 30 to 90% [8]. Rain barrels store the rain water and prevent the runoff from rushing and creating sudden flood damage. Bioretention cells are proven to decrease the cumulative flow rate and flood volume. Permeable pavements increase precipitation losses by enhancing the infiltration capacity of the urbanized land. But in Addis Ababa, the application of such green infrastructure techniques to mitigate flood risks is not common. If they are carefully designed and constructed, these techniques are even proven to be economical than extending the existing conventional drainage systems [9]. It is also important to select the feasible LID control to avoid flood risk at a minimum cost;

## 1.2 Statement of the problem

Damages related with flooding have been increasing for the last fifty years in Africa [10]. Half of the total destructions recorded in sub Saharan countries are related with flooding [11]. As of Addis Ababa, urbanization and development have highly been increasing for the past two decades. The city is the capital of Ethiopia and the seat of African Union in which quarter of the urban population dwell. About half of the national gross domestic product of the country is contributed by the city [12]. It is challenged by flooding as a result of urbanization and the rapid economic growth; which is reflected by the immense alteration of permeable surfaces into impermeable roads and roofs.

In the city, areas located near rivers are susceptible to flooding damages as a result of activities on upper watersheds. In most cases, these areas are vulnerable to flooding because of the weak conventional drainage systems [11]. An analysis on the rainfall pattern of the city over the past 100 years revealed that there has been an increment of about 18mm every ten years from 1951-2002 [13]. An increase in rainfall in the city was also shown by a recent study [14].

The increase in population, rapid urbanization, and fast economic development; coupled with the inadequate drainage systems appear to increase the risk of flooding in the city [15]. The alteration of pervious areas into impervious pavements decreases green environments as a result of deforestation, which minimized water retention capacity of the land, and reduced evapo-transpiration, increasing runoff quantity: which the current conventional drainage systems in the city cannot adequately manage on their own in many cases [12]. Due to one or more of these reasons, one of the main roads of Addis Ababa which is Ethio-China Friendship Street (Gotera to Wollo sefer), has been flooded at the time of high rainfall intensity. Because of this, problems on market areas, traffic jam, and crossing difficulties are apparent.

Although LID controls have the capacity to minimize flood problems by supporting conventional drainage systems and are exercised in many countries [5,7,8], this way of controlling flood is not commonly practiced in developing areas of the city including the area from Wollo sefer to Gotera.

## 1.3 Research Questions

- Is the current drainage system of the study area adequate to manage flooding?
- Can LID controls significantly reduce runoff volume and peak discharge, and prevent the area from flood problems?
- What is the minimum area an LID control can be applied upon the study area to avoid flooding problems
- Which LID control is capable of avoiding flood after being installed on the least area of application possible?

## 1.4 Objective

### 1.4.1 General Objective

- Carry out comparative assessment of hypothetical LID practices to mitigate flood risks considering Wollo sefer-Gotera route as a case study

### 1.4.2 Specific Objectives

- To find peak runoff generated from a watershed.
- To identify spots along the chosen route with insufficient drainage capacity.
- To compare the system with and without LID controls regarding runoff peak and volume reduction, and flood prevention.
- To find the minimum area upon which an LID control can be applied on the study area to remove flood.
- To compare and select the feasible LID control that can be integrated with the existing drainage system and mitigate flood.

## 1.5 Significance of the study

Studies on comparison between different LID controls on the basis of feasible flood mitigation are not common in Ethiopia. This study will certainly fill the research gap and be utilized as a source of valuable information for other researches yet to be conducted, for engineers, contractors, and policy makers on the drainage problems of the area selected for this study, and gives guidance on the cost effective low impact development control that should be installed upon the study area to tackle flood issues.

## 1.6 Scope of the study

This research is geographically constrained in the route from Wollo sefer to Gotera to perform the analysis. It is also concerned on the problems and mitigations of runoff quantity, not quality. Out of the various modeling tools available, the research will be limited on simulating rainfall-runoff analysis using SWMM. The comparison was also made between four selected LID practices for feasible flood mitigation.

## 1.7 Thesis Layout

This thesis is divided into five chapters with an adequate explanation of the information found in each of them. The first chapter incorporates the background information on the capacity of LID controls to mitigate flood problems caused by urbanization, the statement of the problem, the research questions, the general and specific objectives, the significance, and the scope of the research.

The second chapter reviews different literatures related with the topic of this research. It shortly reviews the hydrologic cycle, water balance, catchment, rainfall-runoff relationships and flood, basic concept of urban drainage, stormwater modeling and urbanization, literatures related with LID controls, and different modeling tools used in simulating rainfall-runoff relations.

Chapter three focuses on the methods employed, the materials used, and the procedures followed in this research to meet its objectives. Chapter four is a presentation of the results found after carrying out number of analyses, and related discussions. The last chapter includes the conclusion reached and the recommendation given regarding flood problems in the study area, and the feasible LID control that should be implemented to mitigate this problem.

# CHAPTER TWO

# 2. LITERATURE REVIEW

## 2.1 Hydrologic Cycle

Hydrologic cycle is also called water cycle; which can be defined as the ceaseless motion of water on, above, and below earth's surface. Solar energy radiated from the sun starts the cycle resulting in evaporation of water from oceans, lakes, ponds, and seas; and evapotranspiration (ET) of water from plants and soil in the form of vapors. The vapors would then be lifted up to the sky and get condensed there to make clouds resulting in precipitation of different forms (rain, snow, and hail). Some of this precipitation moves on the surface of the earth to become runoff; and some infiltrate into the earth's surface to build the water table in it. The runoff unites with rivers and gets accumulated on water tanks. Portion of the runoff and the ground water would end up flowing into oceans; and evaporation would take place from there to restart the cycle [1].

## 2.2 Water Balance

The water balance also called mass balance is defined as the basis for the availability and transportation of water for a certain area which can be a continent, a country, a region, or a catchment. There is finite and preserved quantity of water with varying distribution across the earth. Yearly water balance of the earth is presented in table 2.1. The water balance equation sets out that the change in storage equals the difference between the overall inflow and the overall outflow of a catchment [1,16,17]. For a specific area and specific time period, the water balance equation can be written as shown below;

$$P - R - E = \Delta S \quad \ldots\ldots\ldots\ldots\ldots 2.1$$

Where: -

P: Precipitation, R: Runoff, E: Evaporation, $\Delta S$: Storage Change

Table 2.1: Earth's yearly water balance (source: [17])

| | **Ocean** | **Land** |
|---|---|---|
| Area (*10^6km$^2$) | 361.3 | 148.8 |
| Precipitation (*10$^3$km$^3$/year) | 458 | 119 |
| Precipitation (mm/year) | 1270 | 800 |
| Evaporation (*10$^3$km$^3$/year) | 505 | 72 |
| Evaporation (mm/year) | 1400 | 484 |
| Runoff to Ocean | | |
| Rivers (*10$^3$km$^3$/year) | | 44.7 |
| Groundwater (*10$^3$km$^3$/year) | | 2.2 |

Of all the elements in the hydrological cycle, runoff is the most important one to model stormwater. The total amount of water that is intercepted through evaporation and absorbed into groundwater before runoff begins is known as initial abstraction. After runoff begins, water still infiltrates into the soil until it becomes saturated. Where there is insignificant size of surface water, evaporation is often considered to be negligible.

Runoff = Total precipitation − Initial abstraction − Infiltration – Evaporation ..............2.2

Rainfall is the major form of precipitation and the major reason for flood issues. A storm hyetograph is the best way to present a storm event because it shows the instantaneous rainfall intensity with respect to time. Intensity is defined as the rate of rainfall and is typically expressed in units of millimeters per hour [16,17].

Although rainfall intensity varies during precipitation events, many of the procedures used to derive peak flow are based on simplified constant rainfall intensity. Average precipitations are usually measured by rain gauges in many rain stations. Based on the precipitation data measured over long historic records, a standard Intensity–Duration–Frequency (IDF) curve can be developed for a specific area. An IDF curve provides a summary of a site's rainfall characteristics by relating storm duration and exceedance probability (frequency) with rainfall intensity (assumed constant over the duration). With IDF curves, rainfall depth and total rainfall volume can be calculated according to the area of interest. If IDF curves are not available, a designer needs to develop them on a project-by-project basis [16,17].

## 2.3 Catchment

Water balance equation is most often performed for an area known as a Catchment/Watershed/Drainage Basin/River Basin. A catchment is an area of land where rain water accumulates into a common discharge point or outlet. The area of a catchment is dependent on the location and altitude of the outlet and is determined by the water divides. A water divide is a border of a catchment over which the water cannot flow and is a separation between adjacent catchments [4,17]. Water balance of a catchment is presented in figure 2.1

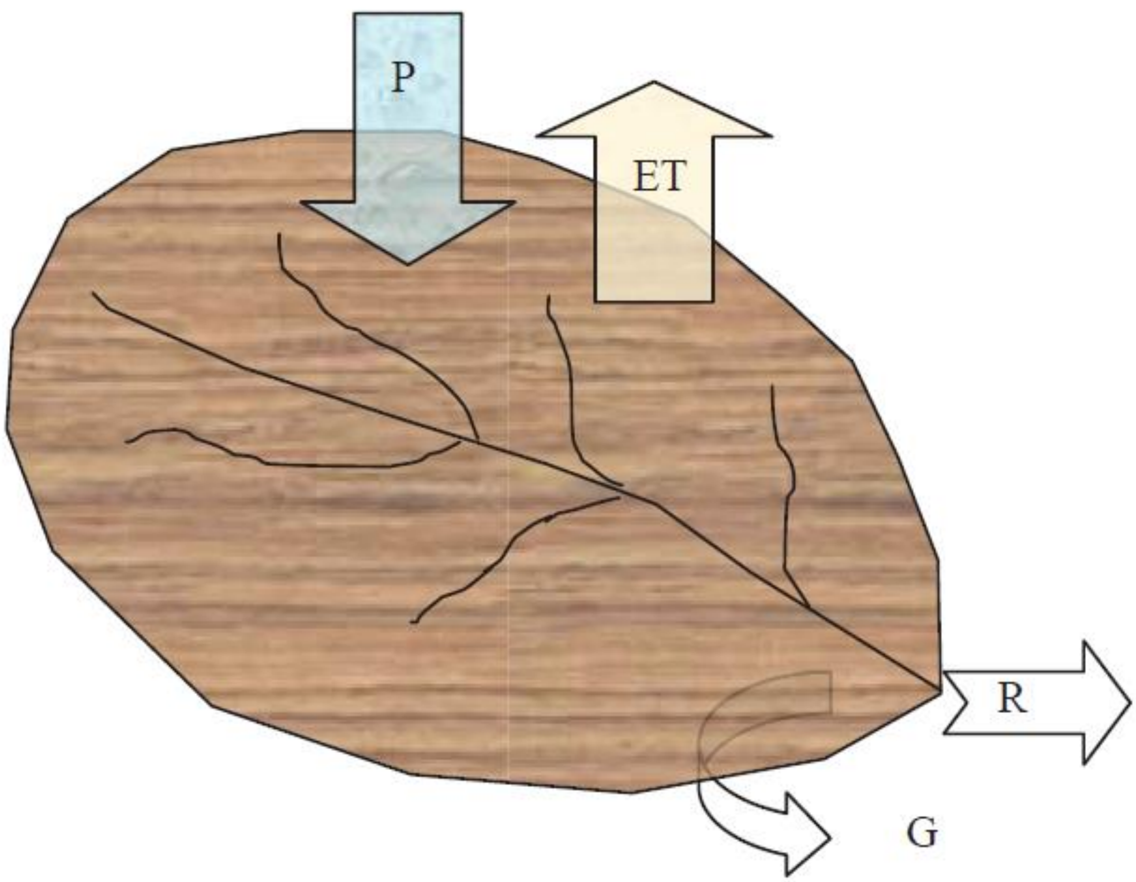


Where: ET: - Evapotranspiration, G: - Ground water runoff

Figure 2.1: Water balance of a catchment (source: [17])

## 2.4 Rainfall-Runoff relationships and Flood

To manage stormwater effectively, a detailed knowledge of rainfall-runoff characteristics is vital. In rainfall-runoff relationship, both runoff coefficient (*C*) and curve number (CN) provide a simplified relationship between rainfall and runoff based on local land use, soil storage and infiltration conditions. Time of concentration (Tc) is also a synthesis parameter to favor stormwater modeling. It is defined as the time required for water to travel from the hydraulically most remote point of the basin to the point of interest. Peak flow is usually calculated to size drainage systems such as pipes, culverts, channels, and weirs, and is also used for selecting measures for erosion control. Peak flows are generally adequate for the design and analysis of conveyance systems such as storm drains or open channels.

Flood occurs when water flow exceeds the capacity of the drainage system. In stormwater modeling, a standard flood or standard project flood is usually selected for rainfall–runoff calculation**.** A 100 year storm event does not mean that kind of storm event occurs once every 100 years; instead, by definition, the chance of that storm event occurring in a year is 1% [1,16,17]

The probability that a flood event (X) in any year will equal a design basin flood with a recurrence interval T is;

P (X event occurs in 1 year) = 1/T ..............2.3

## 2.5 Basic Concept of Urban Drainage

The relationship between the natural hydrological cycles and human activity demands the need for drainage systems. Humans use this cycle to cover their need of water supply in one way, and avoid the water in the name of development altering the natural permeable land into impermeable one in another. These relations demand drainage systems for two types of fluids namely; wastewater and stormwater. Both types must be taken under consideration to achieve a healthy condition for humans and the environment [16].

### 2.5.1 Components of Urban Drainage

Urban drainage systems are needed in developed urban areas because of the interaction between human activity and the natural water circulation. The urban drainage systems can be completely artificial, or combination of manmade sewer facilities and natural watercourses. The system can be represented as a network consisting of catchments and subcatchments, nodes, links and outlet. The components of the system are defined below [18]

**Catchment: -** A catchment is the area collecting water from nearby higher terrain surface, which is delineated by topographic contour lines. A catchment is usually described by its parameters (catchment area, the percentage of impervious area, average slope, the longest flow length and approximate shape).

**Nodes: -** are junctions to link the sewers. They also provide stormwater transition between surface and subsurface systems. Typical examples of nodes are manholes. Manholes should be provided at intersections of stormwater drains, junctions between different size of stormwater drains, where a stormwater drain changes direction/gradient and on long straight lengths.

**Links: -** transport flow in the system, and are often open channels or closed sewers with regular or irregular cross sections.

**Outlet: -** The most downstream component of the urban drainage system, which discharges the sewage from the system to receiving waters.

### 2.5.2 Historical Perspectives

There were different views in history as to what urban drainage is. Through the course of history, some used to view it in relation with flood control; some with respect to wastewater management; and some others as a purification system. There were also some with perspectives of it as an important natural resource, and others viewing it as an ideal place for disease causing pathogens to be transmitted. Such perspectives have generally been influenced by factors such as; religious beliefs, climate, topography, geology, construction, engineering and construction capabilities; factors which played a positive role in providing direction for urban drainage remedies, and a negative role in limiting their development [1,16,17]

### 2.5.3 Development of Modern Urban Drainage

The beginning of modern urban drainage practices was initiated in European cities during the nineteenth century. One critical turning point in urban drainage occurred during the middle of the nineteenth century. During the first half of the nineteenth century sanitary wastes were discharged from buildings to privy vaults and cesspools. Most sewers were designed exclusively for stormwater drainage. Sanitary wastes accumulated in privy vaults and cesspools and were periodically collected by scavengers and transported to a suitable disposal location (e.g., farm, dump outside city). As the nineteenth century progressed the concept of urban drainage changed with the incorporation of water-carriage sanitary waste collection into the urban drainage systems. Sanitary connections to the sewers were made legal and new sewers were constructed to drain stormwater and sanitary wastewater.

The public perspective of urban drainage changed during the nineteenth century from a neglected afterthought to a vital public works system. The public also shifted their stance regarding funding the construction and maintenance of sewer systems. The shift in public perspective was driven by many factors, but the most important was probably the scientific evidence accumulated during the second half of the century linking sanitary wastes and disease transmission.

The perspective of urban drainage also changed from a design standpoint during the nineteenth century. Most sewers constructed before the nineteenth century were not planned or designed by an engineer using numerical calculations. Instead a trial-and-error process was executed, which in some cases eventually produced well-functioning systems. Regarding flood management, the historical perspective and approach is widening the pipes and upgrading the capacity of the existing drainage systems [19].

### 2.5.4 The need for Sustainable Urban Drainage

In many urban areas, drainage is based on a completely artificial system of sewers: pipes and structures that collect and dispose of this water. In contrast, isolated or low-income communities normally have no main drainage. Wastewater is treated locally (or not at all) and stormwater is drained naturally into the ground. These sorts of arrangements have generally existed when the extent of urbanization has been limited. However, recent thinking towards more sustainable drainage practices is encouraging the use of more natural drainage arrangements wherever possible [11,19].

So there is far more to urban drainage than the process of getting the flow from one place to another via a system of sewers. There is a complex and fascinating relationship between wastewater and stormwater as they pass through the system, partly as a result of the historical development of urban drainage. When wastewater and stormwater become mixed, in what are called 'combined sewers', the disposal of neither is 'efficient' in terms of environmental impact or sustainability. Also, while the flow is being conveyed in sewers, it undergoes transformation in a number of ways. Another critical aspect is the fact that sewer systems may cure certain problems, for example health risks or flooding, only to create others in the form of environmental disruption to natural watercourses elsewhere.

Overall, urban drainage presents a classic set of modern environmental challenges: the need for cost-effective and socially acceptable technical improvements in existing systems, the need for assessment of the impact of those systems, and the need to search for sustainable solutions. As in all other areas of environmental concern, these challenges cannot be considered to be the responsibility of one profession alone. Policy-makers, engineers, environment specialists, together with all citizens, have a role. And these roles must be played in partnership. Engineers must understand the wider issues, while those who seek to influence policy must have some understanding of the technical problems [20,21].

### 2.5.5 Low Impact Development (LID) Controls

LID Controls are low impact development practices designed to capture surface runoff and provide some combination of detention, infiltration, and evapotranspiration to it. Using LID in urban areas is becoming one of the most popular methods for sustainable stormwater management and flood mitigation [2,20]. LID is a smarter and more sustainable urban development and flood management technique which retrofits the effect of urbanization and reduces the risk of flood through several non-structural and structural measures [7]. Some of these measures include reducing imperviousness, conserving natural resources and ecosystems, as well as constructing Green Infrastructure (GI).

GIs are implemented for LID purposes; some well-known examples of GIs are bio-retention cells, green roofs, permeable pavements, and rain barrels. They are green infrastructures considered as properties of a given subcatchment, similar to how Aquifers and Snow Packs are treated. Stormwater management modeling (SWMM) is a tool used in the research that can explicitly model eight different generic types of LID controls [20]. These LID controls can either be applied new or retrofitted on existing areas.

**Bio-retention Cells:** are depressions that contain vegetation, grown in an engineered soil mixture placed above a gravel drainage bed to capture stormwater runoff and handle flood issues.

Figure 2.2: Bio-retention cells (source: [4])

**Rain Gardens:** types of bio-retention cells consisting of just the engineered soil layer with no gravel bed below them.

Figure 2.3: Rain Gardens (source: [4])

**Green Roofs:** are another variation of a bio-retention cell that have a soil layer laying atop a special drainage mat material that conveys excess percolated rainfall off of the roof.

Figure 2.4: Green Roofs (source: [4])

**Infiltration Trenches:** are narrow ditches filled with gravel that intercept runoff from upslope impervious areas. They provide storage volume and additional time for captured runoff to infiltrate the native soil below.

Figure 2.5: Infiltration Trenches (source: [4])

**Continuous Permeable Pavement:** are excavated areas filled with gravel and paved over with a porous concrete or asphalt mix. Normally all rainfall will immediately pass through the pavement into the gravel storage layer below it and infiltrate into the soil

Figure 2.6: Permeable Pavement (source: [4])

**Rain Barrels (Cisterns)**: are containers that collect roof runoff during storm events and can either release or re-use the rainwater during dry periods.

Figure 2.7: Rain Barrels (source: [4])

**Rooftop Disconnection:** has downspout discharge to pervious landscaped areas and lawns instead of directly into storm drains. It can also model roofs with directly connected drains that overflow onto pervious areas.

Figure 2.8: Rooftop Disconnection (source: [4])

**Vegetative Swales:** are channels or depressed areas with sloping sides covered with grass and other vegetation. They slow down the conveyance of collected runoff and allow it more time to infiltrate the native soil beneath it.

Figure 2.9: Vegetative Swales (source: [4])

Based on the main functions they have LID controls are categorized into two namely; storage LID controls and storage + infiltration LID controls. The storage LID controls are those that are only capable of retaining or storing stormwater and not infiltrating it. Green roofs and rain barrels are grouped under this category. The storage + infiltration LID controls as the name indicates are capable of both storing and infiltrating stormwater. Permeable pavements and bio-retention cells are grouped in this category.

## 2.6 Stormwater Management and Urbanization

Stormwater management is an endeavor to reduce and detain runoff of rainwater or melted snow into streets, lawns and other sites and the improvement of water quality. When rain falls, part of the water is lost by evapo-transpiration due to interception of leaves, part of it infiltrates into the ground, and the remaining part runs off the surface land. This is how the hydrological cycle operates naturally. Urbanization alters permeable surfaces into impermeable ones, which prevents the water from soaking into the ground, minimizing the amount of infiltration, increasing the volume of runoff, and causing flood issues as a result. Also, stormwater that flows on a natural land moves slower than when it runs off impermeable urbanized lands. This decreases the time for the runoff to reach its peak and creates possibility of sudden flood damages [1,16,22].

To tackle this problem, conventional drainage systems replaces one part of the natural hydrological cycle. In order to prevent the stormwater from running off the streets and cause flood issues, artificial piping systems are commonly constructed. Gutters and downspouts for roof systems, pipes, manholes, and culverts for streets are commonly built to drain off the storm to nearby water bodies before inundating the area [17].

### 2.6.1 Stormwater Management Condition in Ethiopia

In Ethiopia, where watersheds of many urban centers receive significant amount of annual rainfall and where rainfall intensity is generally high, control of runoff at the source, flood protection, and safe disposal of the excess water/runoff through proper drainage facilities is vital. Drainage problems in Ethiopian urban centers include flooding, deterioration of roads, land degradation, sedimentation, water logging, blockage of drainage facilities and the like [12,18].

With urbanization, impermeability increases with the increase in impervious surfaces (i.e. residential houses, commercial buildings, paved roads, parking lots, etc.), drainage pattern changes, overland flow gets faster, flooding and environmental problems such as land degradation increases. It is a problem facing the existing and future environmental conditions of urban centers [22].

### 2.6.2 Stormwater Management Condition in Addis Ababa

Addis Ababa lacks adequate stormwater management system. Gotera - Wollo Sefer road, Saris- Gotera road and on the ring road and in Addis Ketema Sub-city are some example areas found in the city where flooding problem is common. Congested traffic due to flooding of roads after small depth of rainfall, erosion of pavements resulting in reduction of service life of road infrastructure and impact of road flooding on nearby community are consequences of poor drainage system in the city. The pattern of urbanization and modernization in Ethiopia has meant increase densification along with urban infrastructure development [23].

The combined effect of these results in higher rain drop intensity and consequently accelerated and concentrated runoff. Inadequate integration between road and urban stormwater drainage infrastructure coupled with poor management exposes significant proportion of urban areas in the city to flooding risks [24]. These problems can effectively be tackled if LID controls are integrated with the artificial drainage systems [25].

## 2.7 Stormwater Modeling

Stormwater modeling is used to understand the flow direction, flow rates, water elevations, pollutant loads, and contaminant concentrations at any location of interest during and after a specific storm event. The modeling results are usually then used for a master plan, storage and drainage design, or water treatment analysis.

For a large drainage area with complex drainage routes, the basin–node–link (BNL) methodology is usually used for stormwater modeling. Many stormwater modeling software have been developed based on this methodology. In the BNL method, the drainage basin of interest is divided into a certain number of sub-basins (subcatchments) depending on the level of service. A node is then assigned to each sub-basin. Water in each sub-basin is assumed to accumulate to the node. Nodes are also assigned to each end of any conveyance sections. The nodes are connected by drainage links (such as pipes, channels, weirs, drainage structures, pumps, percolation, etc.).

The United States Environment Protection Agency (USEPA) developed the most widely used stormwater modeling software (Stormwater Management Model [SWMM]) by utilizing the BNL methodology. Stormwater modeling results usually yield the stage (water level) at any point of interest, flow rate at any conveyance, and runoff volume in any basin at any time. The modeling results are then used as a basis for master planning, land development, and detail drainage design. Modeling results also form the basis for floodplain maps, which are produced to show inundated areas under a certain storm event [4,17].

## 2.8 Literatures related with the four LID controls

In certain highly urbanized areas, green roofs constitute of between 30 and 50% of the roof surfaces [5,6]. Experiments on vegetated roofs reveal that they are capable of decreasing overall runoff peaks and volumes by 30 to 90% [8]. Rain barrels store the rain water and prevent the runoff from rushing and creating sudden flood damage. Bio-retention cells are proven to decrease the cumulative flow rate and flood volume. Permeable pavements increase precipitation losses by enhancing the infiltration capacity of the urbanized land.

However, in Addis Ababa the application of such green infrastructure techniques to mitigate flood risks is not common. If they are carefully designed and constructed these techniques are even proven to be economical than extending the existing conventional drainage systems [9]. To achieve maximum runoff peak and volume reduction at a minimum cost, selecting the feasible LID control is vital. Generally, LID controls that are applied on wide areas are not economical. This would mean that, the LID control that can avoid flood problem with minimum area of application is the feasible one [9,19]. The following section reviews some literatures related with the LID controls applied in the research.

A research done in Chile, the city of Curico revealed the capability of green roofs in managing flooding damages caused mainly by shortage of green areas in the city, increase in population, and urbanization. The study utilizes stormwater management modeling (SWMM) tool to analyze areas highly affected by increased runoff quantity by considering different distributions and types of green roof surfaces. The research came up with a result of significant decrease of runoff quantity in flood impacted areas by adopting green roof surfaces. For moderate occurrences of precipitation, if half the area is covered by green roofs, flooding can be removed regardless of the type of green roofs implemented. The study states that, for strong rainfall events, 60-95% of buildings of the area should be covered by green roofs to avoid flooding [26].

Another study conducted in Italy on Seveso river basin demonstrated that significant reductions in terms of runoff quantity can be achieved as a result of implementing green roof surfaces. The surroundings of the watershed under study are very congested many times annually due to occurrences of flooding. Recently, an increase in both frequency and intensity of such flooding occurrences on the area was seemed to emerge. The study added that, extending the conventional drainage systems is impossible because of the intense urbanization and development taken place around the area. The study modeled the changes by three hypothetical roof greening scenarios applying. 5, 30, 100% alteration of the conventional roof surfaces to green roofs using SWMM and compared with that of the current impermeable roof surfaces. After this, it came up with a result that, on applying green roofs fully, 30-35% reduction in runoff quantity can be achieved [27].

A study examined the feasibility of rain barrel, Rain Water Harvesting (HRW) system at a distributed scale within an urbanized area located in the northwestern part of Chittagong City that experiences flash flooding on a regular basis. For flood modeling, the stormwater management model (SWMM) was employed with rain barrel low-impact development (LID) as a flood reduction measure. The result showed that, by adopting LID, i.e., RWH, about 28.66% reduction of flood was achieved. Moreover, the study showed that 10%-60% imperviousness of the subcatchment area can yield a monthly RWH potential of 0.04-0.45 $m^3$ from a square meter of rooftop area [28].

A research done on the capacity of bio-retention cells to manage storm water on a 93% impervious site having 7840 $m^2$ area was carried out using SWMM. The result has shown that the bio-retention system reduces the cumulative flow rates by over 55% and the flood wave volume by over 54%. It states that, application of professional computer programs, such as SWMM, enables performing multivariate hydrodynamic calculations that consider also the influence of local rainwater management devices such as bio-retention systems. The study concludes that bio-retention offers an alternative to classic solutions providing a relief to drainage systems in urbanized areas [29]

Permeable pavement is part of the low impact development (LID) measurement, which can decrease urban surface runoff coefficient and flood peak flow. A research conducted on a two-way, six-lane road in Nanjing using SWMM was used to simulate the effect of different pavement structures (drainage surface, permeable pavement, and permeable road) under different rainfall conditions on reducing surface runoff and controlling urban stormwater. The simulation results show that the drainage surface can reduce part of surface runoff, but it has no influence on the reduction and lagging of flood peak. The permeable pavement can reduce part of surface runoff and flood peak and can delay peak time. The study further stated that the permeable road did better in reducing flood peak; which could effectively reduce the pressure on drainage systems and the risk of flood [30].

## 2.9 Feasible LID controls

The above literatures testify that adopting LID controls help reduce the stress on piped drainage system by decreasing the quantity of runoff to mitigate flood risks. Although, retrofitting LID controls with the existing area reduce the adverse effect of urbanization on flood management, selecting the cost effective one is necessary. Generally, LID controls applied on large areas are not economical. There is a direct relationship between the cost and area of application of LID controls. As the area of LID application increases, the cost also increases. Therefore, to be economical, LID controls that can be applied on a minimum area of a catchment should be selected [19].

## 2.10 Related Researches in the context of Addis Ababa

There were researches used in this paper as a source of information that were done in the context of Addis Ababa regarding flood problems and the influence of low impact development controls to mitigate this problem. Researches related with drainage system and flood problems were ‘’Investigation of Flooding Problems in Urban Drainage Systems: the Case at Zenebe Werk in Addis Ababa, Ethiopia.” [23], Impacts of Land Use/Cover on Surface Water Quantity and Quality: Case of Akaki Catchment, Ethiopia” [31], ‘’Flood Assessment on Addis Ababa Light Rail Transit System (LRT): Meshualekiya to Gotera” [22]. In all of these studies, the research areas were found to face flood issues as a result of increasing urbanization and insufficient capacity of conventional drainage system provided.

There were some researches that incorporated in their studies the application of LID controls to mitigate flood issues. The first one was ‘’Integrated Urban Drainage System: The Case of Ayat to Megenagna Light Rail Transit System Route.” [32]. This research concluded the existence of flood problem in the mentioned study area which can be improved by applying rain barrels. The second was ‘’Evaluating the Impact of Land Use Change on Urban Drainage System and Proposed Low Impact Development Measures in Addis Ababa, Ethiopia (case study of Megenagna - Bole Ring Road)” [33]. In this research, it was explained that conventional drainage systems in the mentioned area under study was not sufficient; which resulted in flood problems. It further recommended permeable pavements to be applied to improve the problem.

The last one was ‘’Sustainable Storm Water Management by Implementing low impact development in JEMO, Addis Ababa.” [24]. This research also testified the presence of insufficient drainage capacity and flood problems in the study area. It suggested the implementation of Rain Gardens to better manage problems related with flood.

## 2.11 Modeling Tools

This part reviews different modeling tools capable of simulating the proposed LID practices. There are many tools that incorporate LID practices for modeling storm water which are not only available commercially but also utilized by researchers.

### 2.11.1 Water Environment Research Foundation (WERF) BMP SELECT Model

WERF modeling tools are developed for nine green infrastructure (GI) or LID practices, they being; extended detention basin, retention pond, swale, permeable pavement, green roof, large commercial cisterns and residential rain garden, curb-contained bio retention and in-curb planter vault: mainly suitable for conducting planning level cost estimates. The user inputs for the model are general information of the treatment devices such as system size, drainage area and system type. Furthermore, the tool gives users an option of selecting the sensitivity analysis in the planning and designing stage. Illustration of the results by present value graphs is important output that WERF BMP modeling tools can produce. WERF modeling tools for LID and BMP comes with an interface for the data entry in the format of an excel spreadsheet which makes the handling of software easy for different levels of user groups [33].

### 2.11.2 Storm Water Management Model (SWMM)

SWMM is a well-known rainfall runoff modeling tool that incorporates green infrastructure practices of rain gardens, infiltration trenches, street planters, green roofs, permeable pavements, rain barrels and vegetated swales. It can be applied both in a site and in a catchment scale. Subcatchment based approach is incorporated in this model to model the runoff generated from rainfall [33].

SWMM routes runoff for subcatchments with storm drains, combined sewers, and natural drainage through a network of pipes, channels, and storage/treatment units. SWMM simulates three primary processes: stormwater infiltration, surface runoff, and flow routing. The latest versions of SWMM, like SWMM 5.1 can model hydrologic performance of typical conventional and LID controls with varying sizes, coverage, and geographic distributions [27].

Width and slope of the subcatchment, rainfall data, percentage imperviousness, manning's 'n' values and depression storage for pervious and impervious areas are the input data needed for SWMM. Also, sizing characteristics of different GI practices are required to model the effectiveness on managing urban runoff. For these inputs, output report is produced that contains the model status. The report can be in the form of time series graph, tables, and statistical analysis of simulation results [33].

SWMM consists of runoff yield model, infiltration model, surface runoff concentration model and pipe hydraulic dynamic model. The modeling tool is capable of solving hydraulic systems under three different conditions: steady flow, kinematic wave, and dynamic wave. The robustness and effectiveness of the hydraulic calculation engine have been successfully tested since the early 1970s in thousands of international academic and professional projects. This tool is free and open source; which makes it possible to improve and customize it by creating and incorporating additional features [4,20,27].

SWMM has a user friendly graphical user interfaces (GUI) which enables more visualization of the study area by importing CAD or GIS files. Handling of SWMM requires knowledge of fundamental processes with regard to hydrological modeling which limits its application to within specific user groups [30,33].

### 2.11.3 EPA System for Urban Stormwater Treatment and Analysis Integration Model (SUSTAIN)

SUSTAIN is an ArcGIS based decision support system developed by the US EPA to guide water resource management professionals for the design and implementation of management plans to preserve water and meet water quality goals in catchment scales. It also includes the application of GI controls in stormwater management projects and allows the users to optimize practices in terms of both environmental and economic perspective. SUSTAIN consists of seven key components, being: framework manager, ArcGIS interface, catchment module, BMP module, optimization module, post-processor, and Microsoft Access database. The currently supported GI practices by SUSTAIN includes: bio retention, cistern, constructed wetland, dry pond, grassed swale, green roof, infiltration basin, infiltration trench, porous pavement, rain barrel, sand filter (surface and non-surface), vegetated filter strip and wet pond [34].

The economic component for GI, BMP construction, has a more sophisticated manner, compared to others, for analyzing the unit costs of individual segments. The cost estimation and cost optimization module in SUSTAIN are the main two components of the software used to analyze the economic benefits of the GI in stormwater management. The cost data in the cost estimation module are obtained directly from industry and the unit cost approach in SUSTAIN is designed to minimize the errors that can result by considering the bulk construction cost of GI on a country wide basis.

The GI optimization module uses a tiered approach for the analysis of cost effectiveness of individual and combined catchment scale applications. The decision criteria in SUSTAIN is user defined and to meet that criteria, evolutionary optimization techniques are used. The two search algorithms currently in use for this application are scatter search and non-dominated sorting genetic algorithm-II. An optimal cost effectiveness curve is the outcome of this module for the desired water quantity or water quality control targets [35].

The input data required for the model are, the land use data, catchment data and the designing details of different quantity reduction. The model can be used to select optimal GI scenarios according to their cost effectiveness. SUSTAIN integrates GIS data for the analysis which makes the data input to the program more comprehensive and the level of complexity is higher. Therefore, the end user needs to have sufficient knowledge of stormwater management practices and GIS software package. Thus the software program is mainly suitable for large scale projects which need more accuracy on the basis of both environmental and economic aspects [33,34].

### 2.11.4 CNT Green Values National Storm water Management Calculator

The Center for Neighborhood Technology (CNT) national stormwater management calculator which is also known as National Green Values Calculator (GVC) is tools that was developed to compare the performance, costs and benefits of GI with conventional stormwater management practices. The step by step procedure of the calculator allows the users to set up a runoff reduction goal for their sites by considering the optimum runoff reduction efficiency through a set of GI practices.

The GI practices that are incorporated in national GVC include; green roof, planter boxes, rain gardens, cisterns/rain barrels, native vegetation, vegetated filter strips, amended soils, roadside swales, trees, swales in parking lot, permeable pavement on parking, permeable pavement on drive ways and alleys, and permeable pavement on sidewalks. The calculator is designed to be used in site scale and therefore the tool is incapable of handling evaluations from neighborhood scale to catchment scale.

CNT uses the Soil Conservation Service (SCS) runoff curve number method to calculate the volume of runoff generated. The effect on the GI for infiltration, evapo-transpiration and reusing the storm water runoff is calculated by modeling the ability of each and every practice's ability to capture runoff [27,33]. The user inputs for national GVC contains site specific parameters such as land cover distribution, soil type, runoff reduction goal and attributes of the different GIs that are being used for the analysis. Runoff volume reduction and cost benefit analysis results of different GI are displayed directly on screen in different tabs, as outputs. National GVC is available as a web based freely available tool and the simple interface makes it easy to handle for users at any knowledge level. However, the tool cannot be applied for different geographical regions since it contains data for US based context only [33].

### 2.11.5 Source Loading and Management Model for Windows (WinSLAMM)

WinSLAMM was initially developed as a model to study the relationship between pollutants of urban runoff and runoff quality. With the advancement of GI as a stormwater source control measure, the tool has been upgraded by adding modules which have the capability of modeling the performances and life cycle costs of different practices such as infiltration/bio-filtration basins, street cleaning, wet detention ponds, grass swales, green roofs, filter strips and permeable pavements [36]. The tool supports modeling in different spatial scales such as site, catchment and regional scales.

WinSLAMM is commonly used as a planning tool and can be applied for the hydrology of different types of storms including small storms. The model can evaluate long series of rain events and the impacts of urban soils on runoff are also considered. The biological conditions of the receiving waters are calculated according to the type of GI practice which has been used and the characteristics of the site. WinSLAMM can be integrated with a number of other drainage models when a detailed analysis of runoff is required. The model also contains inbuilt Monte-Carlo components for considering uncertainties [36].

The tool uses directly measured input parameters such as areas and characteristics of contributing catchments to the catchments and the pollutants associated with particulate solids in these areas. The calculated model outputs from the WinSLAMM model are runoff volumes and quality of predevelopment. One of the important features of this model is that the outputs can be imported to a number of other models and also can be integrated in Geographic Information Systems (GIS) platform. The users require fundamental knowledge of urban hydrology and storm water management procedures in order to handle the model [33,36].

# CHAPTER THREE

# 3. METHODS, MATERIALS, and PROCEDURES

## 3.1 Study Area

### 3.1.1 General Description

The study area is located in central Addis Ababa, the road from Wollo sefer to Gotera (Ethio-China Street): including wide areas of right and left sides of the road as shown in figure 3.1. The soil type in the area is mainly clayey and most section is covered by expansive soil. The elevation of the study area ranges from 2200 to 2320 a.m.s.l. Its slope is below 12%; which makes it suitable for LID application. It is a highly urbanized area covered with mostly commercial including residential buildings; which is an ideal environment for LID controls such as rain barrels.


Figure 3.1: Geographic Location of the study area

From figure 3.1, it can be seen that there is a water body adjacent to the study area. This water body is called Bulbula River which comes from Kebena River and makes its way to the Great Akaki. This river serves as an outfall for the stormwater generated from the catchment of the study area that moves through the drainage system installed in it.

With respect to administrative boundary, out of the ten sub cities in Addis Ababa, the study area is found in wereda 19 of Bole sub city; one of the highly urbanized and developed areas of the city. The following figure shows all the administrative boundaries of the city of Addis Ababa, and Bole sub-city where the study area is located was given the 8th number.

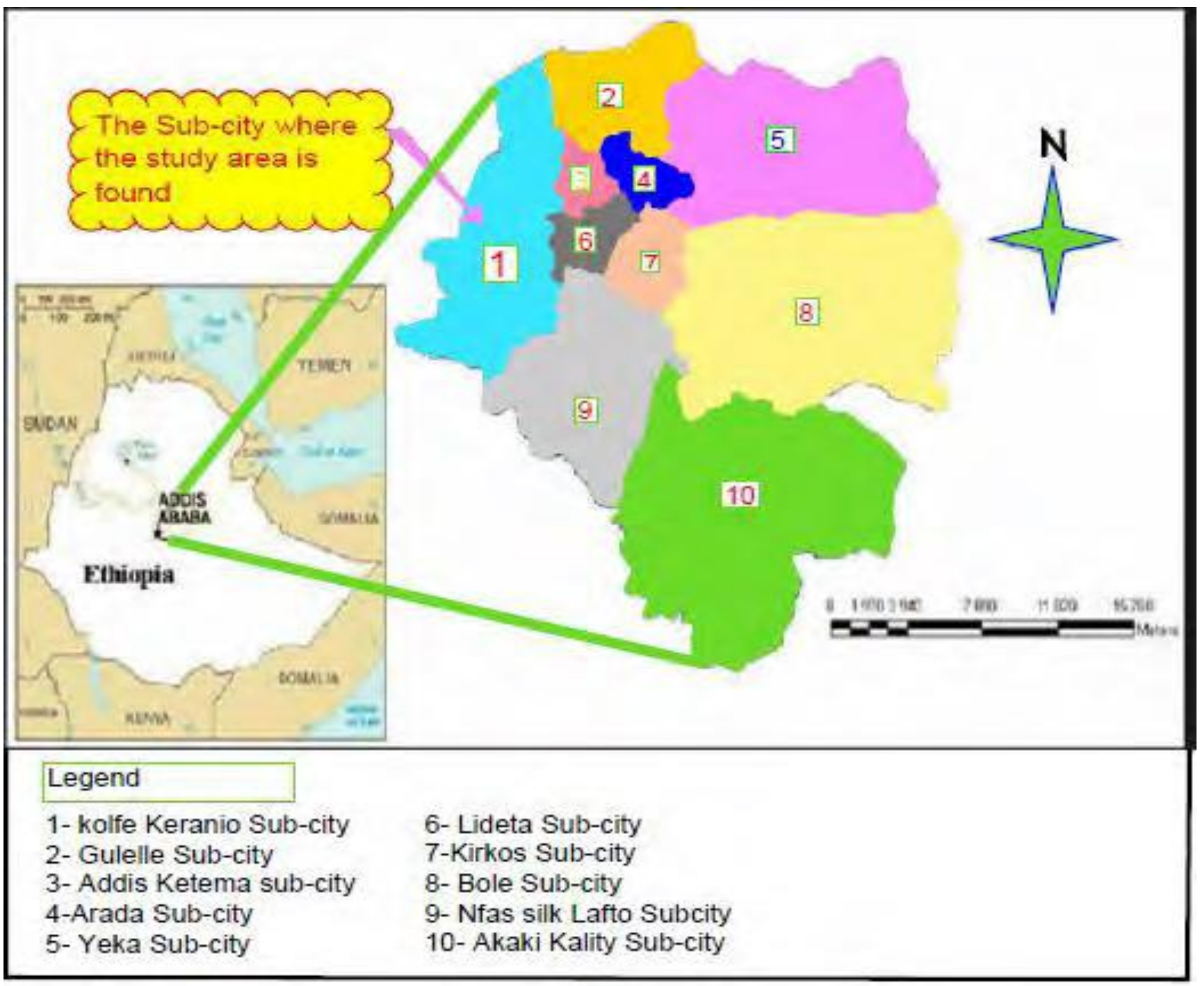


Figure 3.2: Sub cities of Addis Ababa (Source [23])

## 3.1.2 Climatic Condition

Addis Ababa is located on the tropical climatic zone with four climatic seasons namely: Kiremt or summer (June, July, and August), Bega or Winter (December. January, and February), Belg or Autumn (September, October, and November), and Tsedey or Spring (March, April, and May). The city is located around the equator having a high altitude in the subtropics, which is why variation of temperature from one month to another does not exceed 10℃.

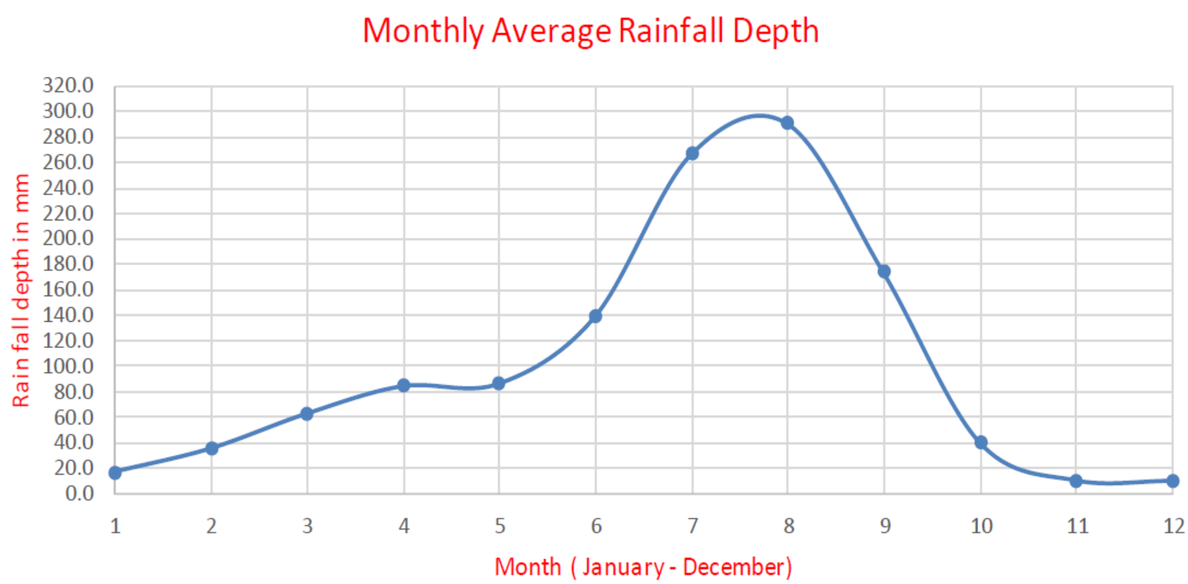


Figure 3.3: Mean monthly rainfall of Addis Ababa: observatory gauging station (1976 to 2015) (source: [23])

From the above figure, it can be seen that volume of rainfall increases from June to September. The forty years (1976-2015) data reveals that the rainfall reaches its peak in the month of August: with an average rainfall depth of about 292 mm.

## 3.1.3 Temperature

On the basis of the climatic zones that prevail to the city and data samples retrieved from the national meteorological agencies of the federal democratic republic of Ethiopia, the effective mean annual temperature of Addis Ababa city is in the order of $10^{o}c$ - $30^{o}c$. It is characterized by cold to moderately hot weather condition.

### 3.1.4 Vegetation

Since Ethiopia has a wide altitudinal range from 120m amsl at Dalol to 4,533m amsl at Ras Dashen, the country is endowed with diversity of vegetation. Starting from 1886, a number of eucalyptus plantations become dominant around Gullelle and Yeka sub-cities. Eucalyptus tree aggravate surface flow of water for flooding since it doesn`t allow undergrowth and insects to exist. Currently the city is endowed with 15 parks with a total area of 817,164 meter square, and 8148 hectare of urban forests.

### 3.1.5 Development and Socio-Economy

The area is observed to rapidly growing economically. The growing lifestyle of the people, availability of better infrastructure and its downtown location are some of the main reasons behind its development. This economic growth is the function of urbanization which alters the natural permeable surfaces by impermeable ones. This phenomenon minimizes the capacity of the land to infiltrate and store stormwater; and changes the natural hydrologic cycle by increasing the amount of runoff.

### 3.1.6 Land Use Land Cover

Addis Ababa has land use ranging from agricultural to high density commercial areas. Information about changes in land use land cover (LULC) provides valuable insights while planning future natural resource management strategies. Remotely sensed data, serve as an effective tool for deriving this kind of information. Land sat Thematic Mapper images of 1987 and 1999 were used to extract LULC change of the city of Addis Ababa and the surrounding area. Analysis of the multi-temporal Landsat images of the city has clearly revealed the loss of forest to urban and residential sprawl within the city limit and the surrounding area. The implication of LULC change testifies the increase in runoff and intensity of rainfall for which adequate drainage system is required to avoid flood damages.

Figure 3.4 shows Addis Ababa is in a high state of urbanization; an indication of the need for some sort of flood prevention mechanism. The urbanization difference is even conspicuous when compared with what the city used to look like years before.

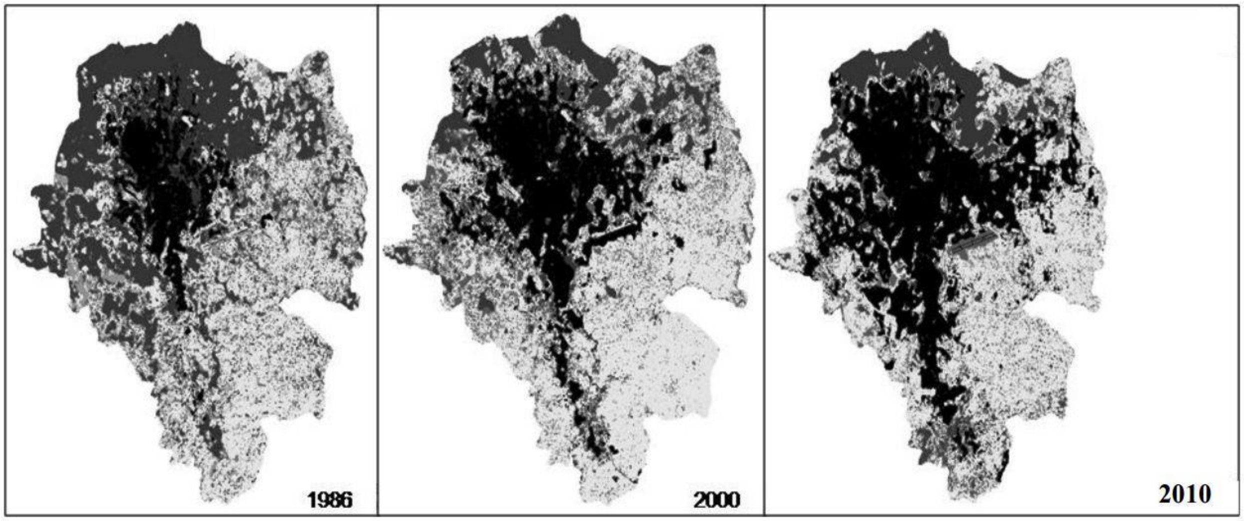


Figure 3.4: Land use map of Addis Ababa in different times (source: [37])

From figure 3.4, it can be seen that urbanization kept on growing from time to time. Another figure was also extracted from a research paper done in 2015 [37] that shows the then land use condition of the city and displayed below together with the study area of this research;

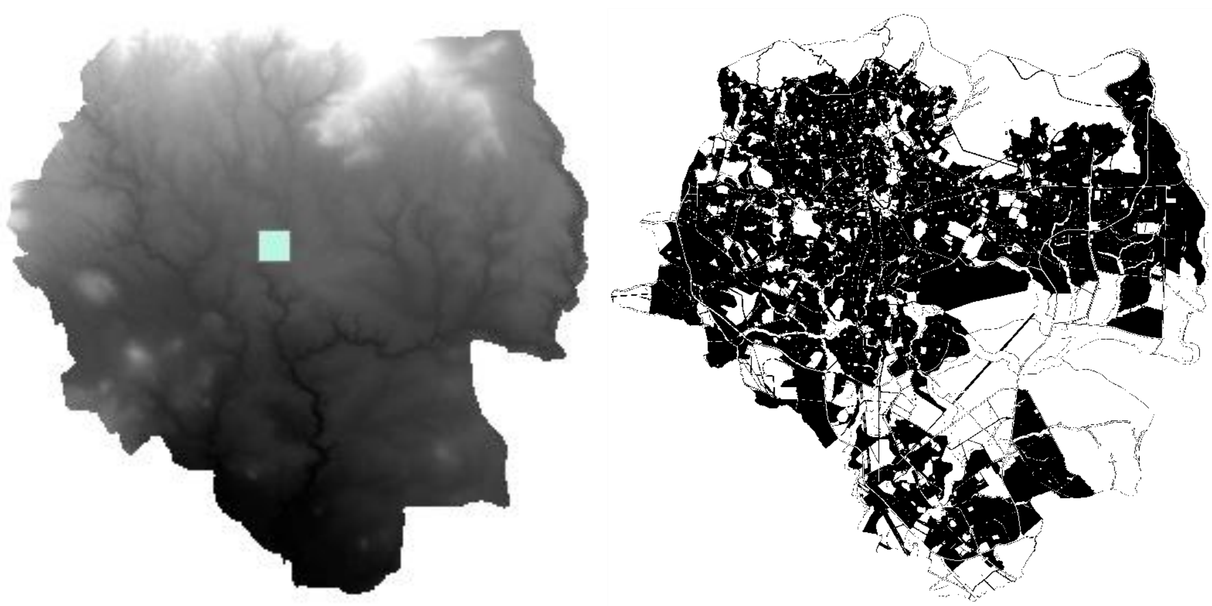

Figure 3.5: The study area and Addis Ababa Land Use in 2015

In figure 3.6, the study area inside Addis Ababa and the land use condition of Addis Ababa in 2015 are displayed from left to right. In the right figure, the dark areas represent highly urbanized places, whereas forest, green areas, and areas along a river are represented by lighter ones. By comparing the study area map with that of the land use map, it can be seen that the study area was under the category of highly urbanized areas.

Another research done in 2016, also testified the above reality [36]. Land use classification for years (1986, 2000, and 2015) was prepared by this research which can be seen in figures 3.6. The research confirmed about the decreasing amount of permeable surface in the mentioned area within this 30 years. It stated that within three decades, urban green spaces, forestland, grassland, and cultivated land minimized annually at rates of 5.9%, 3.3%, 5.4%, and 3.7% respectively. Whereas, built up areas and transport areas were maximized at 5.7%, and 1.3% respectively per year. The research also put forward the land use land cover classification of Bole area as shown in table 3.1.

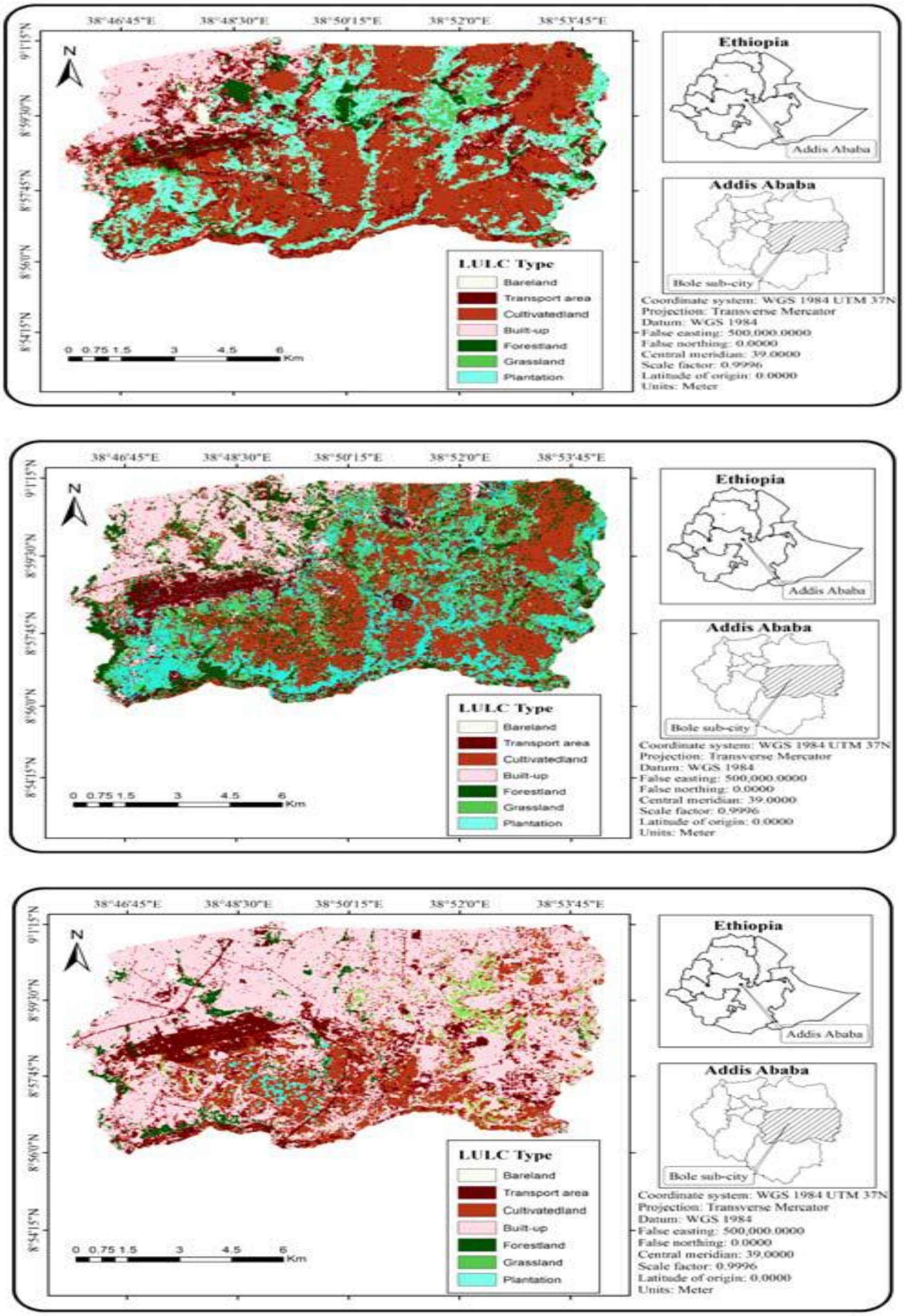


Figure 3.6: LULC classification of 1986, 2000, and 2015 respectively (source: [38])

Table 3.1: Land use change within three decades (source [38])

| LULC | 1986 | | 2000 | | 2015 | |
|---|---|---|---|---|---|---|
| | **Ha** | **%** | **Ha** | **%** | **Ha** | **%** |
| **GS** | 754.6 | 6.3 | 1780.3 | 14.8 | 135.3 | 1.1 |
| **TA** | 1346.6 | 11.2 | 1438.4 | 11.9 | 1979 | 16.4 |
| **FL** | 1077 | 8.9 | 1346.7 | 11.2 | 408.4 | 3.4 |
| **GL** | 1951 | 16.2 | 1819.7 | 15.1 | 414.2 | 3.4 |
| **BL** | 436.9 | 3.6 | 97.6 | 0.8 | 122.2 | 1 |
| **CL** | 5076.6 | 42.2 | 3627.1 | 30.1 | 1736.8 | 14.4 |
| **BA** | 1395.5 | 11.6 | 1950.9 | 16.2 | 7242.3 | 60.2 |
| **TOTAL** | **12038** | **100** | **12038** | **100** | **12038** | **100** |

Where: -

GS: Green space, TA: Transport Area, FL: Forestland, GL: Grassland

BL: Bare land, CL: Cultivated land, BA: Building area

From table 3.1, it can be seen that the coverage of all LULC decreased through time except transport and building areas. This proved the intense alteration of pervious surfaces into impervious ones in the name of urbanization and development. The Google earth map presented in figure 3.1 and a field survey of the study area also confirmed this. In this research, land use map was generated using image taken from Google earth, and classification of different land use was performed in ArcGIS.

### 3.1.7 Flood Problems

The area selected for the research is Ethio-China Friendship Street (from Gotera to Wollo sefer route) which is getting highly urbanized. Flooding is a major problem in the area. Inconveniency in business areas and traffic jamming are some of the problems caused due to this. There are especially certain places of the area where inundation of the road happens on summer. These are; from surroundings adjacent to the main road (from mina building down to the main road end up flooding the area), around INSA, and from Medco building to Gorgorios roundabout. Photographs of some of these areas were taken and are presented below.

Picture 3.1: A man trying to get into his car near Gorgorios Roundabout

Picture 3.2: The same person having a hard time crossing the road (flood coming from adjacent areas and inundating the main road)

Picture 3.3: Inundation of the study area after less intense storm took place.

### 3.1.8 Focus Area

This research was mainly focused on studying the area from around Wollo sefer roundabout to Gorgorios roundabout rather than the whole route as presented in figure 3.1. There were mainly two reasons to select this area. One was because flooding problem is apparent in this place as has been mentioned earlier on; which made it a good representative of the flooding problem in the whole route. The other was the limitation of time and resource. In this study intensive field assessments and data collection was carried out as will be discussed in the coming sections. These were the major reasons for this research to be constrained on the mentioned focus area.

## 3.2 Data Collection

In this study, Primary and secondary data were collected from site and from different sources respectively. These data were the main input parameters for the entire analyses. The primary data that were collected from field were the total number of manholes and their invert elevations, pipe dimensions, maximum water depth, surface water level, the study area's land use type, and photographs of flooding areas. These data were used as input parameters while carrying out model analysis and in evaluating and calibrating the model.

The pipe dimensions include diameter, shape, length, and material type of the conduits. Invert elevations (elevation of the bottom part of a pipe) and maximum water depth (elevation from invert to the ground surface) of the manholes, in the study area were also collected at the field. These parameters were used on the rainfall runoff analysis carried out using stormwater management model (SWMM).

In addition to these, depth of water level for each manhole (water surface at each node) was measured at the study area on August 13, 2021. This data was used to evaluate the model and calibrate it. The land use type of the study area was also verified on the field. This data was used to label the runoff coefficient and to verify land use classification. Some photographs of runoff inundating the study area were also taken on September 11, 2021 at site (pictures 3.1, 3.2, and 3.3) to make sure the existence of flooding problem on ground.

The secondary data gathered in this study were distance from the study area to different stations, thirty years of daily rainfall data from four stations (Bole, Observatory, Intoto, and Akaki), shape file of study area, Digital Elevation Model (DEM) of Addis Ababa, and the land use classification of the study area. The distance between the study area and different rainfall stations found in Addis Ababa were measured using Google map to gather rainfall data from the closer. Daily rainfall data was collected from the selected station out of which annual maximum rainfall data was extracted for further analysis. Shape file for the study area was also produced from Google earth and DEM data of Addis Ababa from Ministry of Water, Irrigation, and Energy. The land use classification of the study area was produced using image of the study area taken from Google earth and analyzing it in Arc GIS. The classified map was used to make comparison between Low Impact Development (LID) controls.

## 3.3 Materials

In this research 26 manholes were counted and a number of tools were utilized while collecting and analyzing the input data discussed in section 3.2. The pipe dimensions, maximum water depths, and the depths of surface water at each node were measured using conventional tape meters. Global Positioning System (GPS) was utilized to measure the invert elevations of the manholes. The distance between the study area and the area where different stations found in Addis Ababa was measured by Google map. The shape file of the study area was obtained using Google earth. Google earth was also used to obtain the image of the study area for the purpose of Land use classification. To present visual subcatchment land use, overlaying was performed on Google earth.

After collecting these data, they were analyzed using different tools. EXCEL 2010 was used in the process of testing the quality of the rainfall data and creating intensity-duration-frequency relationship out of it, and making calibration analysis. EasyFit 5.6 was adopted in selecting the right probability distribution method. A DEM of the study area was clipped from the DEM of Addis Ababa using Geographic Coordinate System (GIS). With GIS delineation of catchment to produce subcatchments of the study area and their respective areal coverage, average slope, and flow length was performed. GIS was also used to classify the image of the study area from Google earth and to obtain the areas of each of the land use classes. Stormwater management model (SWMM) was adopted as the major tool to analyze rainfall-runoff relations and to make comparative assessment between different LID controls.

## 3.4 Procedures

The first step taken in this study was determining the closer station for the study area to collect daily rainfall data from. After the closer station was known to be Bole station as can be seen in table 3.2., thirty years of daily rainfall data was gathered from there, and missing data was filled using interpolation technique, and annual maximum values of the data was extracted as presented in table 3.3. The quality of the data was then checked using outlier test.

Table 3.2: Distance between study area and different stations

| From | To station | Distance (km) |
|---|---|---|
| Study area | Intoto | 9.13 |
| Study area | **Bole Airport** | **1.57** |
| Study area | Ayertena | 8.66 |
| Study area | Observatory | 4.37 |
| Study area | Kality | 10.77 |
| Study area | Akaki | 12.64 |
| Study area | Kotebe | 8.02 |

The next thing was developing IDF relationship and curve based on annual maximum of the collected rainfall data shown in table 3.3, a set of return periods (2, 5, 10, 25, 50, and 100 years), and a goodness of fit analysis. The goodness of fit analysis was carried out using EasyFit 5.6 with the target of choosing the probability distribution that better fits the daily maximum rainfall data. The choice was made between Log Pearson Type III and Extreme value type I (Gumbel) as suggested by Addis Ababa City Road Authority (AACRA) [39].

After this, collecting elevation data from Google earth and ArcGIS followed. Shape file of the study area was first obtained from Google earth, and DEM data of Addis Ababa from Ministry of Water, Irrigation, and Energy. And then clipping study area, catchment delineation, stream network generation, and area, average slope, and flow length calculations was analyzed using ArcGIS

Table 3.3: Annual maximum of Bole station

| Year | Value (mm) | Year | Value (mm) | Year | Value (mm) |
|---|---|---|---|---|---|
| 1991 | 59.6 | 2001 | 32.4 | 2011 | 36.9 |
| 1992 | 44.3 | 2002 | 28.6 | 2012 | 64.7 |
| 1993 | 40.6 | 2003 | 34.6 | 2013 | 42.6 |
| 1994 | 38.2 | 2004 | 29 | 2014 | 27.2 |
| 1995 | 64.7 | 2005 | 44.5 | 2015 | 60.5 |
| 1996 | 37.5 | 2006 | 61.7 | 2016 | 52.3 |
| 1997 | 37.3 | 2007 | 71.2 | 2017 | 53.4 |
| 1998 | 60.1 | 2008 | 61.2 | 2018 | 54.4 |
| 1999 | 37.8 | 2009 | 51.2 | 2019 | 46.5 |
| 2000 | 47 | 2010 | 54.4 | 2020 | 62 |

Hydraulic data such as the number of manholes, invert elevations, maximum water depths, conduit dimension (shape, length, diameter, material) were collected and rainfall runoff analysis followed using stormwater management model (SWMM). On SWMM, the first thing to do was setting the default, map display, and dimensions options. The next step was drawing objects by adding sub-catchments, nodes, outfall, links, and rain gages successively. After editing some properties, filling time series data, and determining flow routing option to be Kinematic wave and infiltration method to be Modified Green Ampt followed. Finally, running the model was carried out successfully.

The next thing was collecting water level depth data from the field to evaluate the model result. Calibration analysis was then performed by adjusting the most sensitive parameters (% impervious area and slope). Based on that, running the software was once again performed and a detailed result about the drainage system emerged; which verified the existence of flooding nodes in the area under study.

Performing analysis on hypothetical feasible LID practices with the target of mitigating flood risk in the study area was the next work. A detailed analysis on four LID controls was carried out using extensive trials and errors. The first step was searching for the least area upon which it would be possible to install one of the four LID controls to avoid flooding. Based on the land use of the study area, comparison between the four LID controls were then made as to which was capable of meeting the target mentioned above. Finally, the study was concluded recommending the LID control that met the target.

## 3.5 Hydrological Processes

### 3.5.1 Meteorological Data

Rainfall is the most common factor used to predict design discharge. Thirty years of daily rainfall data was first collected from Addis Ababa Bole Station; where the study area was closer to. After this, analysis on the continuity of the data was performed gathering rainfall data from three other stations. Then, testing the data for outliers followed. Annual maximum rainfall data was later used to develop IDF curves. After making a comparison between the analyzed IDF with an IDF curve made by Ethiopian Road Authorities (ERA), the ERA's IDF curve was chosen to be conservative, and intensity of the 10 years return period and 30 minutes duration was extracted out of it for further analysis.

### 3.5.2 Data Continuity: Missing Rainfall Data Estimation

In order to perform frequency analysis, an adequate rainfall data record should be available. For part of a day, month, or year there may be missed data due to gauge problem, absence of observer, shielding trees, exposure to a newly built infrastructures, reading mistake, etc. These missing data can and should be filled using interpolation or simple proportion (normal ratio method).

Given the annual precipitation values P1, P2, P3,….Pm at neighboring M stations 1,2,3,……M respectively, it is required to find the missing annual precipitation Px at a station X not included in the above M stations. Further, the normal annual precipitation N1, N2, N3, ......., Ni,.....at each of the above (M+1) stations, including station are known. If the normal annual precipitation at various stations are within about 10% of the normal annual precipitation at station X, then a simple arithmetic average procedure is followed to estimate Px, but if the normal annual precipitation vary considerably, the normal ratio method which is computed using the following formula should be adopted;

$$Px = P1\ (Nx/N1) + P2\ (Nx/N2) + \ldots + Pn\ (Nx/Nn) \ \ldots\ldots\ldots\ldots 3.1$$

Provided that: N1, N2, or N3 differ by more than 10% of Nx

Where:

- N1, N2, ........., Nx : annual rainfall of known stations,
- Nx : annual rain fall of unknown station

### 3.5.3 Test for Outliers

An outlier is a measured value that significantly departs from a trend of the other data, and according to a statistical test, is unlikely to have been drawn from the same population as the remainder of the sample data. Different types of tests exist, e.g.: Log Pearson Type III, Dixon-Thompson, Rosner tests, etc. The following frequency equations are used to detect higher and lower outliers.

$$Y_H = \bar{Y} + KnSy \ \ldots\ldots\ldots\ldots 3.3$$

$$Y_L = \bar{Y} + KnSy \ \ldots\ldots\ldots\ldots 3.4$$

$$X_H = 10^{Y_H} \ \ldots\ldots\ldots\ldots\ldots 3.5$$

$$X_L = 10^{Y_L} \ \ldots\ldots\ldots\ldots\ldots 3.5$$

Where: -

- $Y_H$ and $Y_L$ are higher and lower outlier thresholds in log units respectively,
- $\bar{Y}$ and Sy are the mean and standard deviations of the natural logarithm of the annual rainfall peaks respectively,
- Kn is the critical deviate taken from a standard table given in table 3 of the appendix part.
- $X_H$ and $X_L$ are the higher and lower outlier thresholds respectively.

If the logarithms of the values in a sample are greater than $Y_H$, and lower than $Y_L$**,** they are considered as high and low outliers respectively. If historic information is available that indicates a high outlier is the maximum over an extended period of time, the outlier is treated as historic data and excluded from the analysis. If useful information is not available, then the outlier stays as part of the analysis. Low outliers are deleted from the systems after detected, and the frequency analysis continues with the rest of the data.

## 3.5.4 Intensity-Duration-Frequency (IDF) curve

A convenient form of rainfall information is the intensity-duration-frequency (IDF) relationship. The IDF relationships are used for determining the design rainfall or intensity, when designing drainage works for any engineering project, and allow the engineer to design safe and economical flood control measures. A typical set of IDF curves is given in the figure below where it can be seen that, for an event with a particular return period, rainfall intensity and duration are inversely related. As the duration increases, the intensity reduces.

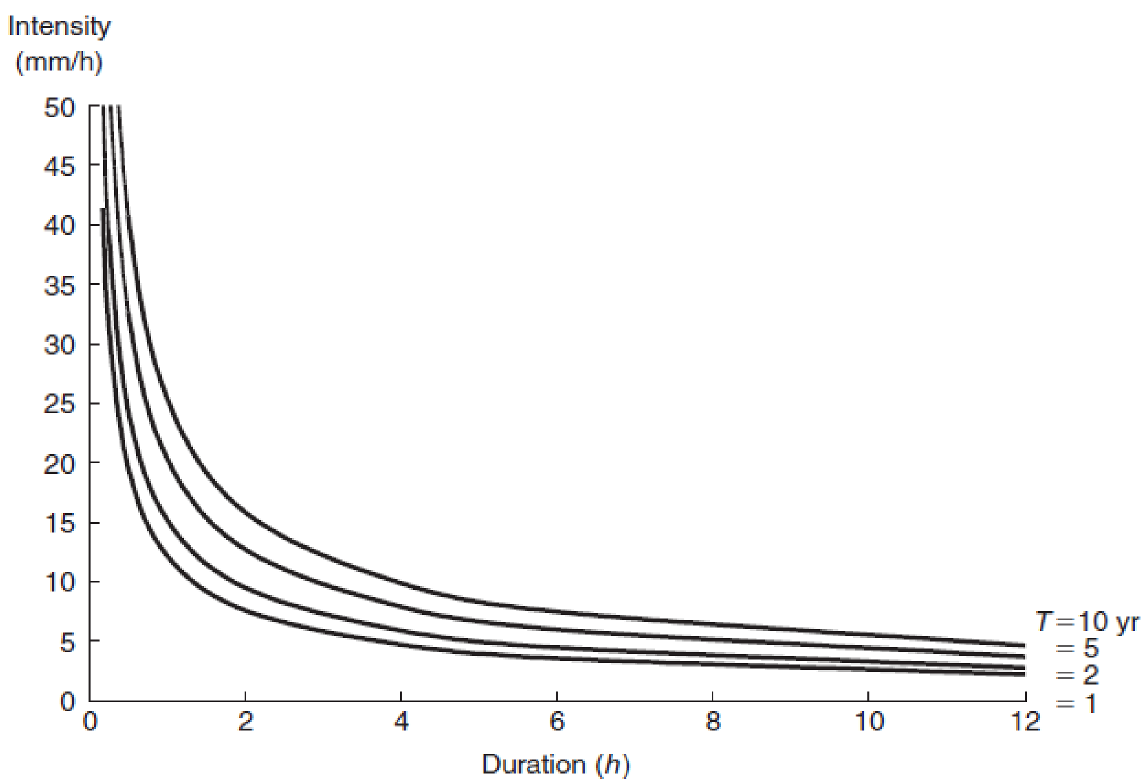


Figure 3.7: Typical IDF curve (source: [16])

Here, extreme rainfall depths related with exceedance probability should be determined. Ethiopian Road Authority (ERA) [40] has prepared IDF curves for different regions of the country as shown in figure 3.8;

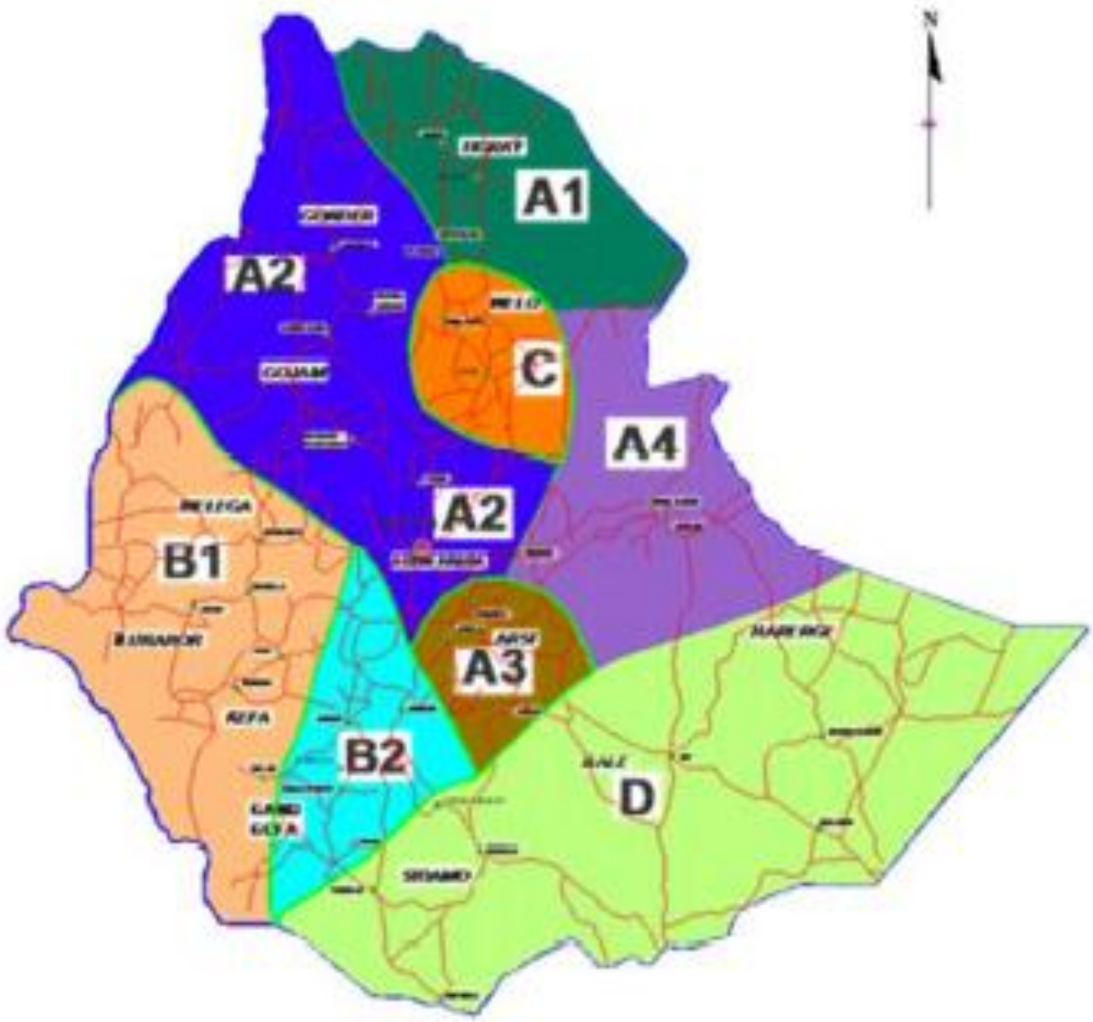


Figure 3.8: Rainfall Regions of Ethiopia (source: [40])

From the above figure, Addis Ababa can be seen located in the region A2. Therefore the area in this study falls in the same region having an IDF curve prepared by ERA and shown in the figure below;

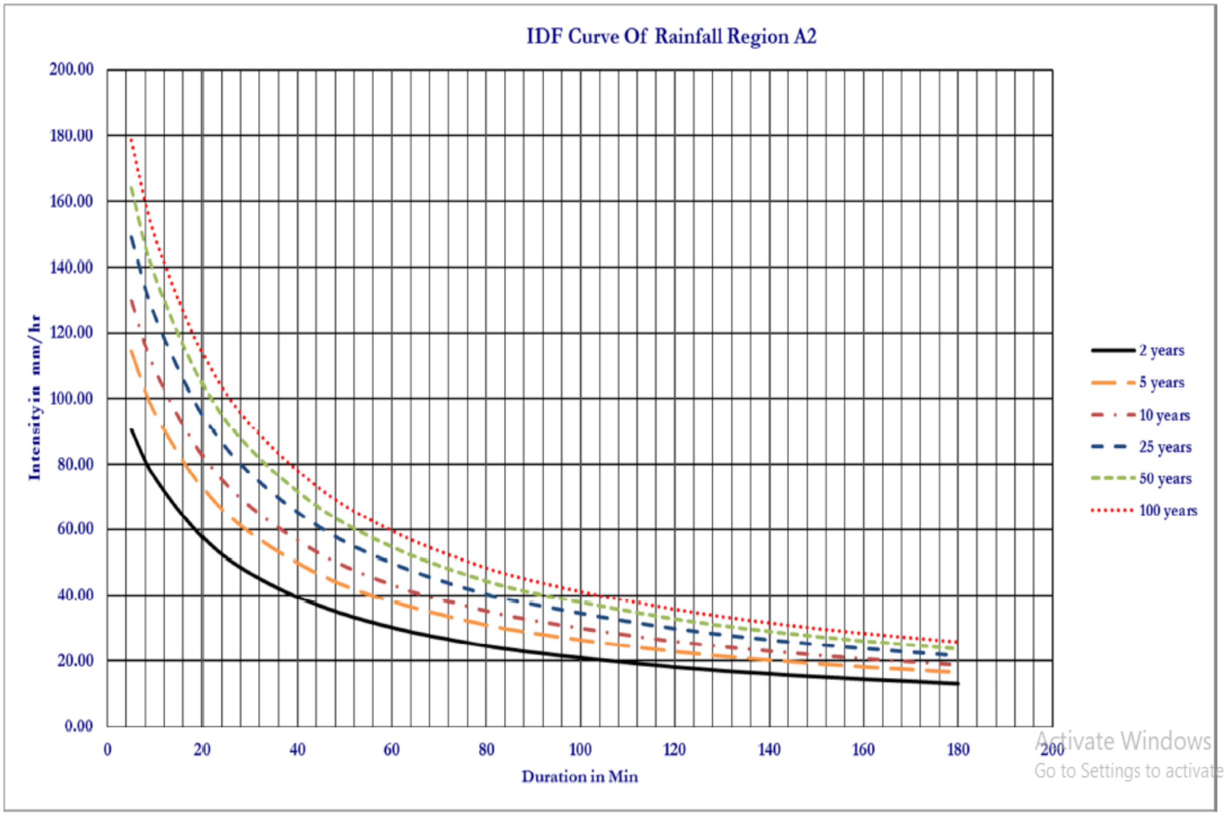


Figure 3.9: IDF curve of A2 (source [38])

In this study, comparison between the IDF curve generated from Bole station and that of the A2 IDF curve was made. To do this, first the intensity-duration-frequency (IDF) curve for the data from Bole station was prepared using rainfall ratio method. Rainfall ratio method was used to estimate the rainfall depth to be distributed on a given duration based on a 24 hour rainfall result. This method can be expressed using the following formula;

$$Rt/R24 = (t / 24) [(b + 24)n / (b + t)n] \ldots\ldots\ldots\ldots\ldots 3.7$$

Where: -

- RRt = rainfall ratio = Rt: R24,
- Rt = rainfall in given duration,
- R24 = rainfall in 24 hour,
- t = time in hour,
- n = 0.9 (0.78 ≤ n ≤ 1.09),
- b = 0.3 (based on studies of large number of gauges in east Africa).

The following steps were used to develop IDF curves on EXCEL;

i. Prepare the maximum daily rainfall data
ii. For each duration (5-min, 10-min, 15-min, 20-min, 30-min, 60-min, 90-min, 120-min), compute the rainfall ratio and the associated sample mean and sample standard deviations of the series of annual maxima, (x1, ……., xm) .

$$\bar{X} = \frac{1}{m}\sum_{i=0}^{m} Xi \ldots\ldots\ldots\ldots\ldots 3.8$$

$$S = \frac{1}{m-1}\sum_{i=0}^{m} (Xi - \bar{X})^2 \ldots\ldots\ldots\ldots\ldots 3.9$$

Where: -

- $\bar{X}$ is mean of rainfall values $x$,
- $S$ is standard deviation of $x$

iii. Compute the frequency factor (KT) using the selected Gumbel probability distribution (based on a goodness of fit analysis) for return periods (T=2, 5, 10, 25, 50, and 100 years) as the following

$$K_T = \frac{-\sqrt{6}}{2a}\left[0.5772 + \ln\left(\ln\left(\frac{T}{T-1}\right)\right)\right] \ldots\ldots\ldots\ldots\ldots 3.10$$

iv. Compute the Rainfall (RF) (XT) that is related with a certain return period (T), using;

$$X_T = \bar{X} + K_T\, S \ldots\ldots\ldots\ldots\ldots 3.11$$

v. Compute also the intensity by dividing the Rainfall result to the durations.
vi. Finally, plot the result

### 3.5.4.1 Selected Probability Distributions

**I. Gumbel (Extreme Value Type I): -** is a probability distribution function useful for hydrologic analysis, particularly rainfall analysis**.** It was selected after carrying out the goodness of fit test. By fitting a distribution to a set of data, a great deal of probabilistic information in the sample can be compactly summarized in the function and its associated parameters [37]. The frequency factor ($K_T$) is derived by substituting the frequency equation of 3.11.

$$K_T = -(6^{0.5}/\pi)\ [0.5772 + \ln(\ln(\frac{T}{T-1}))] \text{ ...............3.12}$$

And the return period (T) can be expressed in terms of frequency factor (KT) as;

$$T = \{1 - \exp\ [-\exp(-0.5772 - \pi K_T/\ 6^{0.5})]\}^{-1} \text{ ...............3.13}$$

After the IDF curve was created, the intensity of the 10 year return period was selected for further analysis.

**II. Log Pearson Type III: -** For the log-Pearson Type III distribution, the first step is to compute the logarithms of the hydrologic data, y = log x. Logarithms to base 10 are usually used. The mean y standard deviation (Sy), and coefficient of skewness (Gs) are calculated for the logarithms of the data. The frequency factor depends on the return period (T) and Gs. When Gs = 0, the frequency factor is equal to the standard normal variate (z). When Gs is different from 0, Kt is approximated;

$$K\ (T, Gs) = z + (z^2 - 1)k + \frac{1}{3}(z^3 - 6z)k^2 - (z^2 - 1)k^3 + zk^4 + \frac{1}{3}k^5 \text{ ...............3.14}$$

Values of the frequency factor for the Pearson Type III (and log- Pearson Type III) distribution for various values of the return period and coefficient of skewness can also be found from any standard table. Frequency factor equation for Log Pearson Type III probability can be written in discharge form as follows;

$$\text{Log } Q_T = \bar{Y} + K\ (T, Gs) * Sy \text{ ...............3.15}$$

Where;

- $Q_T$ is the discharge for T-year return period.

### 3.5.5 Testing Goodness of Fit (GOF)

GOF measures the compatibility of a random sample with a theoretical probability distribution function. These tests show how well the selected distribution fits to data. In this study a probability distribution was selected after carrying out a goodness of fit analysis using EasyFit 5.6 according to the tests described below.

#### 3.5.5.1 Chi-Square Test

The Chi-Squared test is used to determine if a sample comes from a population with a specific distribution. This test is applied to binned data, so the value of the test statistic depends on how the data is binned. Although there is no optimal choice for the number of bins (k), there are several formulas which can be used to calculate this number based on the sample size (N). For example, Easy Fit employs the following empirical formula:

$$k = 1 + \mathrm{Log}_2 N \ \ldots\ldots\ldots\ldots\ldots 3.16$$

The data can be grouped into intervals of equal probability or equal width. The first approach is generally more acceptable since it handles peaked data much better. The Chi-Squared statistic is defined as,

$$X^2 = \sum_{i=0}^{k} \frac{(Oi-Ei)^2}{Ei} \ldots\ldots\ldots\ldots\ldots 3.17$$

Where F is the CDF of the probability distribution being tested, and x1, x2 are the limits for bin i. When comparing different distribution, lower statistics means better fit.  Easy Fit 5.6 Professional software will be applied for testing goodness of the recommended Log Pearson-III and Gumbel Methods.

#### 3.5.5.2 Kolmogorov Smirnov

This test is used to decide if a sample comes from a hypothesized continuous distribution. It is based on the empirical cumulative distribution function (ECDF). Assume that we have a random sample $X1$, ………., $Xn$ from some continuous distribution with CDF F(x). The empirical CDF is denoted by;

$$Fn\ (X) = \frac{1}{n}\ [\text{Number of observations} \leq X] \ \ldots\ldots\ldots\ldots\ldots 3.18$$

The Kolmogorov-Smirnov statistic (D) is based on the largest vertical difference between F(x) and ($x$).

#### 3.5.5.3 Anderson Darling Test

The Anderson-Darling procedure is a general test to compare the fit of an observed cumulative distribution function to an expected cumulative distribution function. This test gives more weight to the tails than the Kolmogorov-Smirnov test.

The Anderson-Darling statistic ($A2$) is defined as;

$$A^2 = -n - \frac{1}{n} \sum_{i=1}^{n} (2i-1) * [\ln F(Xi) + \ln(1 - F(Xn\text{-}1+1))] \quad \ldots\ldots\ldots\ldots\ldots 3.19$$

The hypothesis regarding the distributional form is rejected at the chosen significance level (alpha) if the test statistic, $A^2$ is greater than the critical value obtained from a table. When comparing different distribution, lower statistics means better fit.

## 3.6 Digital Elevation Model (DEM)

A DEM is a grid of square cell; and each cell value represents the elevation of the land surface. DEM is important to know the existing ground surface area flow of water, direction of flow and to identifying and selecting catchment locations. There are different techniques to get DEM data for study locations. There are open and commercial sites where global digital elevation maps/ DEM data can be acquired from satellite imagery.

For this research, first the DEM of Addis Ababa was obtained from ministry of water, irrigation, and energy; and then shape file of the study area was imported from Google earth and clipped using ArcGIS. After this, hydrological processes of fill, flow direction, and flow accumulation were carried out. Subcatchment delineation using pour points was then applied. Finally, the areas, the flow lengths, and the slopes of each subcatchment were generated, and calculating the widths of each subcatchment by dividing the areas by the flow lengths was performed.

## 3.7 Runoff Computation using SWMM

SWMM adopts the three well known principles: conservation of mass, conservation of energy, and momentum. The runoff component of SWMM operates on a collection of sub catchment areas that receive precipitation and generate runoff using water balance mechanism and route it using Manning's equation for partially full pipes [36,38]. Manning's equation is given in SI units as;

$$Q = \frac{1}{n} AR^{2/3} So^{0.5} \ldots\ldots\ldots\ldots\ldots 3.20$$

Where: -

- Q is flow rate/discharge/runoff in $m^3/s$
- V is the velocity of flow in m/s
- A is drainage area in $m^2$
- R is hydraulic radius in m
- n is manning's roughness coefficient
- So is channel slope in m/m

In the above equation, a direct relationship between Q and A, Q and R, and Q and So can be seen; which indicate an increase in one or more of the three parameters (A, R, So) would result in an increase in the flow rate and vice versa. For fully pressurized pipes either Darcy Weisbach or Hazen William equation is used as given below respectively;

$$Q = \sqrt{8g/f}\, AR^{0.5} So^{0.5} \ \ldots\ldots\ldots\ldots\ldots 3.21$$

$$Q = 1.318\, CAR^{0.63} So^{0.54} \ \ldots\ldots\ldots\ldots\ldots 3.22$$

Where: -

- g is gravitational acceleration in $m^2/s$,
- f and C are factors

In this paper, kinematic wave method of flow routing through the drainage system was adopted ruling out the possibility of pressurized flow. Also the Modified Green Ampt method was used as the infiltration method. Also the runoff coefficient was filled in accordance with the land use of the area under study. Since the study area is a commercial type, runoff coefficient (C) value between 0.7 and 0.95 was used according to the recommendation given by

Addis Ababa City Road Authority (AACRA) presented in table 4 of the appendix part.

To model the study area on SWMM, setting the defaults, drawing a network representation of the physical components of the study area, editing the properties of the objects that make up the system, selecting a set of analysis options, running the analysis, and viewing the result was carried out sequentially.

## 3.8 Model Calibration

To check which parameters affect the rainfall-runoff simulation the most, sensitivity analysis done by literatures was taken. Sensitivity analysis is a technique of identifying the responsiveness different parameters involving in the simulation of the hydrological process. The most sensitive parameters that influence the catchment represented by SWMM were found to be percent of impervious area and average slope of each subcatchment [41]. After that, the model result was checked against an observed depth data. And then the model was calibrated by altering the previous values of the sensitive parameters using actual measured data according to the following measurement technique

**R-squared ($R^2$): -** is a statistical measure that represents the proportion of the variance for a dependent variable that's explained by an independent variable or variables in a regression model. R-squared explains to what extent the variance of one variable explains the variance of the second variable. So, if the $R^2$ of a model is 0.50, then approximately half of the observed variation can be explained by the model's inputs. The following equation is used to calculate $R^2$

$$R^2 = \left( \frac{\left[\sum_{t=1}^{n} (\text{qtobs} - \text{qtobs.ave})(\text{qtsim} - \text{qtsim.ave})^2\right]}{(\sum_{t=1}^{n} (\text{qtobs}-\text{qtobs.ave})^{0.5}) * (\sum_{t=1}^{n} (\text{qtsim}-\text{qsim.ave})^{0.5})} \right)^2 \quad \ldots\ldots\ldots\ldots\ldots 3.24$$

Where: -

- qtobs is the calculated data, and qtobsave is the average data
- qtsim simulated data, and qtsimave is the average data at time t
- n is total number of time steps

If the result becomes between 0.85 and 1, then it can be concluded that the model is well in explaining the actual scenario.

**Root Mean Square Error (RMSE)**: - is the standard deviation of the residuals (predicted errors). RMSE tells how much the data is concentrated around the best fit line. The RMSE can be explained using the equation shown below.

$$RMSE = \left( \frac{\sum_{t=1}^{N} (\text{Predicted(i)} - \text{Actual(i)})^2}{N} \right)^{0.5} \quad ..............3.25$$

Where: -

- Predicted = simulated or modeled values
- Actual = observed or measured values
- N = Number of sample

To conclude that the model was well concentrated around the best fit line, the RMSE should not be more than 5.

## 3.9 Application of Hypothetical LID controls

In performing hypothetical analyses, the effect of clogging which can progressively reduce the permeability and infiltration rate was assumed to be negligible while making analyses on the effect of Bio-retention cells and Permeable pavements. This was done due to the fact that, clogging is a concern only for infiltration trenches, which are not part of the research. The other parameters SWMM requests were filled according to the recommendations given by the software itself.

Hypothetical LID controls were applied with the objective of avoiding flood risk after being installed on the smallest area possible. To obtain this, extensive trials and errors had to be performed to find the minimum area upon which one of the four LID controls can hypothetically be applied to avoid the risk of flooding in the area.

While attempting to find this least area, the capacities of each LID controls were first tried after being applied on 100% of the areas of the sub-catchments. This was done for each of the four LID controls. The trial continued decreasing the number of sub-catchments till the least number of sub-catchments upon which each LID controls could be applied to avoid flooding of the area was obtained.

After getting the least number of sub-catchment, the minimum portion area out of which the above objective could be achieved was also found using trial and error technique. This area was concluded to be the most feasible area where one of the four LID controls could hypothetically be applied upon to achieve the objective.

## 3.10 Land use classification of desired area

The LID controls were evaluated according to the existing land use classification of the area under study. Land use classification was performed using Google earth and ArcMap. The image of the study area with some place marks on it and points of the place marks was first taken from Google earth. The image and the place marks were imported separately into ArcGIS. Fitting the place marks attached on the image and the points of the place marks was done and the image was rectified and georeferenced.

After this, the georeferenced image was classified into four classes for a desired area located in it. Areas for each of the four classes were then obtained. The areas were used to make a decision as to which LID control was capable of being realized on the least area to meet the target of avoiding flood. The LID control that met the objective discussed above after being applied on the least area was concluded to be the feasible LID control.

## 3.11 Rationale for using SWMM

Out of the various modeling tools available SWMM was selected by considering criterion such as availability, accessibility, accuracy, and regional limits. When looking at the accuracy levels of the different models reviewed, SWMM and WinSLAMM provide the highest level of accuracy as detailed design tools. A number of literature studies on SWMM modeling indicate that SWMM can produce reasonably accurate results when the model outcomes are calibrated and validated [14,28,29,32].

Among the five models SWMM is one of the most sophisticated models which can be used in any geographic region if the particular data are provided. Unlike the other tools, SWMM is freely available on the internet which can easily be downloaded and used. Besides, SWMM analyzes both hydraulic and hydrologic simulations which is simple to analyze and easy to understand. And also, SWMM is dynamic rainfall runoff model used primarily for urban areas.

LID is a decentralized small-scale measure module which is environmentally friendly, easy to construct, small in size, economical, and ornamental as landscape. In SWMM, several LID modules are created, and then added to the corresponding subarea by changing parameters according to the actual situation. Based on the principle of water balance, the SWMM calculates real-time inflow and outflow of the subarea [33,34]. Currently SWMM is the best model used in many countries [36]. These features make SWMM suitable for this research.

# CHAPTER FOUR

# 4. RESULT and DISCUSSION

## 4.1 Results of Hydrological Processes

### 4.1.1 Result of Outlier test

The data was tested against any outliers as presented in the following tables;

Table 4.1: The Bole annual maximum data with its log values

| Year | X | Y = LOG(X) | Year | X | Y = LOG(X) |
|---|---|---|---|---|---|
| 1991 | 59.6 | 1.775 | 2006 | 61.7 | 1.79 |
| 1992 | 44.3 | 1.646 | 2007 | 71.2 | 1.852 |
| 1993 | 40.6 | 1.609 | 2008 | 61.2 | 1.787 |
| 1994 | 38.2 | 1.582 | 2009 | 51.2 | 1.709 |
| 1995 | 64.7 | 1.811 | 2010 | 54.4 | 1.736 |
| 1996 | 37.5 | 1.574 | 2011 | 36.9 | 1.567 |
| 1997 | 37.3 | 1.572 | 2012 | 64.7 | 1.811 |
| 1998 | 60.1 | 1.779 | 2013 | 42.6 | 1.629 |
| 1999 | 37.8 | 1.577 | 2014 | 27.2 | 1.435 |
| 2000 | 47 | 1.672 | 2015 | 60.5 | 1.782 |
| 2001 | 32.4 | 1.511 | 2016 | 52.3 | 1.719 |
| 2002 | 28.6 | 1.456 | 2017 | 53.4 | 1.728 |
| 2003 | 34.6 | 1.539 | 2018 | 54.4 | 1.736 |
| 2004 | 29 | 1.462 | 2019 | 46.5 | 1.667 |
| 2005 | 44.5 | 1.648 | 2020 | 62 | 1.792 |

Where: X is annual maximum rainfall, both X and Yare in mm

Table 4.2: Outlier test summary

| | | |
|---|---|---|
| **Mean** | 1.665 | |
| **Standard Deviation** | 0.121 | |
| **Kn** | 2.563 | |
| **$Y_H$** | 1.974 | No High Outlier |
| **$Y_L$** | 1.356 | No Low Outlier |
| **$X_H$** | 94.3 | |
| **$X_L$** | 22.7 | |

From table 4.2, it can be seen that there was no value (Y) that exceeded the higher outlier ($Y_H$ = 1.974), and no value was below the lower outlier ($Y_L$ = 1.356). Also from higher and lower outlier thresholds, no value was above $X_H$ = 94.3, and no value was below $X_L$ = 22.57. Therefore it was concluded that there were no outliers.

### 4.1.2 IDF Curve Result

#### 4.1.2.1 Result for Goodness of fit analysis

Table 4.3: Goodness of Fit analysis summary

| **Probability Distributions** | **RANK** | | |
|---|---|---|---|
| | **Kolmogorov Smirnov** | **Anderson Darling** | **Chi-Squared** |
| Gumbel | 14 | 4 | 4 |
| Log Pearson III | 12 | 6 | 30 |

From the above comparison between the two probability distributions, Anderson Darling and Chi-squared tests confirmed that Gumbel fitted the data better. On the other hand, Log Pearson type III was better according to Kolmogorov Smirnov. Overall, Gumbel was chosen as a better probability distribution method for further analysis.

#### 4.1.2.2 Frequency factor results

For different return periods (T), using Gumbel probability distribution (based on the result presented in table 4.3), the frequency factor results were generated and are presented in table 4.4:

Table 4.4:- Frequency factor (KT) for different return periods (T)

| **T** | **KT** |
|---|---|
| 2 | 0.16 |
| 5 | 0.72 |
| 10 | 1.31 |
| 25 | 2.04 |
| 50 | 2.59 |
| 100 | 3.14 |

### 4.1.2.3 Rainfall results based on Normal Ratio (RRt)

Table 4.5: Mean and standard deviation of annual maximum rainfall data based on RRt

| **Time (min)** | **5.00** | **10.00** | **15.00** | **20.00** | **30.00** | **60.00** | **90.00** | **120.00** |
|---|---|---|---|---|---|---|---|---|
| **Time (hr)** | **0.08** | **0.17** | **0.25** | **0.33** | **0.50** | **1.00** | **1.50** | **2.00** |
| **t/24** | **0.00** | **0.01** | **0.01** | **0.01** | **0.02** | **0.04** | **0.06** | **0.08** |
| **(b+24)^n** | **17.66** | **17.66** | **17.66** | **17.66** | **17.66** | **17.66** | **17.66** | **17.66** |
| **(b+t)^n** | **0.42** | **0.50** | **0.58** | **0.66** | **0.82** | **1.27** | **1.70** | **2.12** |
| **RRt** | **0.15** | **0.24** | **0.32** | **0.37** | **0.45** | **0.58** | **0.65** | **0.70** |
| **1991** | 8.66 | 14.52 | 18.78 | 22.05 | 26.81 | 34.64 | 38.76 | 41.45 |
| **1992** | 6.44 | 10.79 | 13.96 | 16.39 | 19.93 | 25.74 | 28.81 | 30.81 |
| **1993** | 5.90 | 9.89 | 12.79 | 15.02 | 18.26 | 23.59 | 26.41 | 28.24 |
| **1994** | 5.55 | 9.30 | 12.04 | 14.14 | 17.18 | 22.20 | 24.85 | 26.57 |
| **1995** | 9.40 | 15.76 | 20.39 | 23.94 | 29.10 | 37.60 | 42.08 | 45.00 |
| **1996** | 5.45 | 9.13 | 11.82 | 13.88 | 16.87 | 21.79 | 24.39 | 26.08 |
| **1997** | 5.42 | 9.08 | 11.75 | 13.80 | 16.78 | 21.68 | 24.26 | 25.94 |
| **1998** | 8.74 | 14.64 | 18.94 | 22.24 | 27.03 | 34.93 | 39.09 | 41.80 |
| **1999** | 5.49 | 9.21 | 11.91 | 13.99 | 17.00 | 21.97 | 24.59 | 26.29 |
| **2000** | 6.83 | 11.45 | 14.81 | 17.39 | 21.14 | 27.31 | 30.57 | 32.69 |
| **2001** | 4.71 | 7.89 | 10.21 | 11.99 | 14.57 | 18.83 | 21.07 | 22.53 |
| **2002** | 4.16 | 6.97 | 9.01 | 10.58 | 12.86 | 16.62 | 18.60 | 19.89 |
| **2003** | 5.03 | 8.43 | 10.90 | 12.80 | 15.56 | 20.11 | 22.50 | 24.06 |
| **2004** | 4.22 | 7.06 | 9.14 | 10.73 | 13.04 | 16.85 | 18.86 | 20.17 |
| **2005** | 6.47 | 10.84 | 14.02 | 16.47 | 20.02 | 25.86 | 28.94 | 30.95 |
| **2006** | 8.97 | 15.03 | 19.44 | 22.83 | 27.75 | 35.86 | 40.13 | 42.91 |
| **2007** | 10.36 | 17.36 | 22.47 | 26.38 | 32.07 | 41.44 | 46.37 | 49.59 |
| **2008** | 8.90 | 14.90 | 19.28 | 22.65 | 27.53 | 35.57 | 39.80 | 42.57 |
| **2009** | 4.70 | 7.87 | 10.18 | 11.95 | 14.53 | 18.77 | 21.01 | 22.47 |
| **2010** | 7.91 | 13.25 | 17.14 | 20.13 | 24.47 | 31.61 | 35.38 | 37.84 |
| **2011** | 5.36 | 8.99 | 11.63 | 13.65 | 16.60 | 21.44 | 24.00 | 25.66 |
| **2012** | 9.40 | 15.76 | 20.39 | 23.94 | 29.10 | 37.60 | 42.08 | 45.00 |
| **2013** | 6.19 | 10.37 | 13.42 | 15.76 | 19.16 | 24.76 | 27.71 | 29.63 |
| **2014** | 3.95 | 6.62 | 8.57 | 10.06 | 12.23 | 15.81 | 17.69 | 18.92 |
| **2015** | 8.79 | 14.73 | 19.06 | 22.39 | 27.21 | 35.16 | 39.35 | 42.08 |
| **2016** | 4.70 | 7.87 | 10.18 | 11.95 | 14.53 | 18.77 | 21.01 | 22.47 |
| **2017** | 7.76 | 13.01 | 16.83 | 19.76 | 24.02 | 31.03 | 34.73 | 37.14 |
| **2018** | 7.91 | 13.25 | 17.14 | 20.13 | 24.47 | 31.61 | 35.38 | 37.84 |
| **2019** | 6.76 | 11.32 | 14.65 | 17.21 | 20.92 | 27.02 | 30.24 | 32.34 |
| **2020** | 9.01 | 15.10 | 19.54 | 22.94 | 27.89 | 36.03 | 40.32 | 43.12 |
| **MEAN** | **6.77** | **11.35** | **14.68** | **17.24** | **20.95** | **27.07** | **30.30** | **32.40** |
| **SDEVA** | **1.89** | **3.16** | **4.09** | **4.81** | **5.84** | **7.55** | **8.45** | **9.04** |

Where: SDEVA denotes standard deviation

#### 4.1.2.4. IDF curve result and analysis

After carrying out different analysis steps as was discussed in the previous sections, the following intensity-duration-frequency relationship (IDF) was generated;

Table 4.6:- Intensity duration frequency relationship

| D (hr) | Mean | SDeva | T, KT 2, 0.16 | | T, KT 5, 0.72 | | T, KT 10, 1.31 | |
|---|---|---|---|---|---|---|---|---|
| | | | RF | I (RF/D) | RF | I (RF/D) | RF | I (RF/D) |
| 0.08 | 6.8 | 1.9 | 7.1 | 84.9 | 8.1 | 97.7 | 9.3 | 111.1 |
| 0.17 | 11.4 | 3.2 | 11.9 | 71.1 | 13.6 | 81.8 | 15.5 | 92.9 |
| 0.25 | 14.7 | 4.1 | 15.3 | 61.3 | 17.6 | 70.5 | 20.0 | 80.2 |
| 0.33 | 17.2 | 4.8 | 18.0 | 54.0 | 20.7 | 62.1 | 23.5 | 70.6 |
| 0.50 | 21.0 | 5.8 | 21.9 | 43.8 | 25.2 | 50.3 | 28.6 | 57.2 |
| 1.00 | 27.1 | 7.6 | 28.3 | 28.3 | 32.5 | 32.5 | 37.0 | 37.0 |
| 1.50 | 30.3 | 8.5 | 31.7 | 21.1 | 36.4 | 24.3 | 41.4 | 27.6 |
| 2.17 | 32.4 | 9.0 | 33.8 | 16.9 | 38.9 | 19.5 | 44.2 | 22.1 |

| D (hr) | Mean | SDeva | T, KT 25, 2 | | T, KT 50, 2.6 | | T, KT 100, 3.14 | |
|---|---|---|---|---|---|---|---|---|
| | | | RF | I (RF/D) | RF | I (RF/D) | RF | I (RF/D) |
| 0.08 | 6.8 | 1.9 | 10.6 | 126.8 | 11.7 | 140.5 | 12.7 | 152.8 |
| 0.17 | 11.4 | 3.2 | 17.7 | 106.0 | 19.6 | 117.4 | 21.3 | 127.6 |
| 0.25 | 14.7 | 4.1 | 22.9 | 91.4 | 25.3 | 101.3 | 27.5 | 110.1 |
| 0.33 | 17.2 | 4.8 | 26.9 | 80.6 | 29.7 | 89.2 | 32.3 | 97.0 |
| 0.50 | 21.0 | 5.8 | 32.6 | 65.3 | 36.1 | 72.3 | 39.3 | 78.6 |
| 1.00 | 27.1 | 7.6 | 42.2 | 42.2 | 46.7 | 46.7 | 50.8 | 50.8 |
| 1.50 | 30.3 | 8.5 | 47.2 | 31.5 | 52.3 | 34.8 | 56.8 | 37.9 |
| 2.17 | 32.4 | 9.0 | 50.5 | 25.2 | 55.9 | 28.0 | 60.8 | 30.4 |

Based on the above IDF result, Intensity-duration-frequency curve (IDF curve) was plotted using EXCEL as shown in the figure below;

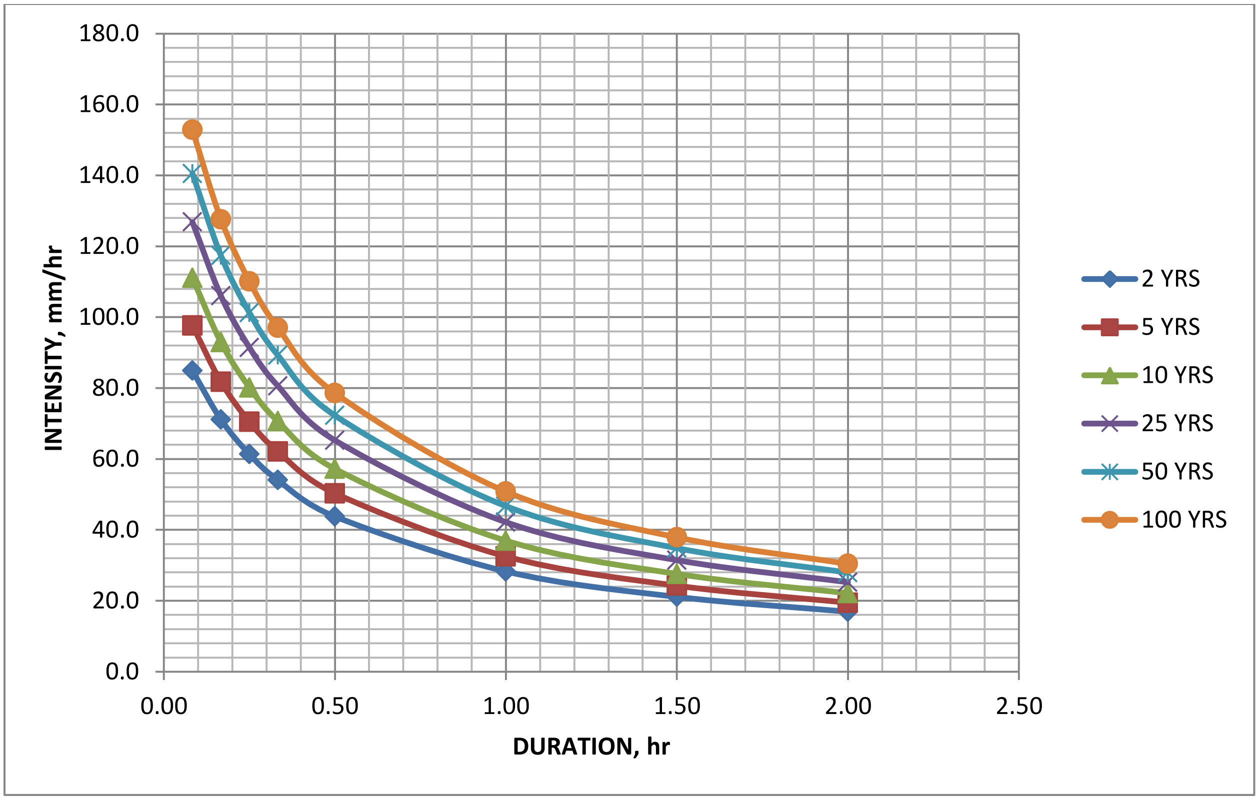


Figure 4.1: IDF curve of Rainfall data from Bole station

After this, a comparison between the IDF curve in figure 4.1 and the A2 IDF curve in figure 3.7 was made and presented in table 4.8. From the comparison, significant differences between the two IDF curves can be seen. The A2 IDF curve has greater intensity values than the Bole IDF curve. This could be because the rainfall data that ERA used while preparing the A2 IDF curve was different from the rainfall data adopted to generate the Bole IDF curve.

Table 4.7:- Comparison between A2 and Bole IDF curves

| D (hr) | T = 2 YEARS | | | T = 5 YEARS | | | T = 10 YEARS | | |
|---|---|---|---|---|---|---|---|---|---|
| | I (A2) | I (BOLE) | D/CE (%) | I (A2) | I (BOLE) | D/CE (%) | I (A2) | I (BOLE) | D/CE (%) |
| 0.08 | 92 | 84.9 | 8.4 | 111 | 97.7 | 13.7 | 127 | 111.1 | 14.3 |
| 0.17 | 78 | 71.1 | 9.7 | 94 | 81.8 | 15.0 | 105 | 92.9 | 13.0 |
| 0.25 | 68 | 61.3 | 10.9 | 80 | 70.5 | 13.5 | 90 | 80.2 | 12.3 |
| 0.33 | 59 | 54.0 | 9.2 | 72 | 62.1 | 15.9 | 82 | 70.6 | 16.1 |
| 0.5 | 48 | 43.8 | 9.7 | 56 | 50.3 | 11.3 | 64 | 57.2 | 11.9 |
| 1.0 | 31 | 28.3 | 9.6 | 37 | 32.5 | 13.8 | 42 | 37.0 | 13.6 |
| 1.5 | 23 | 21.1 | 9.0 | 28 | 24.3 | 15.4 | 32 | 27.6 | 16.0 |
| 2.00 | 17 | 16.9 | 0.5 | 22 | 19.5 | 13.1 | 24 | 22.1 | 8.5 |

| D (hr) | T = 25 YEARS | | | T = 50 YEARS | | | T = 100 YEARS | | |
|---|---|---|---|---|---|---|---|---|---|
| | I (A2) | I (BOLE) | D/CE (%) | I (A2) | I (BOLE) | D/CE (%) | I (A2) | I (BOLE) | D/CE (%) |
| 0.08 | 148 | 126.8 | 16.7 | 164 | 140.5 | 16.7 | 180 | 152.8 | 17.8 |
| 0.17 | 125 | 106.0 | 17.9 | 135 | 117.4 | 15.0 | 151 | 127.6 | 18.3 |
| 0.25 | 105 | 91.4 | 14.8 | 115 | 101.3 | 13.6 | 125 | 110.1 | 13.5 |
| 0.33 | 92 | 80.6 | 14.2 | 102 | 89.2 | 14.3 | 112 | 97.0 | 15.4 |
| 0.5 | 76 | 65.3 | 16.5 | 85 | 72.3 | 17.6 | 90 | 78.6 | 14.5 |
| 1.0 | 48 | 42.2 | 13.8 | 55 | 46.7 | 17.8 | 57 | 50.8 | 12.3 |
| 1.5 | 36 | 31.5 | 14.4 | 40 | 34.8 | 14.8 | 43 | 37.9 | 13.5 |
| 2.00 | 28 | 25.2 | 10.9 | 30 | 28.0 | 7.3 | 32 | 30.4 | 5.3 |

To check this, the rainfall data taken from another station namely observatory station for 30 years (1991-2020 G.C) was analyzed and an IDF curve was produced following the same way and mechanism used to make Bole IDF curve (the detail steps were presented from table 5 to 9 of the appendix part).

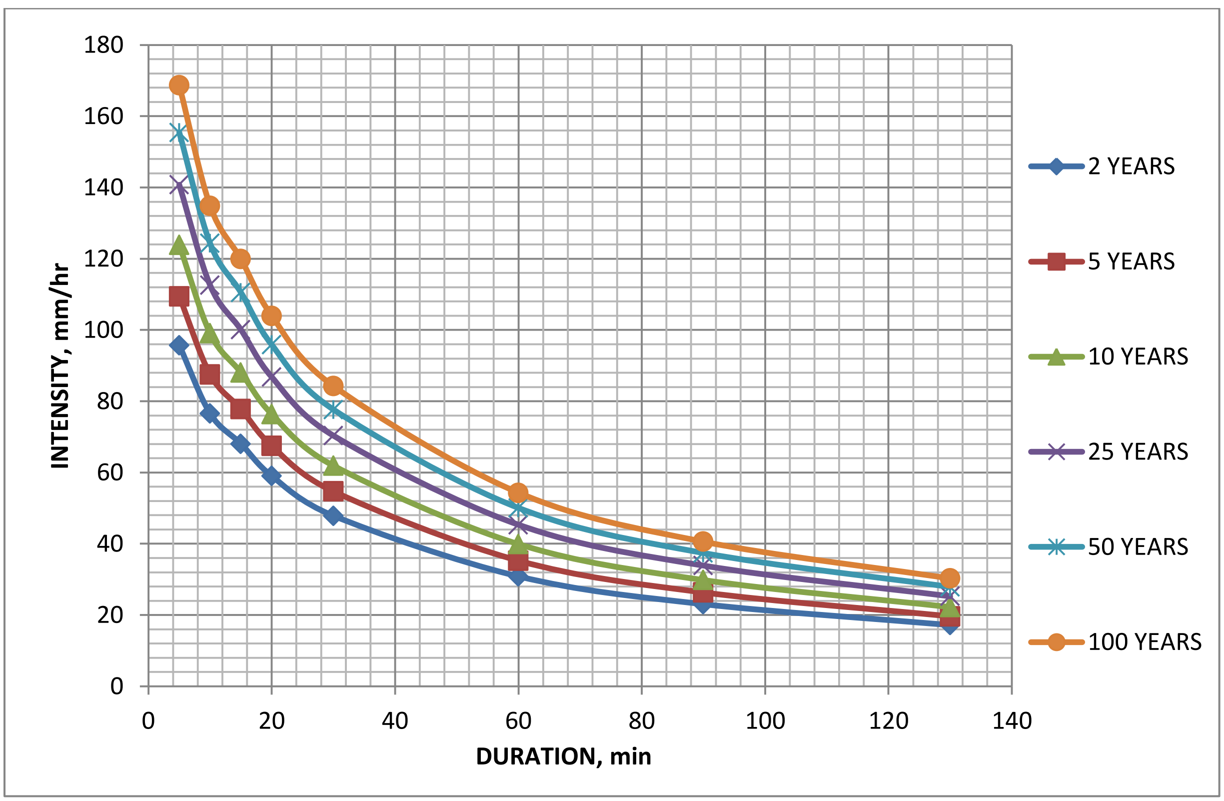


Figure 4.2: IDF curve for observatory station

After this, comparison between the IDF from observatory station and the A2 IDF curve was carried out and shown in table 4.8

Table 4.8: comparison between A2 and observatory station (OBS)

| D (hr) | T = 2 YEARS | | | T = 5 YEARS | | | T = 10 YEARS | | |
|---|---|---|---|---|---|---|---|---|---|
| | I (A2) | I (OBS) | D/CE (%) | I (A2) | I (OBS) | D/CE (%) | I (A2) | I (OBS) | D/CE (%) |
| 0.08 | 92 | 95 | 3.3 | 111 | 111 | 0 | 127 | 125 | 1.6 |
| 0.17 | 78 | 83 | 6.4 | 94 | 94 | 0 | 105 | 105 | 0 |
| 0.25 | 68 | 68 | 0 | 80 | 78 | 2.9 | 90 | 88 | 5.7 |
| 0.33 | 59 | 59 | 0 | 72 | 68 | 1.4 | 82 | 77 | 0 |
| 0.5 | 48 | 48 | 0 | 56 | 55 | 1.8 | 64 | 62 | 3.2 |
| 1.0 | 31 | 31 | 0 | 37 | 35 | 2.8 | 42 | 40 | 10 |
| 1.5 | 23 | 23 | 0 | 28 | 28 | 0 | 32 | 32 | 0 |
| 2.00 | 17 | 17 | 0 | 22 | 20 | 10 | 24 | 22 | 9.1 |

| D (hr) | T = 25 YEARS | | | T = 50 YEARS | | | T = 100 YEARS | | |
|---|---|---|---|---|---|---|---|---|---|
| | I (A2) | I (OBS) | D/CE (%) | I (A2) | I (OBS) | D/CE (%) | I (A2) | I (OBS) | D/CE (%) |
| 0.08 | 148 | 142 | 0 | 164 | 157 | 0.6 | 180 | 170 | 0 |
| 0.17 | 125 | 119 | 0.8 | 135 | 131 | 3.7 | 151 | 141 | 2 |
| 0.25 | 105 | 100 | 5 | 115 | 111 | 3.6 | 125 | 120 | 4.2 |
| 0.33 | 92 | 87 | 5.7 | 102 | 96 | 6.3 | 112 | 104 | 7.7 |
| 0.5 | 76 | 70 | 8.6 | 85 | 78 | 8.9 | 90 | 84 | 7.1 |
| 1.0 | 48 | 45 | 6.7 | 55 | 50 | 10 | 57 | 54 | 5.5 |
| 1.5 | 36 | 34 | 5.9 | 40 | 38 | 5.3 | 43 | 41 | 4.9 |
| 2.00 | 28 | 25 | 12 | 30 | 28 | 7.1 | 32 | 30 | 6.7 |

From the comparison presented in table 4.8, it can be seen that the difference between the intensity values of A2 and observatory station was significantly smaller than the difference between A2 and Bole intensities. This was an indication that the A2 IDF curve was likely generated using rainfall data of the observatory station. Since, the study focused on flood mitigation, to be conservative, the result found from the A2 IDF curve; which was more intense than that of the Bole IDF curve was chosen for further analysis.

## 4.2 DEM (Digital Elevation Model) of study area

The elevation data was first extracted from Google earth. Then, this KML file was imported into ArcGIS, converted into layer, analyzed and finally the following clipped DEM emerged;

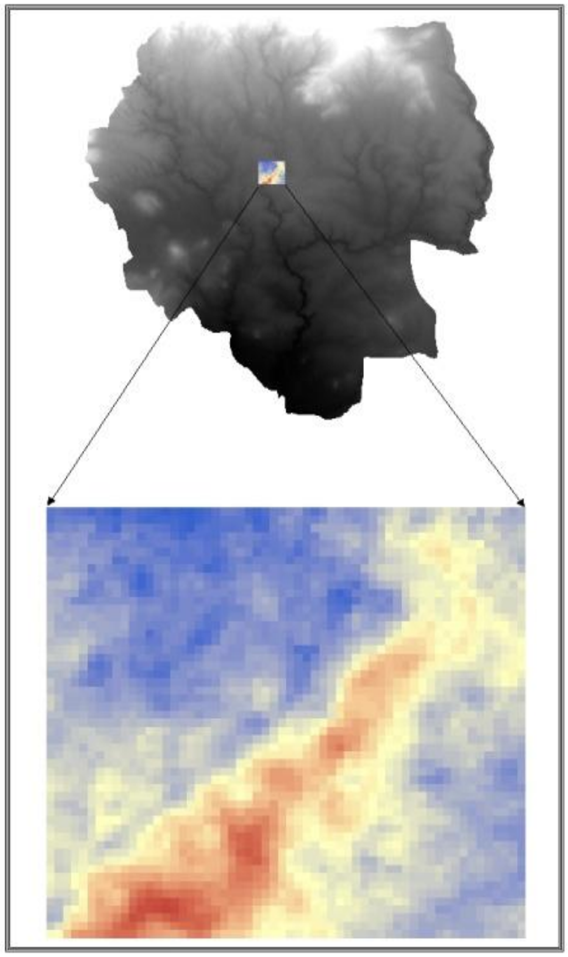

Figure 4.3: The Study Area

Hydrological processes of fill, flow direction, flow accumulation, basin raster, basin vector, clipping study area, generation of stream network continued as shown in figure 4.4. Also, from the flow accumulation raster, eleven subcatchments were delineated using pour point delineation method. The areas, the flow lengths, and the slopes of each subcatchment were generated; and the widths of each subcatchment were calculated dividing the areas by the flow lengths of each subcatchment as presented in table 4.10

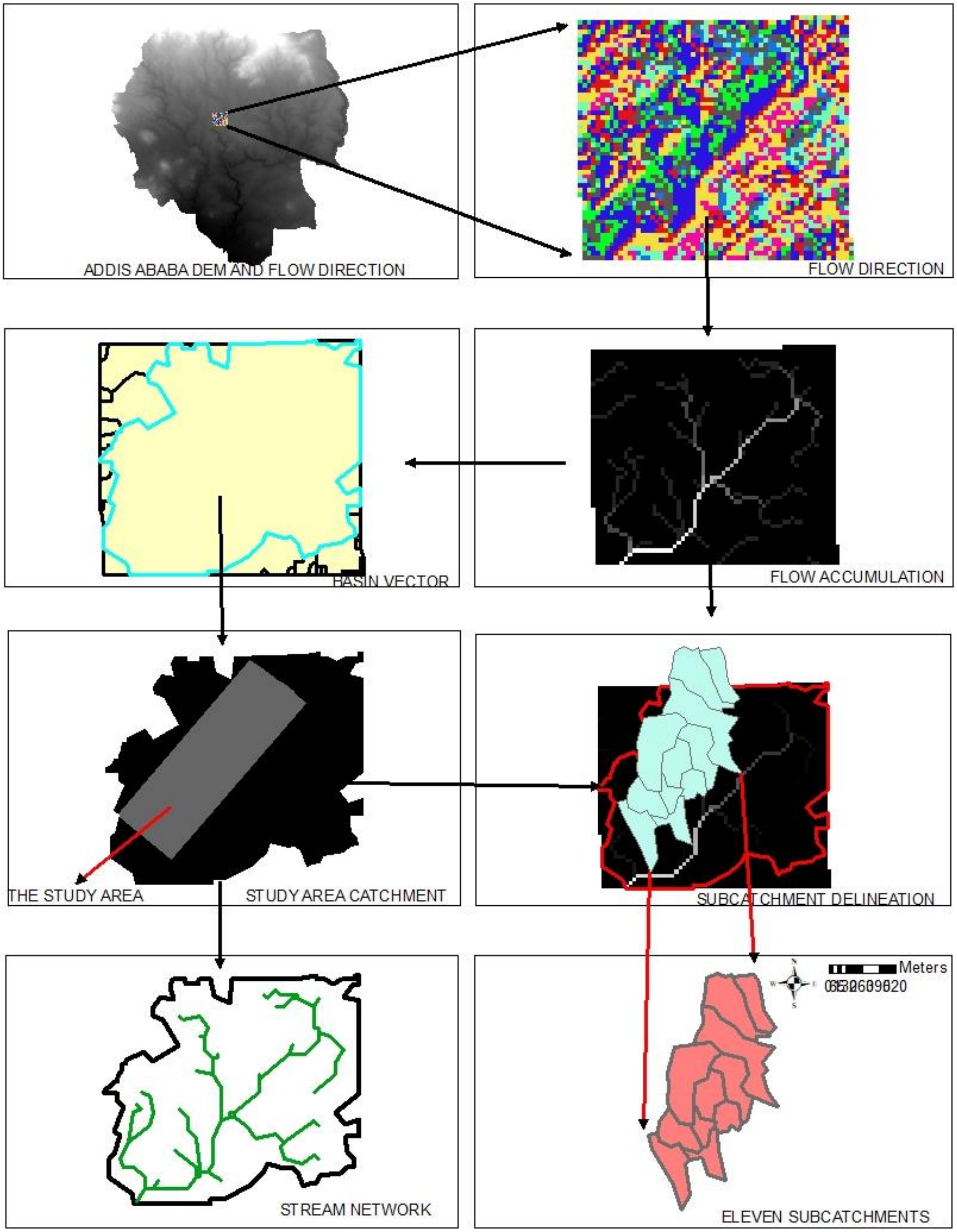


Figure 4.4: Drainage map of the study area

From figure 4.4, it can be seen that eleven subcatchments were generated for the study area. The areas, the flow lengths, the slopes, and the widths of each subcatchment was analyzed and presented in table 4.9

Table 4.9:- subcatchment properties

| Subcatchment | Area (ha) | Flow Length (m) | Width (m) | Slope |
|---|---|---|---|---|
| 1 | 6.3 | 264.8 | 237.9 | 5.5 |
| 2 | 11.5 | 30.7 | 3745.9 | 4.5 |
| 3 | 16.2 | 30.5 | 5311.5 | 7.2 |
| 4 | 6.5 | 61.2 | 1062.1 | 3.4 |
| 5 | 15.1 | 147.7 | 1022.3 | 7.6 |
| 6 | 8.3 | 136.7 | 462.3 | 5.5 |
| 7 | 4 | 68.6 | 587.5 | 7.5 |
| 8 | 2.9 | 263.2 | 111.3 | 4.6 |
| 9 | 6.2 | 214.8 | 288.6 | 8.2 |
| 10 | 4.8 | 30.5 | 1573.8 | 6.6 |
| 11 | 7.9 | 348.4 | 226.8 | 7.5 |
| **Total** | **89.7** | | | |

From the above table, it can be seen that the total area that the study was carried out was about 89.7 hectare (897000 $m^2$). Of all the subcatchments, the 3rd subcatchment was found to have the maximum area of around 16.2 hectare (162000 $m^2$), and the least area was covered by the 7th subcatchment (around 2.9 hectare (29000 $m^2$)).

## 4.3 SWMM analysis and result

After setting map display options to be metric units, and inserting default options, eleven subcatchments, twenty six junctions (nodes or manholes in this case), twenty six conduits (pipes), and a single outfall (Bulbula river that comes from Kebena and makes its way into great Akaki located adjacent to the study area) was plotted as shown in the figure below;

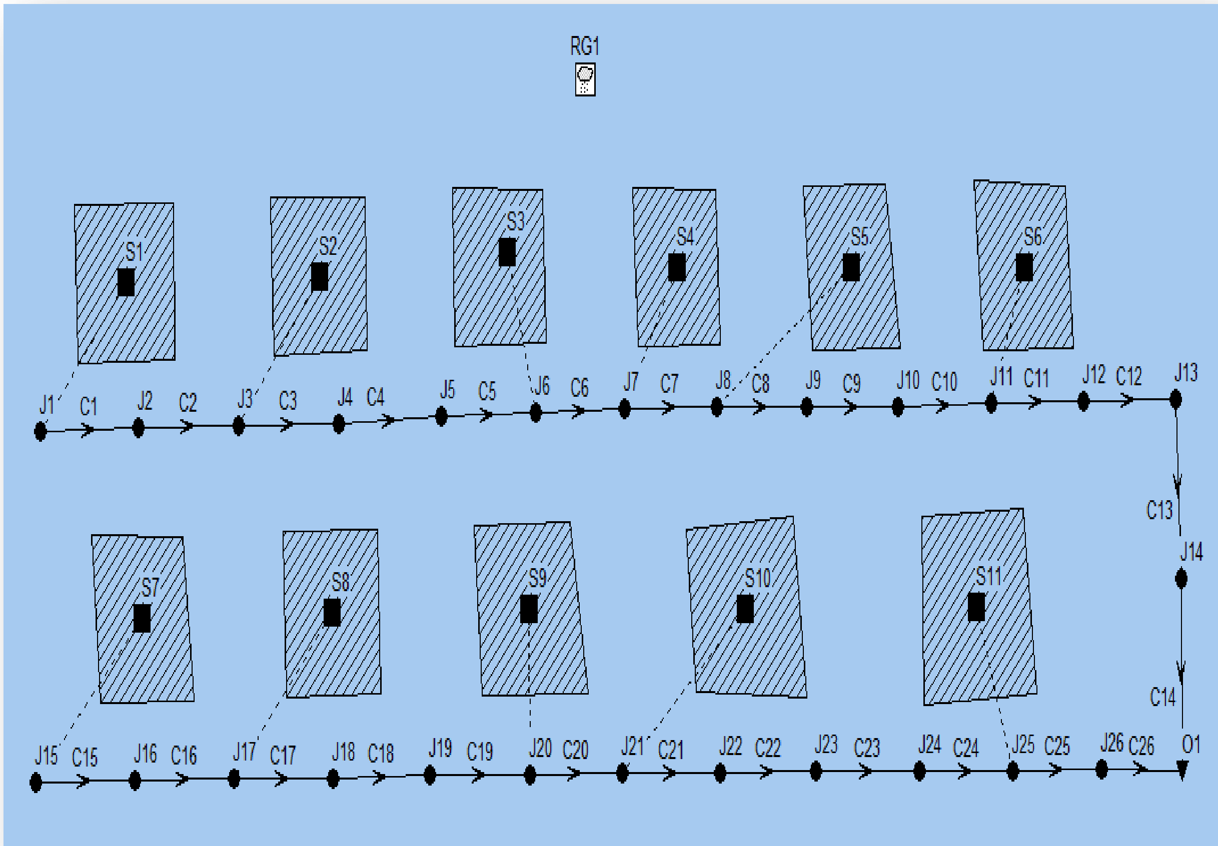


Where: -

- S: Subcatchment, J: Junction/node/manhole, C: conduit, O: Outfall

Figure 4.5: Schematic map of study area objects

In the above map, the conduits (C1 to C14) or the nodes (J1 to J14) can be seen situated to the right side of the road from Wollo sefer to Gorgorios roundabout, and the rest to the left. After plotting the above map, some parameters of subcatchments, nodes and outfalls were edited using SWMM's property editor according to the collected data. Then running it displayed the result about total infiltration, total runoff volume, and runoff peak in table 4.11, and about flooding nodes and conduit surcharge in table 4.10.

Table 4.10: Total infiltration, Runoff Volume and Peak Runoff

| Subcatchment | Total Infiltration (mm) | Total Runoff (mm) | Total Runoff 10^6 Ltr | Peak Runoff (CMS) |
|---|---|---|---|---|
| 1 | 30.97 | 1455.44 | 91.88 | 0.99 |
| 2 | 39.14 | 1448.19 | 166.44 | 1.78 |
| 3 | 45.03 | 1441.34 | 233.5 | 2.46 |
| 4 | 31.33 | 1457.97 | 94.77 | 1.02 |
| 5 | 43.74 | 1442.82 | 217.87 | 2.3 |
| 6 | 30.87 | 1458.44 | 91.88 | 0.99 |
| 7 | 26.27 | 1465.06 | 58.6 | 0.63 |
| 8 | 23.54 | 1469.27 | 42.61 | 0.46 |
| 9 | 30.41 | 1459.19 | 90.44 | 0.94 |
| 10 | 28.02 | 1462.5 | 70.2 | 0.75 |
| 11 | 33.75 | 1454.82 | 114.93 | 1.23 |

Where: -

mm: millimeters, Ltr: liter, CMS: cubic meter per second

### 4.3.1 Node Flooding and Conduit surcharge

SWMM analysis results in node flooding whenever the maximum depth assigned is exceeded by the water surface at a node. In cases like this, the water that is greater than the maximum depth would leave the drainage system and end up inundating the surface. According to the result presented in table 4.11, there was internal flooding in the drainage system on seven nodes (J8-J14).

Table 4.11: Node flooding and conduit surcharge summary report

| Flooding Node | Maximum Rate (CMS) | Total flood volume 10^6 Ltr | Hours Flooded | Conduit Surcharge | Hours both ends full |
|---|---|---|---|---|---|
| J8 | 0.243 | 4.658 | 5.42 | C8 | 6.5 |
| J9 | 0.161 | 3.268 | 3.92 | C9 | 6.5 |
| J10 | 0.101 | 2.222 | 5.08 | C10 | 6.5 |
| J11 | 1.056 | 43.61 | 8.33 | C11 | 15.17 |
| J12 | 0.633 | 21.56 | 3.42 | C12 | 15.17 |
| J13 | 0.395 | 13.969 | 8.08 | C13 | 12.75 |
| J14 | 0.243 | 9.251 | 7.58 | C14 | 12.75 |

The flooding nodes in table 4.11 are located on right side of the road from Wollo sefer to Gorgorios roundabout as indicated in section 4.3. Therefore, flooding was an issue specifically on this side of the road, not on the other. In the same table, it can be seen that as with the seven manholes, equal amounts of conduits with the same identification number were also surcharged (C8-C14). These conduits were at full capacity and therefore were undersized. This has proven the insufficiency of the drainage design in the area under study. SWMM also displayed the water surface depths at each node (manhole or junction) as shown in table 4.12;

Table 4.12: Water surface depth summary

| Node | Water Surface Depth (m) | Node | Water Surface Depth (m) |
|---|---|---|---|
| 1 | 0.26 | 14 | 1.5 |
| 2 | 0.26 | 15 | 0.21 |
| 3 | 0.44 | 16 | 0.21 |
| 4 | 0.44 | 17 | 0.28 |
| 5 | 0.44 | 18 | 0.38 |
| 6 | 0.65 | 19 | 0.38 |
| 7 | 0.75 | 20 | 0.38 |
| 8 | 1.5 | 21 | 0.45 |
| 9 | 1.5 | 22 | 0.45 |
| 10 | 1.5 | 23 | 0.45 |
| 11 | 1.5 | 24 | 0.45 |
| 12 | 1.5 | 25 | 0.56 |
| 13 | 1.5 | 26 | 0.56 |

The nodes J8 to J14 appeaed to have water surface depths higher than the maximum node depths; which created node flooding on those junctions. Whenever such scenarios occur, SWMM displays just the maximum water depth on those junctions found to have water surface heights larger than it.

A profile plot showing the variation of surface water depths across a path of the connected nodes from J1 to J14 all the way to the outfall was also plotted and presented in figure 4.8. From the plot, it can be seen that from J1 to J7 there were no flooding nodes. However, starting from J8 to J14, all the seven nodes can be seen flooding.

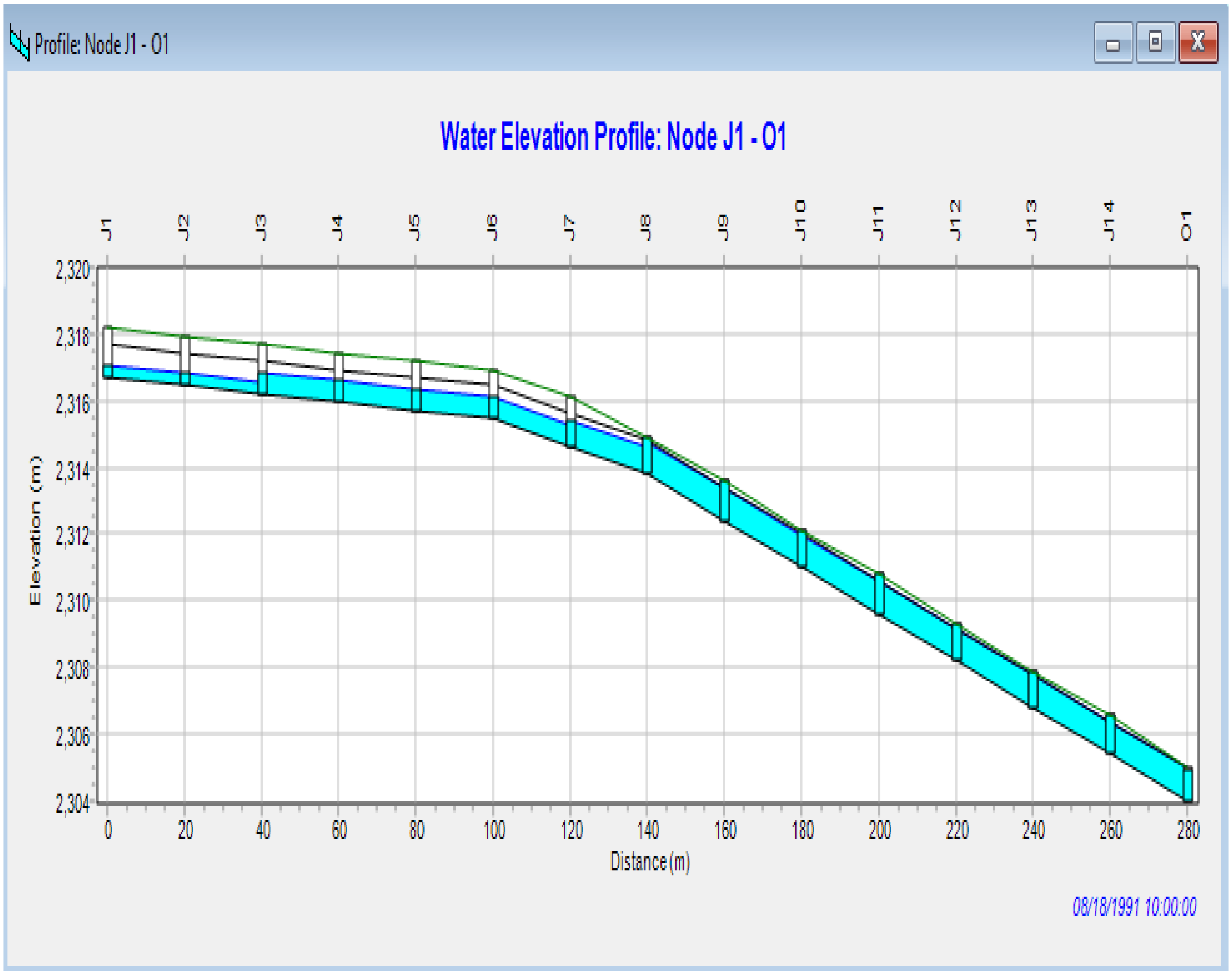


Figure 4.6: Profile plot

## 4.4 Calibration result

Measurements on the 26 manholes were taken on summer, August 13; and data of depth of water surface were collected. Then, a calibration analysis was carried out to see how well the model was when predicting the outcome discussed earlier on. The measured depths and the modeled depths were compared by RSQAURE and ROOT MEAN SQUARE ERROR (RMSE) methods using EXCEL like the manner shown below;

Table 4.13: Comparison between modeled and measured depths

| MH No | Dobs (cm) | Dmod (cm) | r | $r^2$ |
|---|---|---|---|---|
| 1 | 44 | 26 | 18 | 324 |
| 2 | 43 | 26 | 17 | 289 |
| 3 | 70 | 44 | 26 | 676 |
| 4 | 71 | 44 | 27 | 729 |
| 5 | 71 | 44 | 27 | 729 |
| 6 | 94 | 65 | 29 | 841 |
| 7 | 103 | 75 | 28 | 784 |
| 8 | 112 | 150 | -38 | 1444 |
| 9 | 114 | 150 | -36 | 1296 |
| 10 | 113 | 150 | -37 | 1369 |
| 11 | 114 | 150 | -36 | 1296 |
| 12 | 114 | 150 | -36 | 1296 |
| 13 | 112 | 150 | -38 | 1444 |
| 14 | 114 | 150 | -36 | 1296 |
| 15 | 37 | 21 | 16 | 256 |
| 16 | 36 | 21 | 15 | 225 |
| 17 | 46 | 28 | 18 | 324 |
| 18 | 61 | 38 | 23 | 529 |
| 19 | 61 | 38 | 23 | 529 |
| 20 | 61 | 38 | 23 | 529 |
| 21 | 70 | 45 | 25 | 625 |
| 22 | 70 | 45 | 25 | 625 |
| 23 | 71 | 45 | 26 | 676 |
| 24 | 71 | 45 | 26 | 676 |
| 25 | 76 | 56 | 20 | 400 |
| 26 | 77 | 56 | 21 | 441 |
| | | | | **SUM 19648.0** |
| | | | | **SUM/26 755.692** |
| | | | | **RMSE 27.490** |

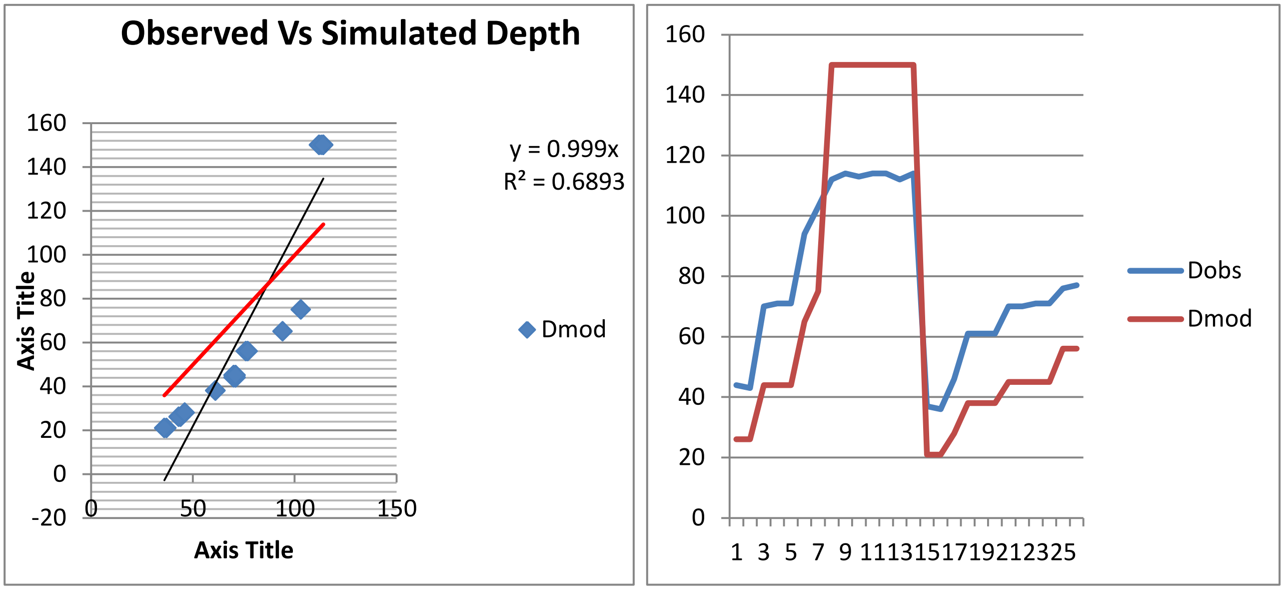


Figure 4.7: measured and modeled depth comparison

Where: -

- Dmod: - simulated/modeled depth,
- Dobs: - measured/observed depth; and both are in cm
- MH No. is manhole (node/junction) number

In figure 4.7, depth results from the SWMM model and measured depths were not close to each other. This was further proved by the results of $R^2$ and RMSE, which were not under acceptable ranges. Therefore, by adjusting the sensitive parameter (percent impervious area, and average surface slope), calibrating the model was found to be necessary.

Table 4.14: Comparison between modeled and measured depths after calibration

| MH No | Dobs | Dmod | r | r² |
|---|---|---|---|---|
| 1 | 44 | 36 | 8 | 64 |
| 2 | 43 | 36 | 7 | 49 |
| 3 | 70 | 67 | 3 | 9 |
| 4 | 71 | 67 | 4 | 16 |
| 5 | 71 | 70 | 1 | 1 |
| 6 | 94 | 100 | -6 | 36 |
| 7 | 103 | 109 | -6 | 36 |
| 8 | 112 | 110 | 2 | 4 |

| | | | | |
|---|---|---|---|---|
| 9 | 114 | 120 | -6 | 36 |
| 10 | 113 | 110 | 3 | 9 |
| 11 | 114 | 120 | -6 | 36 |
| 12 | 114 | 110 | 4 | 16 |
| 13 | 112 | 110 | 2 | 4 |
| 14 | 114 | 115 | -1 | 1 |
| 15 | 37 | 31 | 6 | 36 |
| 16 | 36 | 31 | 5 | 25 |
| 17 | 46 | 41 | 5 | 25 |
| 18 | 61 | 60 | 1 | 1 |
| 19 | 61 | 60 | 1 | 1 |
| 20 | 61 | 60 | 1 | 1 |
| 21 | 70 | 75 | -5 | 25 |
| 22 | 70 | 75 | -5 | 25 |
| 23 | 71 | 75 | -4 | 16 |
| 24 | 71 | 67 | 4 | 16 |
| 25 | 76 | 68 | 8 | 64 |
| 26 | 77 | 69 | 8 | 64 |
| | | | | **SUM 616.0** |
| | | | | **SUM/26 23.692** |
| | | | | **RMSE 4.867** |

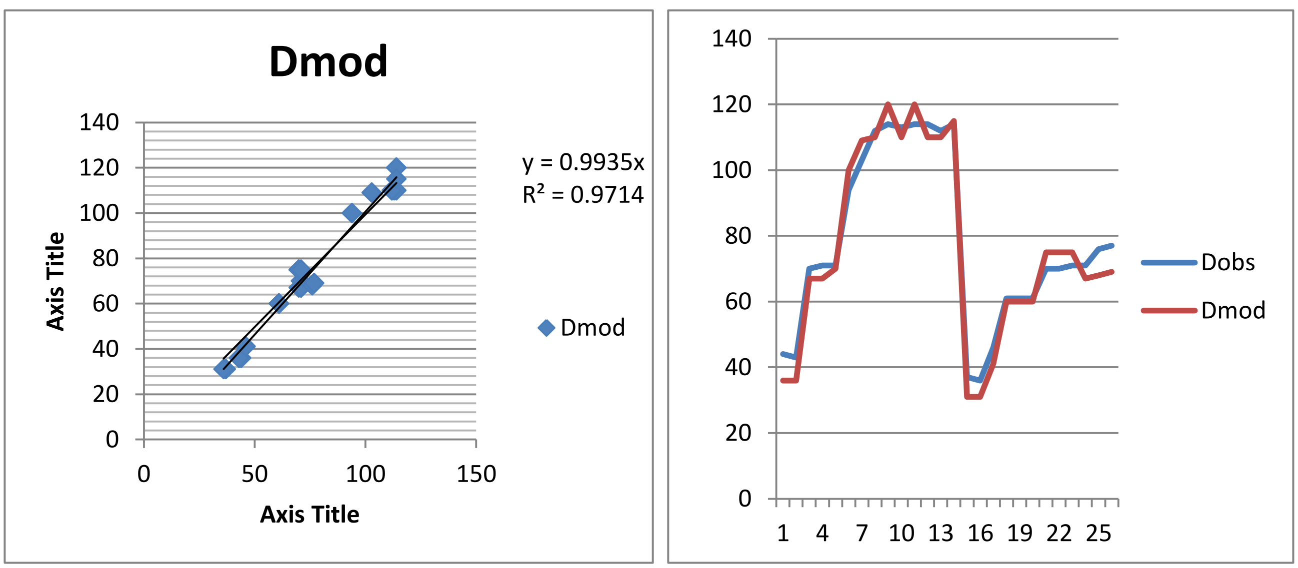


Figure 4.8: measured and modeled depth comparison after calibration

From figure 4.8, it can be seen that the modeled and measured depths got close to each other to acceptable ranges of both $R^2$ and RMSE (0.9714 and 4.867 respectively) after calibration; which proved a good agreement between the model result and the actual measurement.

## 4.5 Result of LID controls

### 4.5.1 Area of application

As discussed in section 3.9, one of the main targets of these analyses was finding the minimum area upon which an LID control could be applied to avoid flood risk. Therefore, analysis on the study area was first carried out with the aim of obtaining a scenario where there are no flooding nodes using LID controls applied on the least area possible. The first task was finding this least area and the right subcatchment/s where this area was located. As it can be seen in table 4.14, many trials proven that all subcatchments were not found to be capable of avoiding flood to the same level after LID application on the same portion of each of the subcatchments. In the same table, the third subcatchment can be seen to be the one where the least area of LID application was found.

Table 4.15: The least area of LID application

| **% area of LID application** | **Subcatchment** | | | | | | | | | | |
|---|---|---|---|---|---|---|---|---|---|---|---|
| | **1** | **2** | **3** | **4** | **5** | **6** | **7** | **8** | **9** | **10** | **11** |
| 100 | X | ✓ | ✓ | ✓ | ✓ | X | X | X | X | X | X |
| 95 | X | ✓ | ✓ | ✓ | ✓ | X | X | X | X | X | X |
| 90 | X | ✓ | ✓ | ✓ | ✓ | X | X | X | X | X | X |
| 85 | X | ✓ | ✓ | ✓ | ✓ | X | X | X | X | X | X |
| 80 | X | ✓ | ✓ | ✓ | ✓ | X | X | X | X | X | X |
| 75 | X | ✓ | ✓ | ✓ | ✓ | X | X | X | X | X | X |
| 70 | X | ✓ | ✓ | ✓ | ✓ | X | X | X | X | X | X |
| 65 | X | ✓ | ✓ | ✓ | ✓ | X | X | X | X | X | X |
| 60 | X | ✓ | ✓ | X | ✓ | X | X | X | X | X | X |
| 55 | X | ✓ | ✓ | X | ✓ | X | X | X | X | X | X |
| 50 | X | X | ✓ | X | ✓ | X | X | X | X | X | X |
| 45 | X | X | ✓ | X | ✓ | X | X | X | X | X | X |
| 40 | X | X | ✓ | X | ✓ | X | X | X | X | X | X |
| **36** | X | X | ✓ | X | X | X | X | X | X | X | X |
| 35 | X | X | X | X | X | X | X | X | X | X | X |

Where: -

- ✓ : flood removal from the drainage system (no flooding nodes)
- X : Flood remains unresolved (there are still flooding nodes).

As it can be seen in table 4.15, after many trials, the least area upon which one of the four LID controls could be applied to remove flood was found to be 36% of the third subcatchment. From table 4.9, the area covered by the third subcatchment was 162000m². Thus, 36% of 162000m² would be 58320m² of area. If one of the four LID controls be installed on such area of the 3rd sub-catchment, all nodes would be free from flooding.

The trials also proven that any area of LID application on the third sub-catchment above this least area would avoid flooding issue. But any area below this would not. Thus, this area (36% of the 3rd subcatchment) (58320 m²) was concluded to be the least area upon which any of the four LID controls could be applied to avoid the risk of flooding (considering 0% roof slope in the case of Green Roofs). Also, no conduits in the whole area would be surcharged if one of the four LID controls be applied on such area. This would mean the conventional drainage system on the study area would be sufficient in mitigating flood issues if supported by one of the four LID controls. After assuming such an area, SWMM displayed the following result on maximum water surface depth; an indicator for the presence of flooding nodes:

Table 4.16: Maximum water surface depth after LID application

| **Node** | **Water Surface Depth (m)** | **Node** | **Water Surface Depth (m)** |
|---|---|---|---|
| 1 | 0.26 | 14 | 0.82 |
| 2 | 0.26 | 15 | 0.21 |
| 3 | 0.44 | 16 | 0.21 |
| 4 | 0.44 | 17 | 0.28 |
| 5 | 0.44 | 18 | 0.38 |
| 6 | 0.65 | 19 | 0.38 |
| 7 | 0.75 | 20 | 0.38 |
| 8 | 0.73 | 21 | 0.45 |
| 9 | 0.73 | 22 | 0.45 |
| 10 | 0.73 | 23 | 0.45 |
| 11 | 0.82 | 24 | 0.45 |
| 12 | 0.82 | 25 | 0.56 |
| 13 | 0.82 | 26 | 0.56 |

From table 4.16, water surface depths can be seen decreased. Particularly, the water surface depths of the flooding nodes (J8 to J14) were significantly decreased after LID application when compared with the one presented in table 4.13 before LID application. These junctions found to have water surface depths less than the maximum assigned depths. As a result of this, no flooding nodes on the entire drainage system were obtained after assuming application of one of the four LID controls on the 36% of the third subcatchment.

This can further be illustrated by the water surface elevation profile shown in figure 4.9. Comparing the profile plots of figure 4.6 and figure 4.9, the water surface depths of the flooding nodes in the analysis without the application of LID controls (J8 – J14) can be seen decreased to the level of no flooding after LID application was assumed. The surcharged conduits in the previous analysis can also be seen undercharged after the application of LID controls.

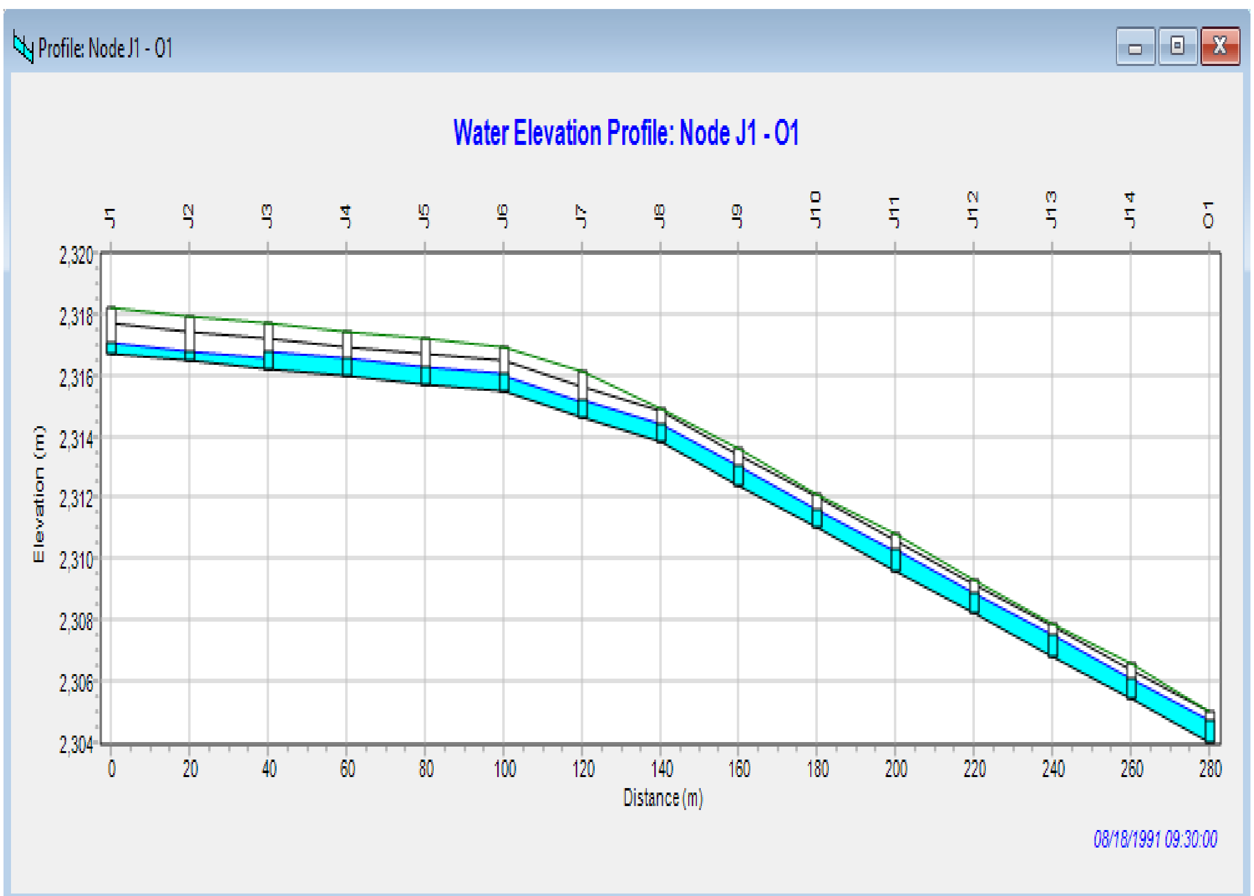


Figure 4.9: Water surface elevation profile after LID application

However, the reduction of runoff volume and peak runoff occurred on only the third subcatchment for all LIDs as indicated in table 4.17. Not only was this, but also infiltration and storage by the LID controls were achieved only on the third subcatchment as shown in table 4.18. This indicated, runoff volume and peak runoff reduction, and increase in infiltration and storage could not be obtained anywhere else other than the subcatchment itself upon which the LID controls were applied.

Table 4.17: LID performance regarding runoff volume and peak runoff reduction

| **Sub-catchment** | **Area of LID application ($m^2$)** | **Area of LID application (%)** | **LID control** | **Reduction in Runoff volume (%)** | **Reduction in Peak Runoff (%)** |
|---|---|---|---|---|---|
| 3 | 58320 | 36 | Permeable Pavement | 114.85 | 112.07 |
| 3 | 58320 | 36 | Bio-retention Cells | 114.85 | 112.07 |
| 3 | 58320 | 36 | Green Roofs | 54.34 | 52.07 |
| 3 | 58320 | 36 | Rain Barrels | 62.8 | 60.07 |

The performance of the LID controls with respect to infiltration and storage was presented in table 4.18. From the result, it can be seen that permeable pavements had the highest capacity in infiltrating more stormwater than the rest. Also, no infiltration took place after installing green roofs and rain barrels. This proved the limited function of green roofs and rain barrels on storage only as described in section 2.5.5. Moreover, rain barrels were found to have the highest performance with regard to storing the stormwater they receive from downspouts of buildings.

Table 4.18: LID performance regarding infiltration and storage

| Subcatchment | LID Control | Infiltration loss (mm) | Final Storage (mm) |
|---|---|---|---|
| 3 | Permeable Pavements | 17407.11 | 34.2 |
| 3 | Bio-retention Cells | 2176.7 | 51.3 |
| 3 | Green Roofs | 0 | 102.6 |
| 3 | Rain Barrels | 0 | 800 |

However, for the case of green roofs, roof slope was assumed to be zero in the previously presented analyses; which was an unrealistic scenario. Roofs are normally designed with at least 5% slopes to drain the stormwater coming on them. When this least roof slope was considered, green roofs could not remove the occurrence of flood after being applied on the 36% of the third sub-catchment. This was due to the direct relationship between runoff quantity and slope. As the slope gets steeper, runoff increases and vice versa as indicated in section 3.7.

After applying 5% roof surface slope for green roofs, SWMM displayed results concerning runoff volume and peak runoff, and infiltration loss and final storage in table 4.19 and table 4.20 respectively.

Table 4.19: Green roofs performance regarding infiltration and storage capacity

| Sub-catchment | LID control | Infiltration Loss (mm) | Final Storage (mm) |
|---|---|---|---|
| 3 | Green Roofs | 0 | 71.3 |

Table 4.20: Green roofs performance regarding runoff volume and peak runoff reduction

| Sub-catchment | LID control | Reduction in Runoff volume (%) | Reduction in Peak Runoff (%) |
|---|---|---|---|
| 3 | Green Roofs | 7.9 | 0 |

From the above tables, it can be seen that Green Roofs has the capacity to minimize runoff volume and store stormwater on the third subcatchment after 5% roof slope was assumed. But, they could not prevent the area from flooding. Even in reducing runoff volume on the third subcatchment, green roofs could not do as good as the other LID controls. While green roofs reduced 7.9% of runoff volume generated from the third subcatchment, the permeable pavements and bio-retention cells reduced 114.85% and rain barrels 62.8%. Also, while the other LID controls reduced peak runoff, green roofs did not. Therefore, the option of considering Green Roofs was taken out and the analyses continued with the three LID controls for further comparison.

### 4.5.2 LID control selection

After this, the three LID controls were compared as to which can be realized on the ground taking into consideration the land use of the third subcatchment. Land use analysis was performed using Google earth and Arc GIS. The image of the study area from February 25, 2021 was first taken from Google earth and imported and georeferenced in Arc GIS. The third subcatchment was then extracted out of it as can be seen in figure 4.10. This image was classified into four classes and the respective areas of each of these classes were obtained as presented in figure 4.11 and table 4.21.

The transport areas upon which the bioretention cells and permeable pavements could be applied constitute 20.4%. The total building area on which rain barrels could be installed was found to be 60%. Since, the target was avoiding flood with the minimum area of LID application (36% of the 3$^{rd}$ subcatchment), this could only be realized using rain barrels as there exists more than adequate amount of building area to host these LID controls. The buildings in the study area, specifically in the third subcatchment use gutters and downspouts to convey stormwater and transport it to the drainage system.

If Rain Barrels were installed, the load on the existing drainage system would be minimized. Retrofitting rain barrels on the urbanized study area and integrating them with the existing conventional drainage system would enable one to avoid flood risk successfully.

Therefore, after making comparison between the four LID controls on the basis of flood removal on the least area of LID application, rain barrels were selected as they proved themselves to be capable of being realized on the study area and meet the target.


Figure 4.10: Georeferenced image of the study area and extracted image of the third subcatchment

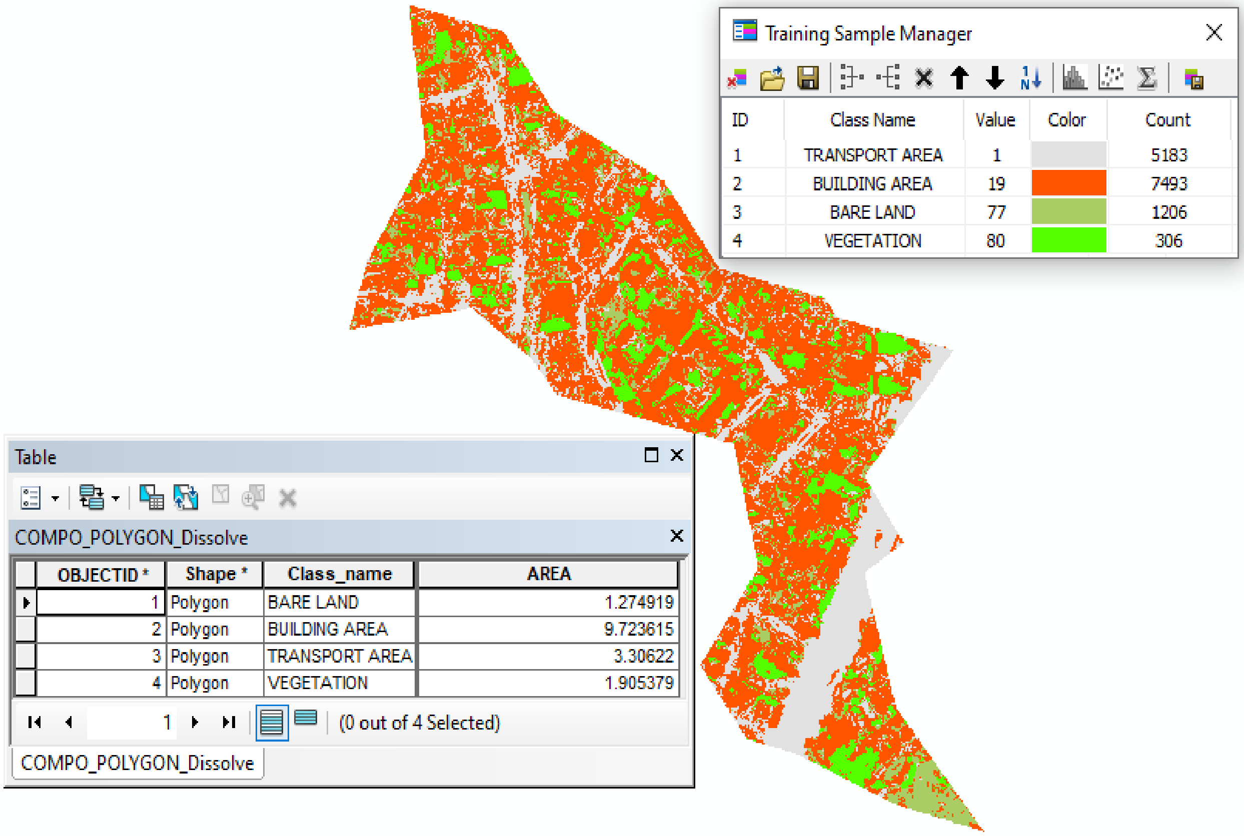


Figure 4.11: Classified map of the third subcatchment with four class names and their respective areas

Table 4.21: Areal coverage of the four classes in percent

| Class Name | Area (ha) | Percent (%) |
|---|---|---|
| BARE LAND | 1.274919 | 7.86 |
| BUILDING AREA | 9.723615 | 60 |
| TRANSPORT AREA | 3.30622 | 20.4 |
| VEGETATION | 1.905379 | 11.75 |
| **Total** | **16.2** | **100** |

# CHAPTER FIVE

# 5. CONCLUSION and RECOMMENDATION

The area chosen for this study encountered flood problems. Flooding was apparent on one side of the study area. From Gorgorios to Wollo sefer the left side of the area, or from Wollo sefer to Gorgorios, the right side of the area was found facing flood problems. Seven of the fourteen nodes in this side were inundated. Thus, it was concluded that the drainage system of the area could not adequately manage flood issues.

Further analysis and trial and errors proved the application of LID controls (bioretention cells, rain barrels, and permeable pavements) was capable of flood removal if applied on at least 36% (58320 $m^2$) of the third subcatchment even if reduction of runoff volume and peak runoff was achieved on only the third subcatchment where the LID was applied. Therefore the most feasible way to remove flood from the area would be the application of one of the three LID controls on the least area possible, which appeared to be 36% of the third subcatchment.

A final analysis was carried out on comparison between the three LID controls as to which could be realized considering the LULC of the study place. The analysis revealed Rain barrels to be the ones that could be installed on the 36% of the third subcatchment and avoid flood risk. Therefore these LID controls were selected as the feasible choice.

In order to control flood risks the area under study faces and will be facing in the future to come because of the increasing urbanization, it is recommended to implement Rain Barrels and integrate them with the existing conventional drainage system. These LID controls were found to be the most feasible choice by which protection of the area from flood damages could be realized. Rain barrels not only protect the area from flooding risks, but also can store the water to be reused.

# REFERENCES


1. Oija, C.S.P, Berndtsson R, Bhunya P. Engineering Hydrology. Oxford University Press. 2008.
2. Stephen T, Toan V, Trung N, et al. The Role of Green Infrastructures in Managing Urban Floods. ISET. 2019.
3. Sherard JA, Jacobs JM, Asce M. Vegetated roof water-balance model experimental and model results. J. Hydrol. Eng. 2012; 17(8).
4. United States EPA. Storm Water Management Model: User's Manual Version 5.1. 2015.
5. Dunnet N., Kingsbury N. Planting green roofs and living walls, Timber Press, Inc, Portland, OR. 2004.
6. Carten TL, Rasmussen TC. Hydrologic Behavior of Vegetative Roofs. JAWRA. 2006; 42(5):1261-1274.
7. Oberndorfer E, Lundholm J, Bass B, et al. Green Roofs as Urban Ecosystems: Ecological Structures, Functions, and Services. BioOne. 2007; 57(10):823-833.
8. Bliss DJ, Neufeld RD, Ries RJ. Storm water Runoff Mitigation Using a Green Roof. J. Environ. Eng. 2009; 26(2):407-418.
9. Cui T, Long Y, Yong Y. Choosing the LID for Urban Storm Management in the South of Taiyuan Basin by Comparing the Storm Water Reduction Efficiency. Int. J. Water. Dec 2019; 11(12):1-18
10. Macchi S, Tiepolo M. (eds), Switzerland. Climate Change Vulnerability in Southern African Cities: Building Knowledge for Adaptation. Springer. 2014; 1-19
11. World Bank, Addis Ababa. Washington D.C. Enhancing Urban Resilience: City Strength Resilient Cities Program. GFDRR. 2015; Working Paper 100980.
12. Douglas I, Alam K, Maghenda M, et al. Unjust Waters: Climate Change, flooding and the urban poor in Africa. E&U. 2008;20(1):187-205
13. Conway D, Mould C, Bewket W. Over One Century of Rainfall and Temperature Observations in Addis Ababa, Ethiopia. Int. J. Climatol. 2014; 24(1):77-91.
14. Li L, Li W, Ballard T, et al. CMIP5 Model Simulations of Ethiopian Kiremt-season Precipitation current climate and future changes. Clim. Dyn. 2015; 46(9-10):2883-2895.

15. CLUVA. Climate Change and Urban Vulnerability in African: Research Brief, Seventh Framework Program Deliverable. CLUVA consortium. 2013; 1-16.
16. Davies Buttler and John W. Davies. Urban Drainage:2nd Edition. 2004.
17. Han D. Concise Hydrology; Dawei Han and Ventus Publishing ApS. 2010.
18. Hailemichael F. Flood Assessment of Addis Ababa Light Rail Transit System (LRT): Meshualekiya – Gotera. AAiT School of Graduate Studies (2015).
19. USKH. Inc (Water Resources Group). Low Impact Development Design Guidance Manual. 2008 Dec; WMPCPg08001
20. Gironas J, Roesner L, Davis J, et al. Storm Water Management Model Application Manual. US EPA. 2009 Jul.
21. Houdeshell C, Pomerev C, Hair L, et al. Cost Estimating Tools for Low-Impact Development Best Management Practices: Challenges, limitations, and implications. J. Irrig. Drain. Eng. 2009;137(3).
22. Huber W.C. New Options for Overland Flow Routing in SWMM. Urban Drainage Modeling. 2001; 22-29.
23. Alemu H. Investigation of Flooding Problems in Urban Drainage Systems: the case at Zenebe Werk in Addis Ababa, Ethiopia. AAiT School of Graduate Studies. 2017.
24. Ketema K. Sustainable Storm Water Management by Implementing low impact development in JEMO, Addis Ababa. AAiT School of Graduate Studies. 2018.
25. Huber W.C., Cannon L., Stouder M. BMP Modeling Concepts and Simulation. US EPA. 2004.
26. Mora-Melia D, Lopez-Aburto C, Ballesteros-Perez P, et al. Viability of Green Roofs as a flood Mitigation Element in Central Region of Chile. Sustainability. Apr 2018. 10(1130):1-19.
27. Burszta-Adamlak E, Mrowlec M. Modeling of Green roofs' hydrologic performance using EPA's SWMM. J.Hydrol. July 2013.68(1):36-42.
28. Akter A, Hasan A, Islam K. Possibilities of urban flood reduction through distributed scale rain-water harvesting. Water Sci. Eng. 2020.13(2):95-105.
29. Wałęga A., Cebulska M., Gądek W. The use of bioretention cell to decreasing outflow from parking lot. J. Water Land Dev. 2018;(36):173-181.n
30. Zhu H, Yu M, Zhu J, et al. Simulation study on effect of permeable pavements on reducing flood risk of urban runoff. IJTST.8(2019):373-382.
31. Atsbha T. Impacts of Land Use/Cover on Surface Water Quantity and Quality: Case of Akaki Catchment, Ethiopia. AAiT School of Graduate Studies. 2019

32. Zewdu A. Integrated Urban Drainage System: The Case of Ayat to Megenagna Light Rail Transit System Route. AAiT School of Graduate Studies, 2015.
33. Paulos W. Evaluating the Impact of Land Use Change on Urban Drainage System and Proposed Low Impact Development Measures in Addis Ababa, Ethiopia (case study of Megenagna - Bole Ring Road). AAiT School of Graduate Studies, 2020.
34. Jayasoriya V, Ng A. Tools for modeling of Stormwater Management and Economics of Green Infrastructure Practices: A Review. Water Air Soil Pollut. 2014;225(8)
35. Shoemaked L, Riverson J, Alvi K, et al. SUSTAIN-A Framework for Placement of Best Management Practices in Urban Watersheds to Protect Water Quality: Report. US EPA. 2009
36. Lai F.H., Dai T. Zhen J, et al. SUSTAIN-AN EPA BMP process and placement tool for urban watersheds. Proceedings of the Water Environment Federation. US EPA. 2007; 1-23.
37. Pitt R. Voorhees J. WinSLAMM and Low Impact Development. LID conference, College Park, Marryland. 2004 Sep; 1-13.
38. Abebe T, Mathias, Megento L, et al. The City of Addis Ababa from 'Forest City' TO 'Urban Heat Island': Journal of Urban and Environmental Engineering, vol. 10, núm. 2, 2016, pp. 254-262
39. Addis Ababa City Road Authority: Drainage Design Manual, 2004
40. Ethiopian Road Authority. Drainage Design manual, 2013
41. Abraha T. Sustainable Urban Drainage Options for Mekelle City. AAiT School of Graduate Studies, 2018

# APPENDIX

Table 1: Soil Characteristics (Clay is soil type of study area) (source [5])

| Soil Texture Class | K | Ψ | ϕ | FC | WP |
|---|---|---|---|---|---|
| Sand | 4.74 | 1.93 | 0.437 | 0.062 | 0.024 |
| Loamy Sand | 1.18 | 2.40 | 0.437 | 0.105 | 0.047 |
| Sandy Loam | 0.43 | 4.33 | 0.453 | 0.190 | 0.085 |
| Loam | 0.13 | 3.50 | 0.463 | 0.232 | 0.116 |
| Silt Loam | 0.26 | 6.69 | 0.501 | 0.284 | 0.135 |
| Sandy Clay Loam | 0.06 | 8.66 | 0.398 | 0.244 | 0.136 |
| Clay Loam | 0.04 | 8.27 | 0.464 | 0.310 | 0.187 |
| Silty Clay Loam | 0.04 | 10.63 | 0.471 | 0.342 | 0.210 |
| Sandy Clay | 0.02 | 9.45 | 0.430 | 0.321 | 0.221 |
| Silty Clay | 0.02 | 11.42 | 0.479 | 0.371 | 0.251 |
| Clay | 0.01 | 12.60 | 0.475 | 0.378 | 0.265 |

**K** = saturated hydraulic conductivity, in/hr
Ψ = suction head, in. φ = porosity, fraction, **FC** = field capacity, fraction
**WP**= wilting point, fraction

Table 2: Manning's n – overland flow (smooth concrete used for permeable pavement analysis) (source [5])

| **Surface** | **n** |
|---|---|
| Smooth asphalt | 0.011 |
| Smooth concrete | 0.012 |
| Ordinary concrete lining | 0.013 |
| Good wood | 0.014 |
| Brick with cement mortar | 0.014 |
| Vitrified clay | 0.015 |
| Cast iron | 0.015 |
| Corrugated metal pipes | 0.024 |
| Cement rubble surface | 0.024 |
| Fallow soils (no residue) | 0.05 |
| Cultivated soils | |
| Residue cover < 20% | 0.06 |
| Residue cover > 20% | 0.17 |
| Range (natural) | 0.13 |
| Grass | |
| Short, prairie | 0.15 |
| Dense | 0.24 |
| Bermuda grass | 0.41 |
| Woods | |
| Light underbrush | 0.40 |
| Dense underbrush | 0.80 |

Table 3: outlier test Kn values at 10% significant level. (Source [16])

| Sample size | K value | Sample size | K value | Sample size | K value | Sample size | K value |
|---|---|---|---|---|---|---|---|
| 10 | 2.036 | 45 | 2.727 | 80 | 2.940 | 115 | 3.064 |
| 11 | 2.088 | 46 | 3.736 | 81 | 2.945 | 116 | 3.067 |
| 12 | 2.134 | 47 | 2.744 | 82 | 2.949 | 117 | 3.070 |
| 13 | 2.175 | 48 | 2.753 | 83 | 2.953 | 118 | 3.073 |
| 14 | 2.213 | 49 | 2.760 | 84 | 2.957 | 119 | 3.075 |
| 15 | 2.247 | 50 | 2.768 | 85 | 2.961 | 120 | 3.078 |
| 16 | 2.279 | 51 | 2.775 | 86 | 2.966 | 121 | 3.081 |
| 17 | 2.309 | 52 | 2.783 | 87 | 2.970 | 122 | 3.083 |
| 18 | 2.335 | 53 | 2.790 | 88 | 2.973 | 123 | 3.086 |
| 19 | 2.361 | 54 | 2.798 | 89 | 2.977 | 124 | 3.089 |
| 20 | 2.385 | 55 | 2.804 | 90 | 2.981 | 125 | 3.092 |
| 21 | 2.408 | 56 | 2.811 | 91 | 2.984 | 126 | 3.095 |
| 22 | 2.429 | 57 | 2.818 | 92 | 2.989 | 127 | 3.097 |
| 23 | 2.448 | 58 | 2.824 | 93 | 2.993 | 128 | 3.100 |
| 24 | 2.467 | 59 | 2.831 | 94 | 2.996 | 129 | 3.102 |
| 25 | 2.486 | 60 | 2.837 | 95 | 3.000 | 130 | 3.104 |
| 26 | 2.502 | 61 | 2.842 | 96 | 3.003 | 131 | 3.107 |
| 27 | 2.519 | 62 | 2.849 | 97 | 3.006 | 132 | 3.109 |
| 28 | 2.534 | 63 | 2.854 | 98 | 3.011 | 133 | 3.112 |
| 29 | 2.549 | 64 | 2.860 | 99 | 3.014 | 134 | 3.114 |
| 30 | 2.563 | 65 | 2.866 | 100 | 3.017 | 135 | 3.116 |
| 31 | 2.577 | 66 | 2.871 | 101 | 3.021 | 136 | 3.119 |
| 32 | 2.591 | 67 | 2.877 | 102 | 3.024 | 137 | 3.122 |
| 33 | 2.604 | 68 | 2.883 | 103 | 3.027 | 138 | 3.124 |
| 34 | 2.616 | 69 | 2.888 | 104 | 3.030 | 139 | 3.126 |
| 35 | 2.628 | 70 | 2.893 | 105 | 3.033 | 140 | 3.129 |
| 36 | 2.639 | 71 | 2.897 | 106 | 3.037 | 141 | 3.131 |
| 37 | 2.650 | 72 | 2.903 | 107 | 3.040 | 142 | 3.133 |
| 38 | 2.661 | 73 | 2.908 | 108 | 3.043 | 143 | 3.135 |
| 39 | 2.671 | 74 | 2.912 | 109 | 3.046 | 144 | 3.138 |
| 40 | 2.682 | 75 | 2.917 | 110 | 3.049 | 145 | 3.140 |
| 41 | 2.692 | 76 | 2.922 | 111 | 3.052 | 146 | 3.142 |
| 42 | 2.700 | 77 | 2.927 | 112 | 3.055 | 147 | 3.144 |
| 43 | 2.710 | 78 | 2.931 | 113 | 3.058 | 148 | 3.146 |
| 44 | 2.719 | 79 | 2.935 | 114 | 3.061 | 149 | 3.148 |

For 30 years of data, Kn = 2.563

Table 4: Runoff Coefficients for Different Land use (source [37])

| Type of Drainage Area | C |
|---|---|
| **Business** | |
| Commercial area | 0.7 - 0.95 |
| Neighborhood area | 0.5 – 0.7 |
| Residential areas | |
| Single family areas | 0.3 – 0.5 |
| Multi units detached | 0.4 – 0.6 |
| Multi units attached | 0.6 – 0.75 |
| Sub-urban | 0.25 – 0.4 |
| Apartment dwelling areas | 0.5 – 0.7 |
| **Industrial** | |
| Light areas | 0.5 – 0.8 |
| Heavy areas | 0.6 – 0.9 |
| Parks cemeteries | 0.1 – 0.25 |
| Play ground | 0.2 – 0.4 |
| Railroad yard areas | 0.2 – 0.4 |
| Unimproved areas | 0.1 – 0.3 |
| **Lawns** | |
| Sand soil, flat < 2% | 0.05 - 0.1 |
| Sand soil, average, 2 to 7% | 0.1 – 0.15 |
| Sand soil, steep > 7% | 0.15 – 0.2 |
| Heavy soil, < 2% | 0.13 – 0.17 |
| Heavy soil, average, 2 to 7% | 0.18 – 0.22 |
| Heavy soil, steep > 7% | 0.25 – 0.35 |
| **Streets** | |
| Asphaltic | 0.7 – 0.95 |
| Concrete | 0.8 – 0.95 |
| Bricks | 0.7 – 0.85 |
| Drives and Walks | 0.7 – 0.85 |
| Roofs | 0.7 – 0.95 |

Table 5: The annual maximum data of observatory with its log values

| Year | OBS (X) | Y = LOG(X) | Year | OBS (X) | Y = LOG(X) |
|---|---|---|---|---|---|
| 1991 | 47.3 | 1.6749 | 2006 | 43.5 | 1.6385 |
| 1992 | 51.4 | 1.7110 | 2007 | 46.3 | 1.6656 |
| 1993 | 53.5 | 1.7284 | 2008 | 53.3 | 1.7267 |
| 1994 | 57 | 1.7559 | 2009 | 54.7 | 1.7380 |
| 1995 | 85.3 | 1.9309 | 2010 | 44.6 | 1.6493 |
| 1996 | 47.6 | 1.6776 | 2011 | 55.8 | 1.7466 |
| 1997 | 46.3 | 1.6656 | 2012 | 36.4 | 1.5611 |
| 1998 | 43.3 | 1.6365 | 2013 | 47.2 | 1.6739 |
| 1999 | 37.4 | 1.5729 | 2014 | 65.4 | 1.8156 |
| 2000 | 37.1 | 1.5694 | 2015 | 47.8 | 1.6794 |
| **2001** | **96.3** | **1.9836** | 2016 | 47.7 | 1.6785 |
| 2002 | 29.5 | 1.4698 | 2017 | 55.2 | 1.7419 |
| 2003 | 46.2 | 1.6646 | 2018 | 49.3 | 1.6928 |
| 2004 | 44.2 | 1.6454 | 2019 | 43.4 | 1.6375 |
| 2005 | 58.6 | 1.7679 | 2020 | 46.9 | 1.6712 |

Table 6: Outlier test summary

| | |
|---|---|
| **Mean** | 1.6924 |
| **Standard Deviation** | 0.100 |
| **Kn** | 2.564 |
| **$Y_H$** | 1.949 |
| **$Y_L$** | 1.436 |
| **$X_H$** | 88.88 |
| **$X_L$** | 27.28 |

Y = 1.98 is a high outlier (historic data)

Table 7: Goodness of fit test for annual max of observatory station (Extreme Value I (Gumbel fits better))

| Probability Distributions | RANK | | |
|---|---|---|---|
| | Kolmogorov Smirnov | Anderson Darling | Chi-Squared |
| Gumbel | 17 | 10 | 3 |
| Log Pearson III | 13 | 12 | 7 |

Table 8: Mean and standard deviation based on normal ratio method

| Time (min) | 5.00 | 10.00 | 15.00 | 20.00 | 30.00 | 60.00 | 90.00 | 120.00 |
|---|---|---|---|---|---|---|---|---|
| **Time (hr)** | **0.08** | **0.17** | **0.25** | **0.33** | **0.50** | **1.00** | **1.50** | **2.00** |
| **t/24** | **0.00** | **0.01** | **0.01** | **0.01** | **0.02** | **0.04** | **0.06** | **0.08** |
| **(b+24)^n** | **17.66** | **17.66** | **17.66** | **17.66** | **17.66** | **17.66** | **17.66** | **17.66** |
| **(b+t)^n** | **0.42** | **0.50** | **0.58** | **0.66** | **0.82** | **1.27** | **1.70** | **2.12** |
| **RRt** | **0.15** | **0.24** | **0.32** | **0.37** | **0.45** | **0.58** | **0.65** | **0.70** |
| **1991** | 7.10 | 11.35 | 15.14 | 17.50 | 21.29 | 27.43 | 30.75 | 33.11 |
| **1992** | 7.71 | 12.34 | 16.45 | 19.02 | 23.13 | 29.81 | 33.41 | 35.98 |
| **1993** | 8.03 | 12.84 | 17.12 | 19.80 | 24.08 | 31.03 | 34.78 | 37.45 |
| **1994** | 8.55 | 13.68 | 18.24 | 21.09 | 25.65 | 33.06 | 37.05 | 39.90 |
| **1995** | 12.80 | 20.47 | 27.30 | 31.56 | 38.39 | 49.47 | 55.45 | 59.71 |
| **1996** | 7.14 | 11.42 | 15.23 | 17.61 | 21.42 | 27.61 | 30.94 | 33.32 |
| **1997** | 6.95 | 11.11 | 14.82 | 17.13 | 20.84 | 26.85 | 30.10 | 32.41 |
| **1998** | 6.50 | 10.39 | 13.86 | 16.02 | 19.49 | 25.11 | 28.15 | 30.31 |
| **1999** | 5.61 | 8.98 | 11.97 | 13.84 | 16.83 | 21.69 | 24.31 | 26.18 |
| **2000** | 5.57 | 8.90 | 11.87 | 13.73 | 16.70 | 21.52 | 24.12 | 25.97 |
| **2002** | 4.43 | 7.08 | 9.44 | 10.92 | 13.28 | 17.11 | 19.18 | 20.65 |
| **2003** | 6.93 | 11.09 | 14.78 | 17.09 | 20.79 | 26.80 | 30.03 | 32.34 |
| **2004** | 6.63 | 10.61 | 14.14 | 16.35 | 19.89 | 25.64 | 28.73 | 30.94 |
| **2005** | 8.79 | 14.06 | 18.75 | 21.68 | 26.37 | 33.99 | 38.09 | 41.02 |
| **2006** | 6.53 | 10.44 | 13.92 | 16.10 | 19.58 | 25.23 | 28.28 | 30.45 |
| **2007** | 6.95 | 11.11 | 14.82 | 17.13 | 20.84 | 26.85 | 30.10 | 32.41 |
| **2008** | 8.00 | 12.79 | 17.06 | 19.72 | 23.99 | 30.91 | 34.65 | 37.31 |
| **2009** | 8.21 | 13.13 | 17.50 | 20.24 | 24.62 | 31.73 | 35.56 | 38.29 |
| **2010** | 6.69 | 10.70 | 14.27 | 16.50 | 20.07 | 25.87 | 28.99 | 31.22 |
| **2011** | 8.37 | 13.39 | 17.86 | 20.65 | 25.11 | 32.36 | 36.27 | 39.06 |
| **2012** | 5.46 | 8.74 | 11.65 | 13.47 | 16.38 | 21.11 | 23.66 | 25.48 |
| **2013** | 7.08 | 11.33 | 15.10 | 17.46 | 21.24 | 27.38 | 30.68 | 33.04 |
| **2014** | 9.81 | 15.70 | 20.93 | 24.20 | 29.43 | 37.93 | 42.51 | 45.78 |
| **2015** | 7.17 | 11.47 | 15.30 | 17.69 | 21.51 | 27.72 | 31.07 | 33.46 |
| **2016** | 7.16 | 11.45 | 15.26 | 17.65 | 21.47 | 27.67 | 31.01 | 33.39 |
| **2017** | 8.28 | 13.25 | 17.66 | 20.42 | 24.84 | 32.02 | 35.88 | 38.64 |
| **2018** | 7.40 | 11.83 | 15.78 | 18.24 | 22.19 | 28.59 | 32.05 | 34.51 |
| **2019** | 6.51 | 10.42 | 13.89 | 16.06 | 19.53 | 25.17 | 28.21 | 30.38 |
| **2020** | 7.04 | 11.26 | 15.01 | 17.35 | 21.11 | 27.20 | 30.49 | 32.83 |
| **MEAN** | **7.65** | **12.24** | **16.32** | **18.87** | **22.95** | **29.58** | **33.15** | **35.71** |
| **SDEVA** | **2.04** | **3.26** | **4.35** | **5.03** | **6.11** | **7.88** | **8.83** | **9.51** |

Table 9: IDF relation of observatory station

| D (hr) | Mean | SDeva | T, KT 2, 0.16 | | T, KT 5, 0.72 | | T, KT 10, 1.31 | |
|---|---|---|---|---|---|---|---|---|
| | | | RF | I (RF/D) | RF | I (RF/D) | RF | I (RF/D) |
| 0.08 | 7.7 | 2.0 | 8.0 | 96 | 9.1 | 109 | 10.3 | 124 |
| 0.17 | 12.2 | 3.3 | 12.8 | 77 | 14.6 | 88 | 16.5 | 99 |
| 0.25 | 16.3 | 4.4 | 17.0 | 68 | 19.5 | 78 | 22.0 | 88 |
| 0.33 | 18.9 | 5.0 | 19.7 | 59 | 22.5 | 67 | 25.5 | 76 |
| 0.50 | 23.0 | 6.1 | 23.9 | 48 | 27.3 | 55 | 31.0 | 62 |
| 1.00 | 29.6 | 7.9 | 30.8 | 31 | 35.3 | 35 | 39.9 | 40 |
| 1.50 | 33.2 | 8.8 | 34.6 | 23 | 39.5 | 26 | 44.7 | 30 |
| 2.17 | 35.7 | 9.5 | 37.2 | 17 | 42.6 | 20 | 48.2 | 22 |

| D (hr) | Mean | SDeva | T, KT 25, 2 | | T, KT 50, 2.6 | | T, KT 100, 3.14 | |
|---|---|---|---|---|---|---|---|---|
| | | | RF | I (RF/D) | RF | I (RF/D) | RF | I (RF/D) |
| 0.08 | 7.7 | 2.0 | 11.7 | 141 | 13.0 | 155 | 14.1 | 169 |
| 0.17 | 12.2 | 3.3 | 18.8 | 113 | 20.7 | 124 | 22.5 | 135 |
| 0.25 | 16.3 | 4.4 | 25.0 | 100 | 27.6 | 111 | 30.0 | 120 |
| 0.33 | 18.9 | 5.0 | 28.9 | 87 | 31.9 | 96 | 34.7 | 104 |
| 0.50 | 23.0 | 6.1 | 35.2 | 70 | 38.8 | 78 | 42.1 | 84 |
| 1.00 | 29.6 | 7.9 | 45.3 | 45 | 50.1 | 50 | 54.3 | 54 |
| 1.50 | 33.2 | 8.8 | 50.8 | 34 | 56.1 | 37 | 60.9 | 41 |
| 2.17 | 35.7 | 9.5 | 54.7 | 25 | 60.4 | 28 | 65.6 | 30 |

Table 10: Node input data

| Node | Type | Maximum Water Depth (m) | Invert Elevation (m) |
|---|---|---|---|
| J1 | Junction | 1.1 | 2315.6 |
| J2 | Junction | 1.1 | 2314 |
| J3 | Junction | 1.1 | 2313.3 |
| J4 | Junction | 1.1 | 2312.4 |
| J5 | Junction | 1.1 | 2311.5 |
| J6 | Junction | 1.1 | 2310.6 |
| J7 | Junction | 1.1 | 2309.9 |
| J8 | Junction | 1.1 | 2309.1 |
| J9 | Junction | 1.1 | 2308.4 |
| J10 | Junction | 1.1 | 2307.8 |
| J11 | Junction | 1.1 | 2307.2 |
| J12 | Junction | 1.1 | 2306.5 |
| J13 | Junction | 1.1 | 2306 |
| J14 | Junction | 1.1 | 2305.2 |
| J15 | Junction | 1.1 | 2316 |
| J16 | Junction | 1.1 | 2315.3 |
| J17 | Junction | 1.1 | 2314.5 |
| J18 | Junction | 1.1 | 2313.8 |
| J19 | Junction | 1.1 | 2313.1 |
| J20 | Junction | 1.1 | 2312.2 |
| J21 | Junction | 1.1 | 2311.3 |
| J22 | Junction | 1.1 | 2310.1 |
| J23 | Junction | 1.1 | 2309.3 |
| J24 | Junction | 1.1 | 2308.4 |
| J25 | Junction | 1.1 | 2307.3 |
| J26 | Junction | 1.1 | 2306.4 |
| Outlet | Outfall | | 2286 |

Table 11: Conduit input data

| Conduit Name | Conduit Shape | Conduit Length (m) | Conduit Diameter (cm) | Maximum Depth (m) | Roughness |
|---|---|---|---|---|---|
| C1 | Circular | 100.0 | 80.0 | 1.0 | 0.014 |
| C2 | Circular | 100.0 | 80.0 | 1.0 | 0.014 |
| C3 | Circular | 100.0 | 80.0 | 1.0 | 0.014 |
| C4 | Circular | 100.0 | 80.0 | 1.0 | 0.014 |
| C5 | Circular | 100.0 | 80.0 | 1.0 | 0.014 |
| C6 | Circular | 100.0 | 80.0 | 1.0 | 0.014 |
| C7 | Circular | 100.0 | 80.0 | 1.0 | 0.014 |
| C8 | Circular | 100.0 | 80.0 | 1.0 | 0.014 |
| C9 | Circular | 100.0 | 80.0 | 1.0 | 0.014 |
| C10 | Circular | 100.0 | 80.0 | 1.0 | 0.014 |
| C11 | Circular | 100.0 | 80.0 | 1.0 | 0.014 |
| C12 | Circular | 100.0 | 80.0 | 1.0 | 0.014 |
| C13 | Circular | 100.0 | 80.0 | 1.0 | 0.014 |
| C14 | Circular | 100.0 | 80.0 | 1.0 | 0.014 |
| C15 | Circular | 110.0 | 80.0 | 1.0 | 0.014 |
| C16 | Circular | 110.0 | 80.0 | 1.0 | 0.014 |
| C17 | Circular | 110.0 | 80.0 | 1.0 | 0.014 |
| C18 | Circular | 110.0 | 80.0 | 1.0 | 0.014 |
| C19 | Circular | 110.0 | 80.0 | 1.0 | 0.014 |
| C20 | Circular | 110.0 | 80.0 | 1.0 | 0.014 |
| C21 | Circular | 110.0 | 80.0 | 1.0 | 0.014 |
| C22 | Circular | 110.0 | 80.0 | 1.0 | 0.014 |
| C23 | Circular | 110.0 | 80.0 | 1.0 | 0.014 |
| C24 | Circular | 110.0 | 80.0 | 1.0 | 0.014 |
| C25 | Circular | 110.0 | 80.0 | 1.0 | 0.014 |
| C26 | Circular | 110.0 | 80.0 | 1.0 | 0.014 |

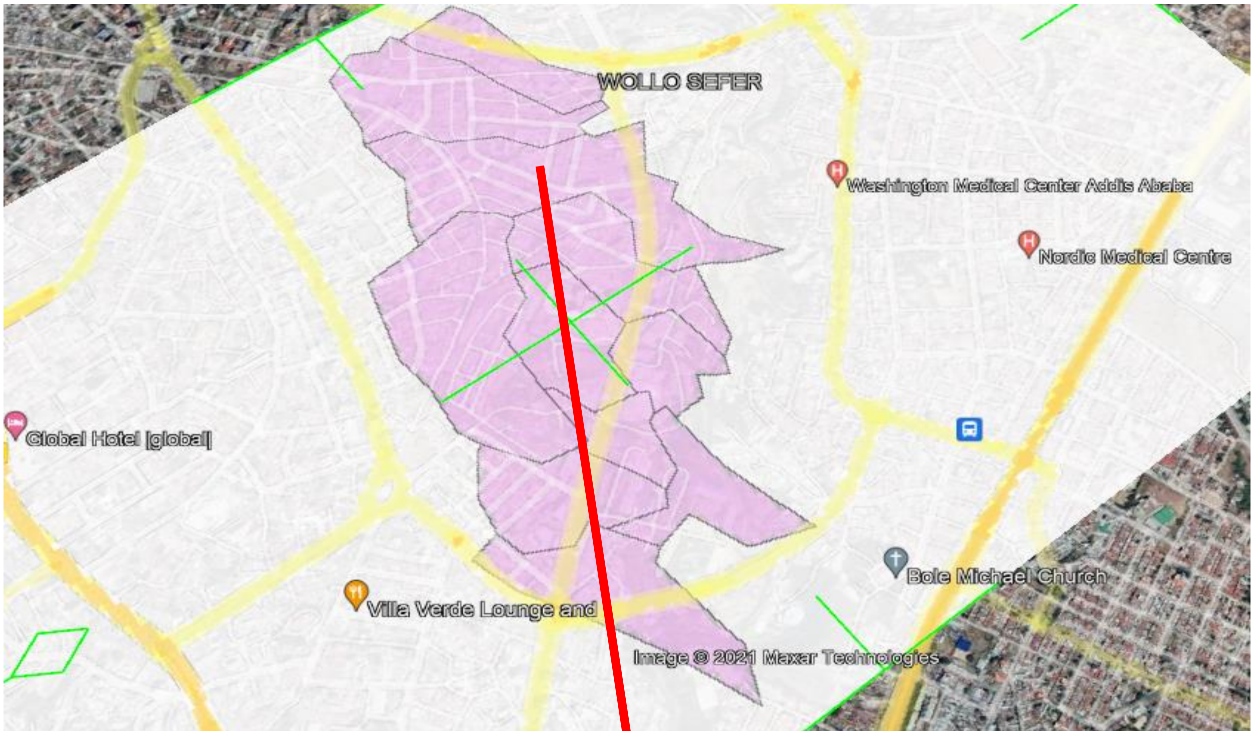


Figure 1: The eleven subcatchments on Google Earth

Figure 2: The third subcatchment

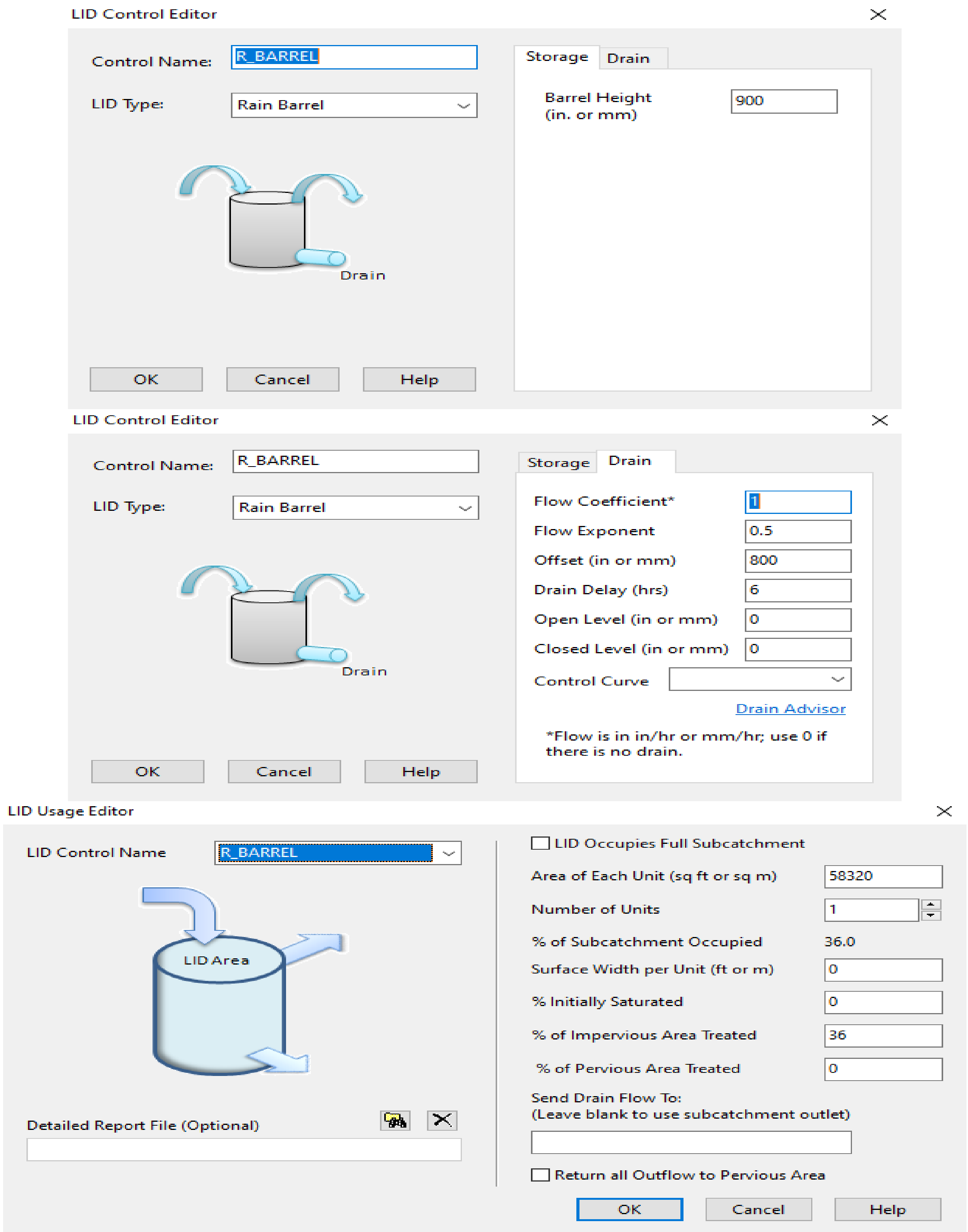


Figure 3: LID Specifications used for Rain Barrels

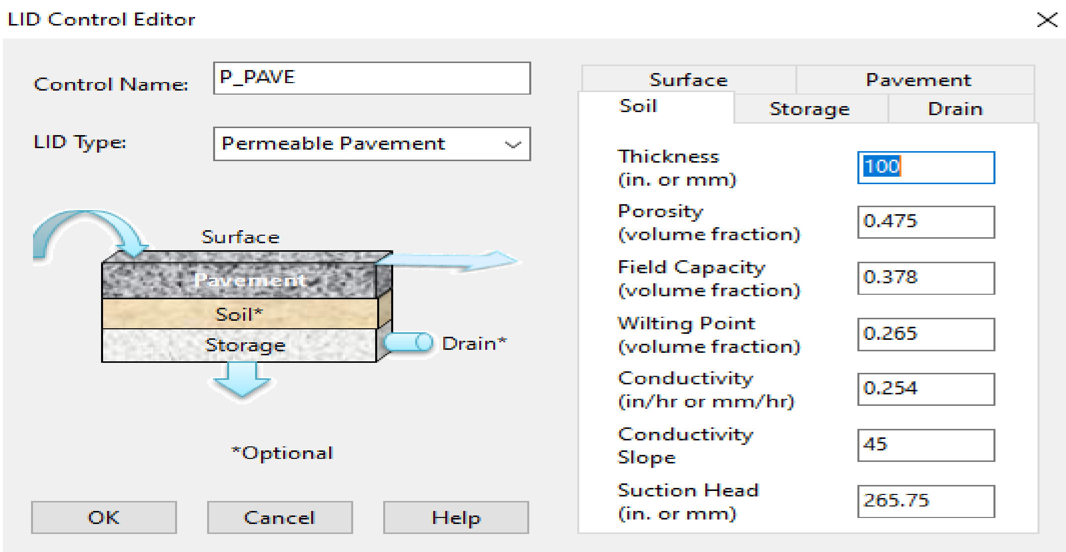
LID Control Editor
Control Name: P_PAVE
LID Type: Permeable Pavement
Surface
Pavement
Soil*
Storage
Drain*
*Optional
OK
Cancel
Help
Surface
Pavement
Soil
Storage
Drain
Thickness (in. or mm) 100
Porosity (volume fraction) 0.475
Field Capacity (volume fraction) 0.378
Wilting Point (volume fraction) 0.265
Conductivity (in/hr or mm/hr) 0.254
Conductivity Slope 45
Suction Head (in. or mm) 265.75

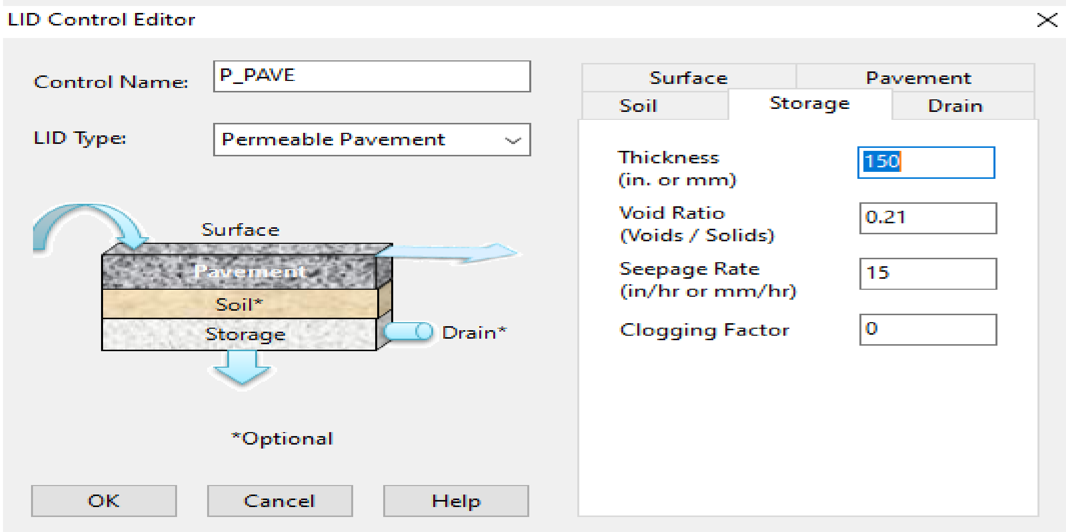
LID Control Editor
Control Name: P_PAVE
LID Type: Permeable Pavement
Surface
Pavement
Soil*
Storage
Drain*
*Optional
OK
Cancel
Help
Surface
Pavement
Soil
Storage
Drain
Thickness (in. or mm) 150
Void Ratio (Voids / Solids) 0.21
Seepage Rate (in/hr or mm/hr) 15
Clogging Factor 0

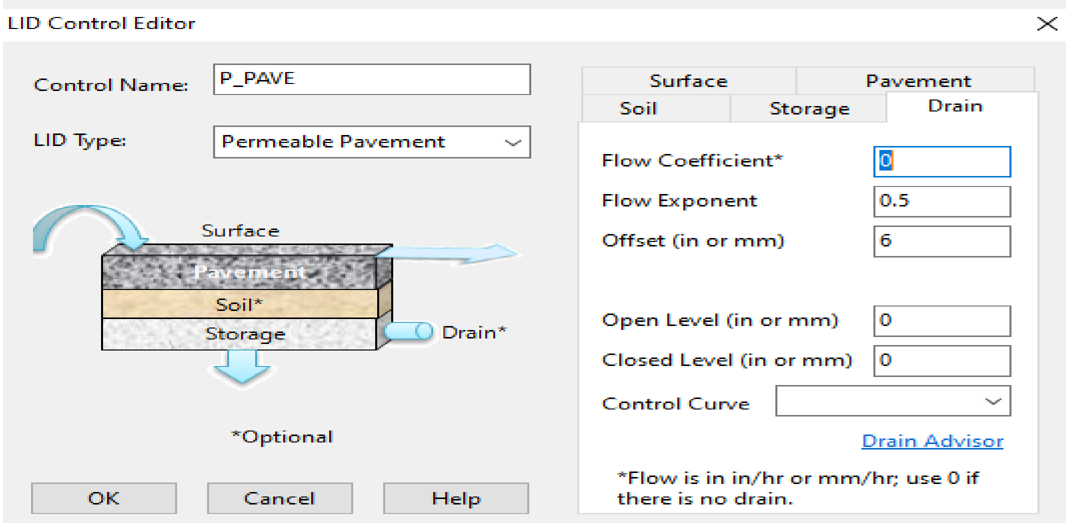
LID Control Editor
Control Name: P_PAVE
LID Type: Permeable Pavement
Surface
Pavement
Soil*
Storage
Drain*
*Optional
OK
Cancel
Help
Surface
Pavement
Soil
Storage
Drain
Flow Coefficient* 0
Flow Exponent 0.5
Offset (in or mm) 6
Open Level (in or mm) 0
Closed Level (in or mm) 0
Control Curve
Drain Advisor
*Flow is in in/hr or mm/hr; use 0 if there is no drain.

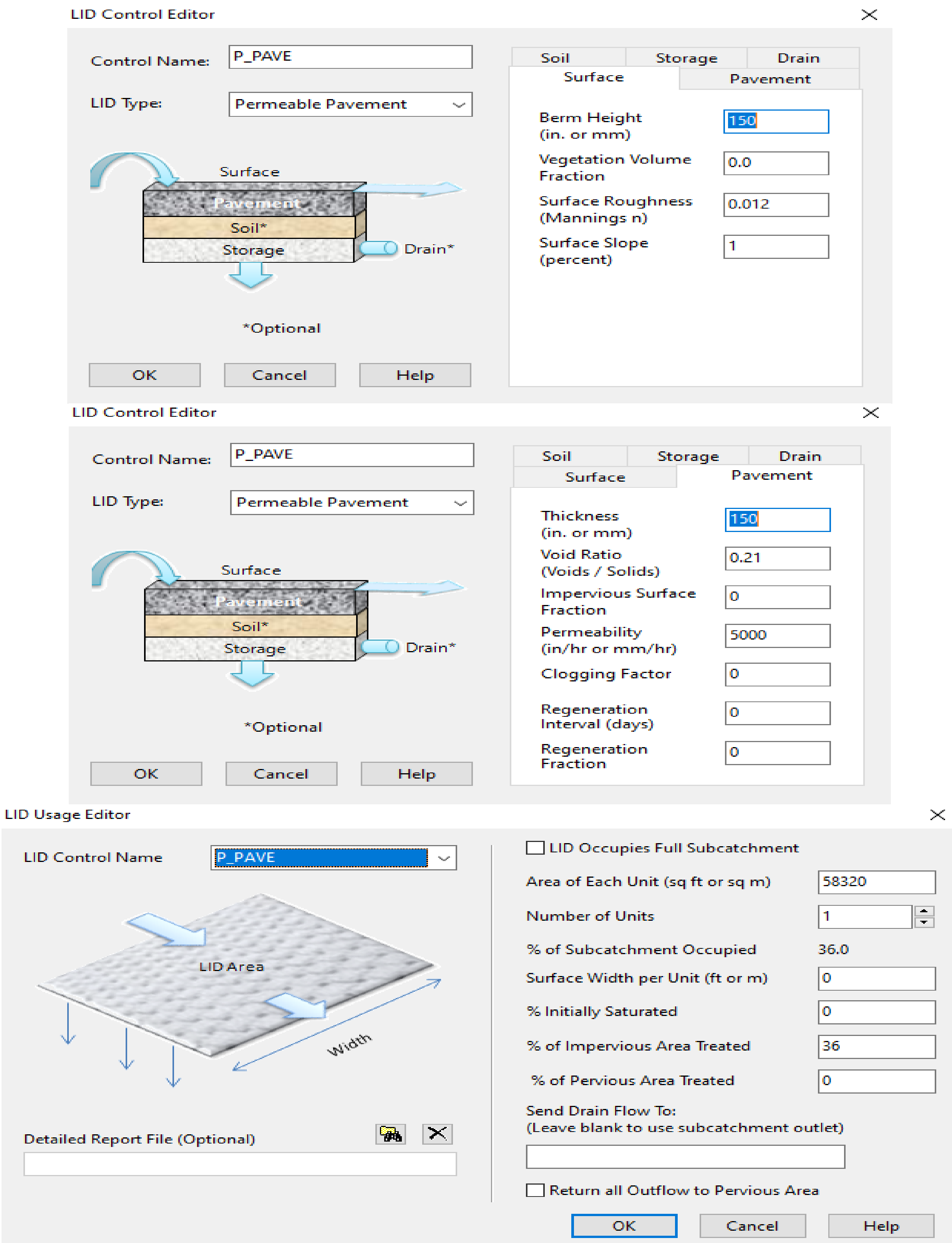


Figure 4: LID specifications used for Permeable Pavements

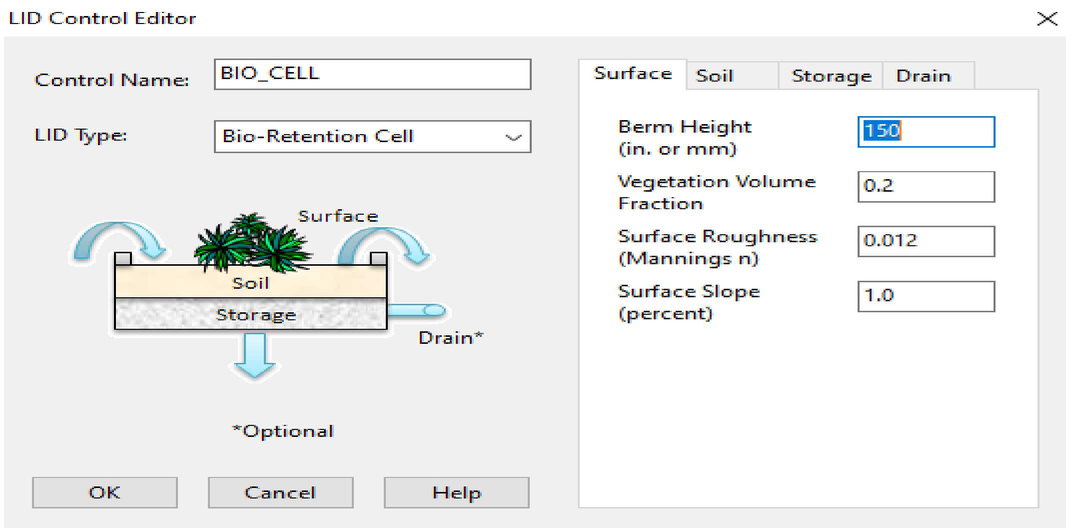
LID Control Editor
Control Name: BIO_CELL
LID Type: Bio-Retention Cell
Surface
Soil
Storage
Drain*
*Optional
OK
Cancel
Help
Surface
Soil
Storage
Drain
Berm Height (in. or mm) 150
Vegetation Volume Fraction 0.2
Surface Roughness (Mannings n) 0.012
Surface Slope (percent) 1.0

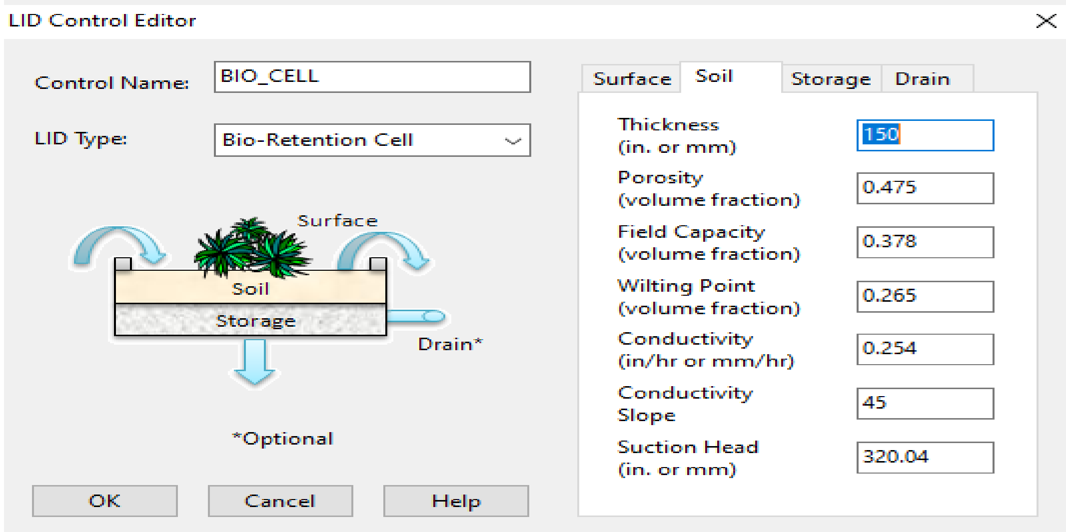
LID Control Editor
Control Name: BIO_CELL
LID Type: Bio-Retention Cell
Surface
Soil
Storage
Drain*
*Optional
OK
Cancel
Help
Surface
Soil
Storage
Drain
Thickness (in. or mm) 150
Porosity (volume fraction) 0.475
Field Capacity (volume fraction) 0.378
Wilting Point (volume fraction) 0.265
Conductivity (in/hr or mm/hr) 0.254
Conductivity Slope 45
Suction Head (in. or mm) 320.04

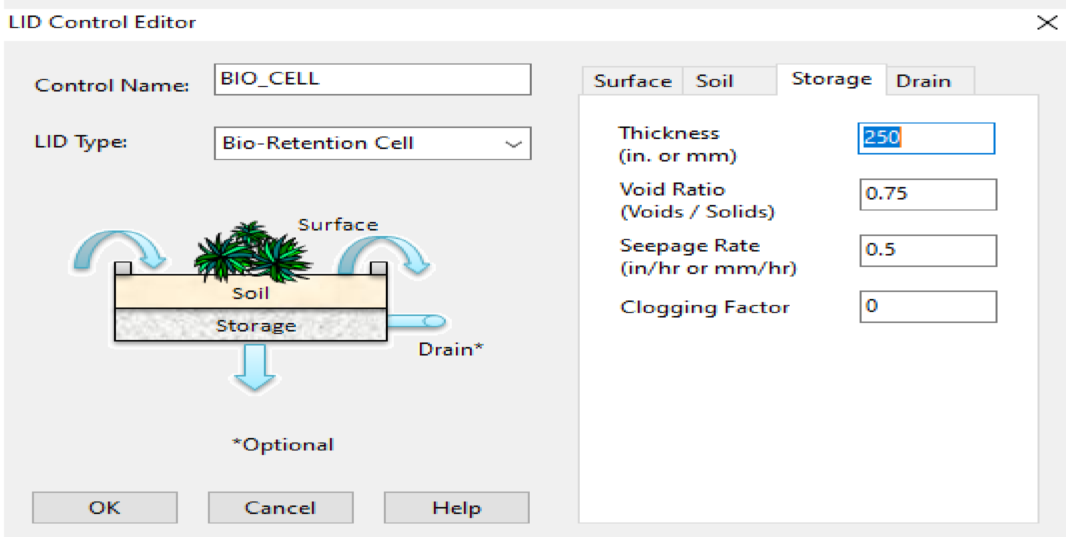
LID Control Editor
Control Name: BIO_CELL
LID Type: Bio-Retention Cell
Surface
Soil
Storage
Drain*
*Optional
OK
Cancel
Help
Surface
Soil
Storage
Drain
Thickness (in. or mm) 250
Void Ratio (Voids / Solids) 0.75
Seepage Rate (in/hr or mm/hr) 0.5
Clogging Factor 0

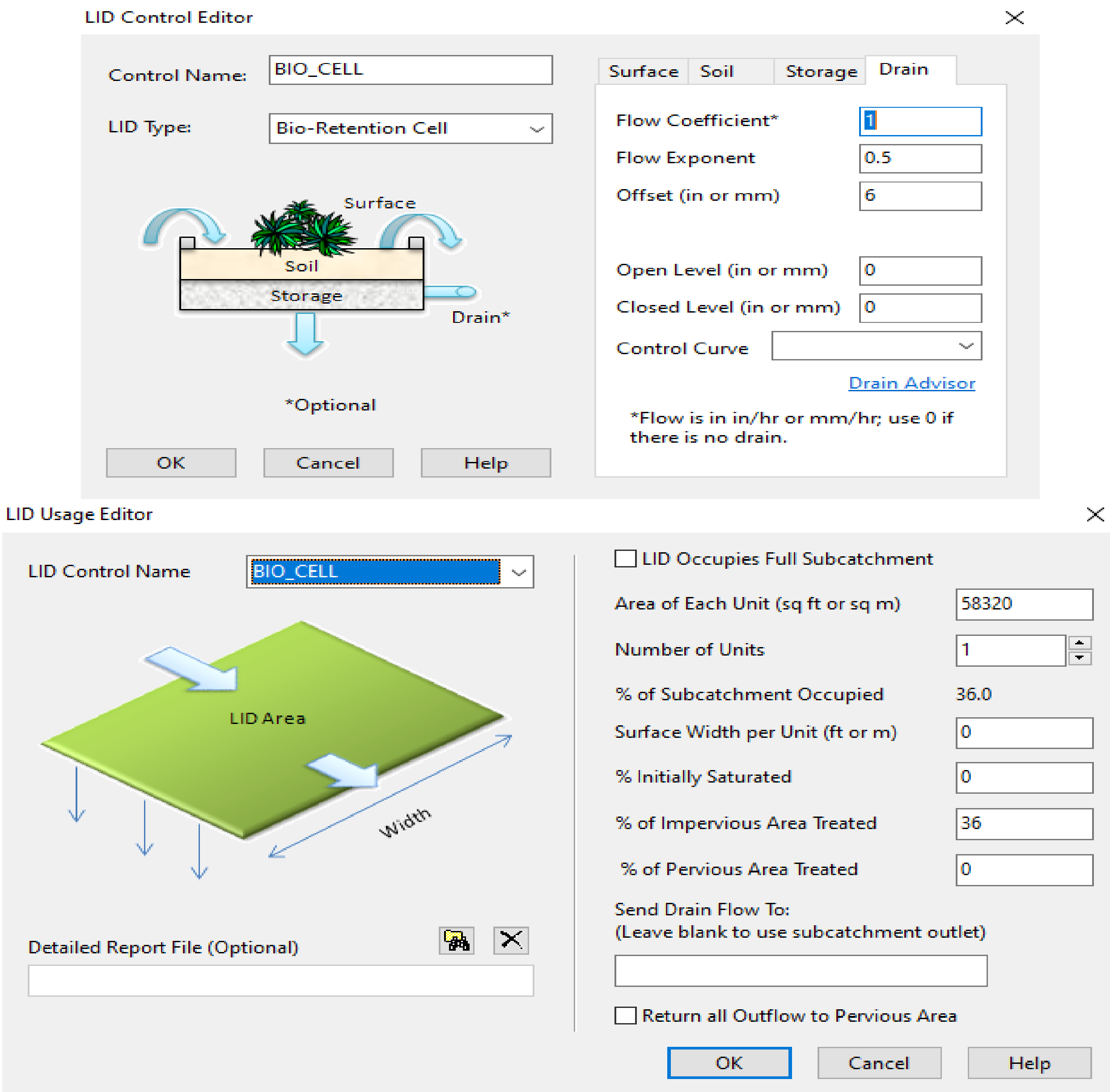


Figure 5: LID specifications used for Bio-retention Cells

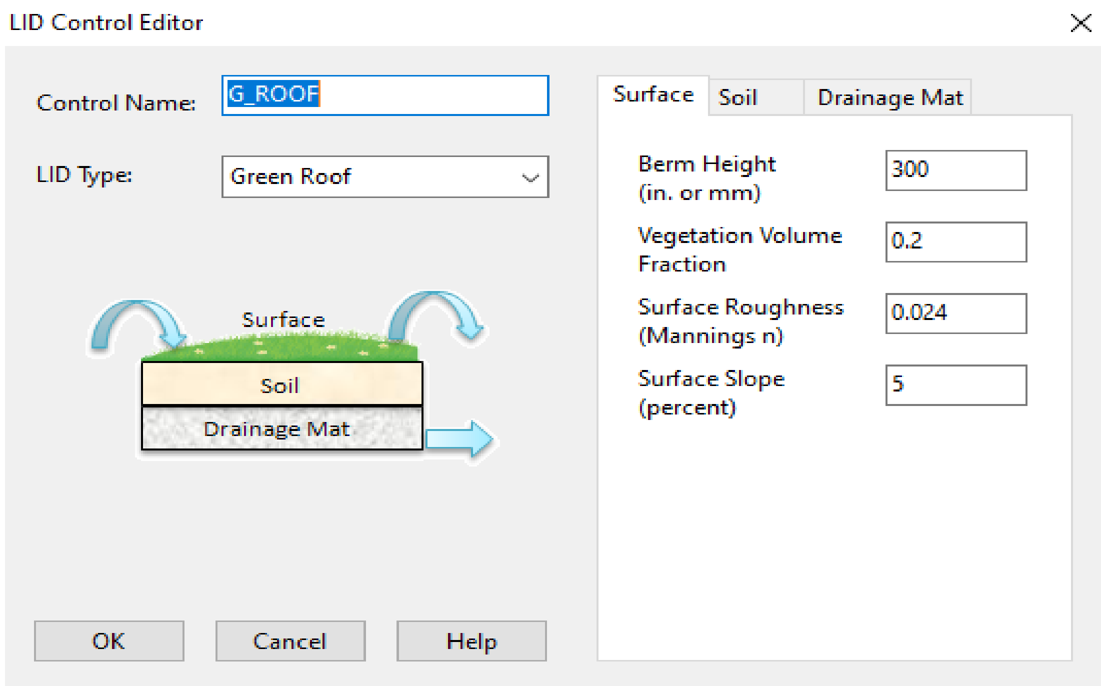
LID Control Editor
Control Name:
G_ROOF
LID Type:
Green Roof
Surface
Soil
Drainage Mat
OK
Cancel
Help
Surface
Soil
Drainage Mat
Berm Height
(in. or mm)
300
Vegetation Volume
Fraction
0.2
Surface Roughness
(Mannings n)
0.024
Surface Slope
(percent)
5
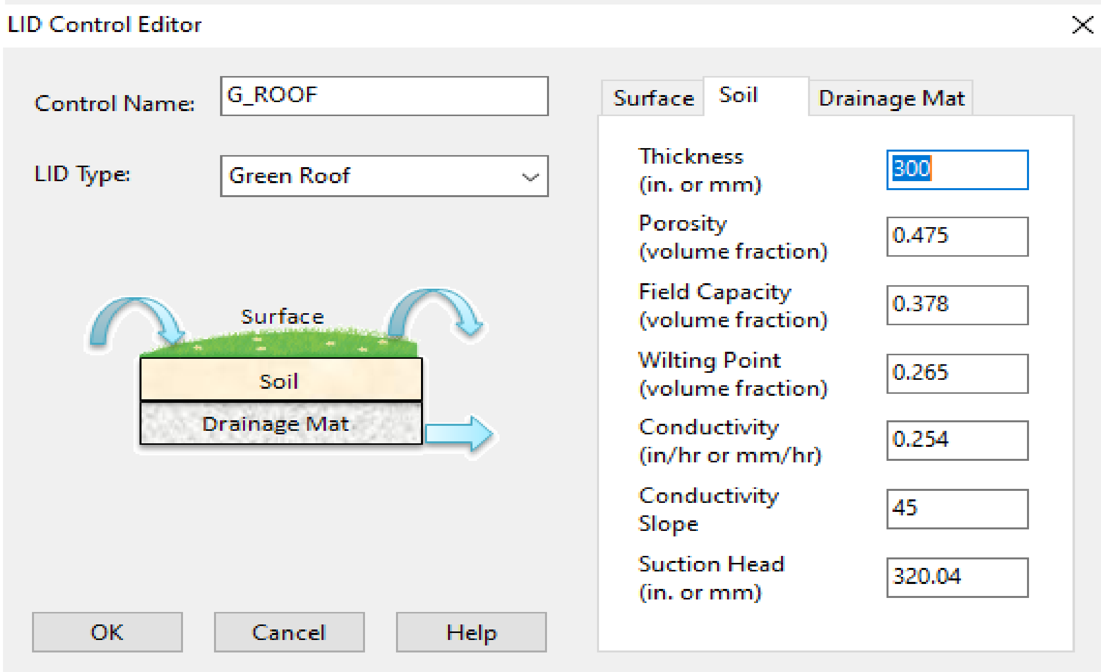
LID Control Editor
Control Name:
G_ROOF
LID Type:
Green Roof
Surface
Soil
Drainage Mat
OK
Cancel
Help
Surface
Soil
Drainage Mat
Thickness
(in. or mm)
300
Porosity
(volume fraction)
0.475
Field Capacity
(volume fraction)
0.378
Wilting Point
(volume fraction)
0.265
Conductivity
(in/hr or mm/hr)
0.254
Conductivity
Slope
45
Suction Head
(in. or mm)
320.04

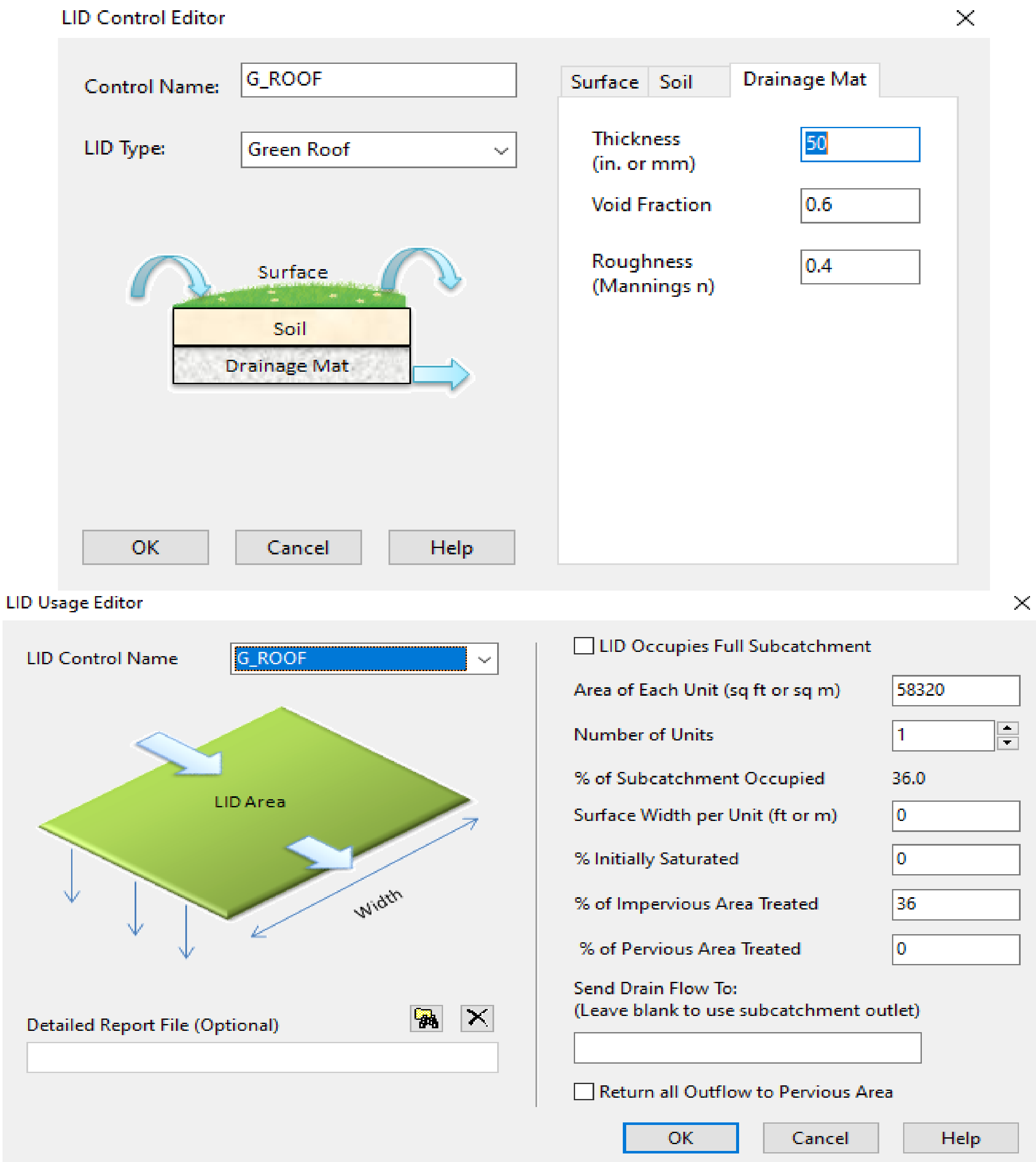


Figure 6: LID specifications used for Green Roofs

N.B: **meters** were chosen as the map units in the map dimensions. Therefore; **mm** and **mm/hr** were used over **in** and **in/hr** where required.